博士論文

Study on economic damage due to pluvial flood in Japan and the world and the impact of climate change

(日本と世界における内水氾濫による経済的被害と気候変動による影響に関する研究)

バッタライ　ラジャン

BHATTARAI RAJAN

Study on economic damage due to pluvial flood in Japan and the world and the impact of climate change

(日本と世界における内水氾濫による経済的被害と気候変動による影響に関する研究)

Rajan BHATTARAI
Student ID: 37-117304

A dissertation submitted to the University of Tokyo in partial fulfillment of the requirements for the degree of doctor of engineering

PhD Dissertation

Department of Civil Engineering
Graduate School of Engineering
The University of Tokyo

June 2014

Doctoral Committee
Prof. Kei YOSHIMURA (Chair)
Prof. Taikan OKI
Prof. Toshio KOIKE
Prof. Kensuke FUKUSHI
Prof. Riki HONDA
Prof. Yoshihide SEKIMOTO

東京大学
THE UNIVERSITY OF TOKYO

Study on economic damage due to pluvial flood in Japan and the world and the impact of climate change

(日本と世界における内水氾濫による経済的被害と気候変動による影響に関する研究)

Rajan BHATTARAI
Student ID: 37-117304

A dissertation submitted to the University of Tokyo in partial fulfillment of the requirements for the degree of doctor of engineering

PhD Dissertation

Department of Civil Engineering
Graduate School of Engineering
The University of Tokyo

June 2014

Approved as to style and content by:

.....	.....
(Chairman of Committee)	(Member)
.....	.....
(Member)	(Member)
.....	.....
(Member)	(Member)

This entire work is dedicated to my beloved mother...Binda devi Bhattarai

Acknowledgement

I would like to express my heartfelt gratitude to my respected supervisor Prof. Kei Yoshimura for his regular assistance, encouragement and valued suggestion without which the completion of this research work was impossible. I also wish to thank with my ample respect to Prof. Taikan Oki, head of Oki laboratory and a committee member, for his continuous support and encouragement to make this work a success. I wish to express my sincere gratitude to all my committee members: Prof. Toshio Koike, Prof. Kensuke Fukushi, Prof. Riki Honda and Prof. Yoshihide Sekimoto for their constructive comments, suggestions and recommendations.

My special thank goes to Prof. Shinta Seto, whose initial advises eased me to forward in research work and Prof. Kazuo Oki whose constructive advises always helped me to do something better. I would like to thank Prof. Hyungjun Kim for his large effort to improve my computer skills and Prof. Goro Mouri and Michio Murakami for their constructive comments and inspiration. My special thanks go to Dr. Masahi Kiguchi, Dr. Keigo Noda, Mr. Shinichiro Nakamura, and Mr. Nobuyuki Utsumi who had a lot of contribution in this research work from data preparation to finalizing the results.

It would be virtually impossible to mention names of all who have lent a helping hand in this work. I would, however, also like to place on record of my gratitude to all my friends in Oki laboratory. Special thanks goes to Ms. Misato Okaneya and Mr. Tomonori Kanazawa who helped me a lot in my initial days in Japan as my tutor. I am always grateful to all my friends: Suryun Ham, Asako Nishijima, Shinijiro Yano, Yusuke Satoh, Atsushi Okazaki, Mehwish Ramzan, Cherry Mateo, Akane Saya, Ronald Muana, Wataru Suzuki, Misako Hatono, Junya Hamada, Natsuki Yoshida, Amelia Lee Zhi Yi, Din Amad Ud, Shizuki Fukuda, Tatsuya Makino, Kiyotaka Mukaida, Daisuke Tokuda and Zhongwang Wei. At this moment I would like to thank Dr. Tomoko Nitta, Dr. Eun Chul Chang, Dr. Zhongfang Liu, Mr. Xiaogang He, Mr. Zero Kakehashi, Ms. Rina Takahashi, Ms. Sachi Abe, and Ms. Naoko Fukubayashi, past members of Oki laboratory, whose helps were really fruitful.

I would also like to extend my sincere thanks to all the professors and staffs in the University of Tokyo. My especial thank goes to the secretaries in Oki laboratory; Ms. Ayako Kurosawa, Ms. Yuki Tsukuda, and Ms. Mari Toi in the Institute of Industrial Science (IIS), Komaba campus and the secretaries in Yoshimura laboratory; Ms. Keiko Motani, Ms. Sunao Noguchi, and Ms. Kumi Miyagi in the Atmosphere and Ocean Research Institute (AORI), Kashiwa campus for their kind cooperation to make my university life easier. I also like to thank the staffs of the department of civil engineering and Foreign Student Office (FSO) for their nice guidance during these three years period. I am highly indebted to the mentors of Japanese Language Class (JLC) in the department of civil engineering for their efforts increasing my Japanese proficiency.

I would like to thank from core of my heart to the government of Japan, providing me financial assistance during these three years through MEXT scholarship program, and the University of Tokyo, giving me an opportunity for studying here with all kind of supports. I would also like to thank Government of Nepal who facilitated me for this study with three years study leave.

Last but not the least; I would like to express my deepest gratitude to all my family members, especially to my wife, *Roshna*, for her patience and tolerance over the last three years in every circumstances.

Abstract

The assessment of flood risk and its future prediction under the anthropogenic climate change are important to policy makers for future preparedness and adaptation planning. Almost all countries in the world including major cities suffer from flood damage every year due to large exposed population and property. Flood losses are increasing more rapidly during the late 20th century and are expected to increase in future too. The intensity of damage varies as per the level of their vulnerability; as a result economic loss intensity due to floods is much higher in developing countries than in developed countries. Even though huge investments for the improvement of flood control infrastructures were made, flooding remains a serious problem throughout the world. Some large scale and record breaking flooding events in recent years in terms of physical losses provided serious attention to world leaders and policy makers towards proper planning and management of flood control infrastructures and formulating future adaptation strategies. It is presumed that future increase in hazards extremes resulting from climate variability and socio-economic development will increase economic losses. Various studies projected a large increment of flood losses in the world by late 21st century, and even worse there will be large spatial and inter-annual variability.

Flooding related to rainfall usually divided into large-scale fluvial floods, and pluvial floods that occur due to excessive rainfall and overwhelms local drainage systems. The share of pluvial flooding to total physical losses cannot be underestimated. The pluvial flood damage, particularly in densely populated urban areas and areas with poor drainage facilities were recorded very high not only during heavy rainfall events, but also at moderate to low rainfall events. Rapid urbanization with poor infrastructures often promotes increasing flood damage not only to economy but also to human lives. Due to the highest concentration of capital in urban regions, a small changes in rainfall intensity can led to large increase in pluvial flood damage and hence pluvial flood damage could be a large component of physical losses in future climate change condition.

In this regards, a proper way of estimating pluvial flood damage amount and thereby assessing its risk in local to global scale in present and future is a demanding task for not only scientific communities, but also indispensable for decision makers.

To this end, various flood damage assessment models have been developed and used. Most studies regarding flood damage assessment have been done for large scale fluvial flooding. Many conceptual models which provide the different vulnerability or risk indices for spatial comparison were used by various organizations. These index-based approaches might be suitable for assessing relative risk distribution; however a decision maker requires proper estimate of economic damage in absolute monetary terms so that economic viability of proposed infrastructure development plan could be justified.

The direct flood damage estimating models so far developed basically utilizes integration of two different sub-models. A hydrological model is used to estimate hydrological parameters and a loss model is used to relate these hydrological parameters to damage amount. However, a hydrological model usually needs large resources and still there is a need of better understanding of flooding characteristics in inner urban areas. Calibration and validation of these models are often difficult due to limited data availability. On the other hand various loss models, so far developed in some local scale using past flooding damage data have serious uncertainties while using for different temporal and spatial regions. Uncertainty related to types of property and its values are also critical in loss models while expanding the model to different regions. Moreover, an extreme event corresponding to large return period is usually taken for damage assessments providing largest possible damage, however total annual damage is usually associated with many high frequency events and reported as equal as extreme events. There is a need of a model which can incorporate all potential events for damage so that proper estimate of annual damage could be made.

To address the aforementioned issues, in this research, we present a novel and robust statistical model for pluvial flood damage assessment particularly for general property.

We used recorded historical daily damage data in Japan that are archived in Ministry of Land, Infrastructure, Transport and Tourism (MLIT) of Government of Japan to produce functions namely damage occurrence probability function and damage cost function. The former function represent the relationship of exceedance probability of rainfall to its corresponding damage probability, and latter represent the relationship of exceedance probability of rainfall to relative damage amount for a particular location. Our statistical approach gives the probability of damage following every daily rainfall event and thereby estimates annual damage as a function of rainfall, population density, topographical slope, and gross domestic product. The newly developed model largely reduces use of sophisticated hydrological models on one hand and current micro-scale loss models in the other hand. The model could be a very light and robust tool for decision makers to estimate annual damage for short term planning and to estimate expected annual damage for long term planning with reasonable level of confidence.

The model was first developed using the damage data for the period of 1993-2002 and validated through 2003-2009, calculating area average total national pluvial flood damage in Japan. The results for Japan showed reasonable agreement with annual damage for the period 1993–2002 in calibration and 2003-2009 in validation. The annual damage variation is well matched with the recorded annual damage in most of the years. The expected annual damage estimated during 1993-2009 by the model (90 billion yen) is also well comparable with recorded average annual damage for the same period (97 billion yen). The average monthly variation of damage is also well matched with the recorded average monthly damage variation, expanding the applicability of the model for seasonal damage estimation. Furthermore, we evaluated uncertainty of our model, basically due to damage data preparation and methodology applied. The regional distribution of expected pluvial flood damage over Japan was also estimated, which reveals that bigger cities had higher absolute damage than smaller cities had. On the other hand, vulnerability of smaller cities seems to be higher than bigger cities. This might be due to lower preparedness for pluvial flooding.

The sensitivity test for different resolution precipitation data shows that the calculated total annual damage is almost insensitive to the horizontal resolution. Flexibility of the model leads us for future projection of pluvial flood damage in Japan and also extending the methodology to entire globe.

Daily precipitation results of multiple climate models were used for Japan to predict future pluvial flood damage under different climate scenarios. The daily precipitation results from MRI-AGCM with 13 different scheme candidates based on their output resolution, convective schemes, and future SSTs (ensemble of three different clusters of CMIP models SST outputs) were used for A1B scenario in far-future [2083-2095]. Five different GCM candidates were used for RCP2.6 and RCP8.5 scenario. The results for ensemble mean of expected annual pluvial flood damage in Japan shows an increment of 105% during far-future [2083-2095] from the base period [1993-2005] in A1B scenario. For this scenario, the pluvial flood damage will be more than double and expected to reach up to 177 (±44) billion yen per year. On the other hand, two RCP scenarios show the ensembles mean increment of about 47% and 247% in RCP2.6 and RCP8.5 respectively during the far-future [2083-2095] from present [1993-2005]. The average annual damage for RCP2.6 scenario will rise up to 116 (± 17) billion yen and that for RCP8.5 is 274 (±92) billion yen at 2005 price during the late 21st century. Also inter-annual variations of damage for RCP8.5 scenarios are significantly higher in far-future than that in the present period. The results of average monthly variation show the damage associated with East-Asian monsoon (June-July) and typhoons (Sep-Oct) both are significantly increases in future climate, however there is a large uncertainty among the ensemble members. Long term future run using four different GCMs for RCP2.6 and RCP8.5 scenarios reveals that there is a continuous rising trend of pluvial flood damage amount for RCP8.5 scenario, however the increment rate will be dramatically rise after 2060s, if present socio-economic development level persists in future too.

The model was further applied to estimate pluvial flood damage in the world. The global daily precipitation data (CPC unified gauge based dataset) along with

population density, gross domestic product, and topographical slope were utilized with 0.5° spatial resolution. The vulnerability of each country was assumed as an inverse function of human development index (HDI). The vulnerability parameters, optimized for Japan, were converted with inverse relationship of HDI of Japan and other countries. The results of global expected damage distribution from the period (1990-2005) shows that the absolute pluvial flood damage was higher in developed regions for example in Eastern USA, Western Europe and Japan. Eastern China, Northern India, including Bangladesh, Pakistan and some South-east Asian nations also had higher absolute damage value. But, relative damage amount with respect to the corresponding gross domestic product shows Central African nations and South Asian nations had higher vulnerability.

Since the absence of global database for pluvial flood damage, it was hard to validate the results of global estimation of pluvial flood damage directly. The capability of the new model was tested with the expected annual national damage estimated by the model for different countries. The correlation of average annual national damage due to general flood damage recorded in EM-DAT was highly correlated with expected pluvial flood damage estimated by this model, showing its capability to produce the average annual damage in each nation. The expected annual global pluvial flood damage for the period 1990-2005 is estimated to be 6.3 billion USD (2000 price), which is about 25% of total approximate flood damage (25 billion USD) during this period.

The entire work is described in the present dissertation through chapter 1 to Chapter 6. Chapter 1 is an introductory one. Chapter 2 reviews the risk assessment and damage modeling techniques for different flood types, damage types for present and future climate along with their limitations. Chapter 3 describes the formulation of the pluvial flood assessment model with detail description of data and methodology and its evaluation in present. Chapter 4 describes the application of the model for future assessment of pluvial flood in Japan in different climate scenarios. Chapter 5 deals a way to widen the model for global assessment and evaluate the results based on current global database. The final section concludes the study with recommendations.

List of Publications

Bhattarai R., Yoshimura K., Seto S., Nakamura S., Oki T., 2014. Statistical model for economic damage from pluvial flood in japan using rainfall data and socio-economic parameters. *Hydrological Sciences Journal.* [Under review]

Bhattarai R., Yoshimura K., Sato Y., Keigo N., Oki T., A projection of future pluvial flood damage in Japan under anthropogenic climate change. [In preparation]

Bhattarai R., Yoshimura K., Mashasi K., Oki T., First estimate of global pluvial flood damage. [In preparation]

List of tables

List of Figures

Table of Contents

1. Introduction

1.1 Motivation

The world faces several natural disaster and thereby billions of dollar economic losses every year. The world bank report (Dilley *et al.*, 2005) marked that earthquakes, floods, drought like natural hazards continue to cause tens of thousands of deaths, hundreds of thousand injuries, and billions of dollar in economic losses every year around the world. Flooding is one of the major causes of physical losses in the world and continually increasing in trend. Globally flood damage have increased from an average of seven billion USD per year in the 1980s to more than twenty billion USD at the end of 2000s (Kundzewicz *et al.*, 2013). Thirty-five percent of physical losses over the past 40 years in the Asia-Pacific region were due to flooding (Asian Development Bank, 2013). Moreover, occurrence of flood is the most frequent among all natural disasters (Jha *et al.*, 2011). Recent large scale and record breaking flooding events in terms of physical losses provided serious attention to the world leaders and policy makers towards proper planning and management of flood control infrastructures and formulating future adaptation strategies. China in 2010 experienced the largest flood damage of 51 billion USD in one single year and the 2011 flood in Thailand caused the most expensive insurance loss ever, worldwide, with total liability estimated at around 15 billion USD (Kundzewicz *et al.*, 2013). Flooding events in Germany and central Europe in May and June, 2013 were the most expensive, costing around 16 billion USD (Wake, 2013). Economic losses due to floods are higher in developed countries, however the economic losses expressed as a proportion of gross domestic product are much higher in developing countries (Handmer *et al.*, 2012). Even a huge investment for improvement of flood control infrastructures, flooding remains a serious problem throughout the Europe (Kundzewicz *et al.*, 2013) and the case of Japan is also similar. Annual expenditure for flood control in government budget is nearly 10 billion USD (about 1 trillion yen) as reported in Kazama *et al.*, (2009) in Japan. Despite the fact that improvement of flood control infrastructures in major rivers, with huge investment, has resulted declining the inundated area in housing or urban land; however inundation damage density and thereby inundation damage for private assets remain very high in Japan (MLIT, 2006). The high potential of flood damage in Japan is basically due to the fact

that approximately 9% of Japan's land area is flood prone, but contains 41% of Japan's population and 65 % of the national assets (Kundzewicz *et al.*, 2013).

A special report of the Intergovernmental Panel on Climate Change (IPCC), often called IPCC SREX (IPCC, 2012) stated that future changes in hazards extremes resulting from climate variability, anthropogenic climate change, and socioeconomic development can alter the impacts of climate extremes on natural and human systems and the potential for disasters. IPCC (2012) also revealed with high confidence that economic losses from weather and climate related disasters have increased, but with large spatial and inter-annual variability. Some researches prevailed that the warming climate in future leads to the increase in flooding in many parts of the world (Hirabayashi *et al.*, 2008, 2013, Seneviratne *et al.*, 2012). Future projections of precipitation and temperature changes imply possible changes in floods in future as it is likely that the frequency of heavy precipitation or the proportion of total rainfall from heavy rainfalls will increase in the 21st century over many areas of the globe (Seneviratne *et al.*, 2012). Bouwer (2013) summarized different studies and concluded that the median increase of all projected flood losses will be 83% by the year 2040, relative to the year 2000. In Europe, the annual damage and the number of people exposed in late 20th century are expected to increase about two fold by the end of 21st century under SREX B2 scenario (low emission) and about three times under SREX A2 scenario (high emission) (Feyen *et al.*, 2012).

A policy report by Ministry of Land, Infrastructure, Transport and Tourism (MLIT) (MLIT, 2008a) mentioned even worse scenarios for Japan. The report cited that there was a significant increasing trend during the last century in number of days with heavy daily precipitation and also stated that there has been an increasing trend in short-time heavy rainfall in the last 30 years as also revealed in Utsumi *et al.* (2011). The reports further revealed based on different studies that future annual precipitation and summer precipitation will increase in most part of Japan. Also it stated that heavy rainfall events become more frequent in most parts of Japan. Owing to the fact of having high concentration of the property and above climatic condition, Japan could

be a hot spot of climate change impact and thereby spot of huge amount of flood damage in the world.

Flooding related to rainfall usually divided into large-scale floods due to high discharges of rivers and stream (fluvial flood), and local and urban floods that occur due to excessive rainfall that overwhelms local drainage capacity (Pluvial flood) (Bouwer, 2013). Even often published flood damage events are from fluvial flood, the share of pluvial flooding cannot be under estimated. The pluvial flood damage, particularly in densely populated urban areas and areas with poor drainage facilities were recorded very high not only during heavy rainfall but also at moderate to low rainfall events. Mouri *et al.* (2013) stated that the pluvial flood is more affected by population than fluvial flood and hence many cities in the world suffer from pluvial flood every year. Rapid urbanization with inadequate engineered in-city drainage infrastructure will promote the damage not only to economy but also to human lives (Kundzewicz *et al.*, 2013). MLIT has shown that 86% of total economic flood damage in the Tokyo metropolitan during 1998-2007 was due to pluvial flood only (MLIT, 2008b). The flood damage in Kochi in September 1998 (Yamamoto *et al.*, 1999) was largely due to the pluvial flood damage and also failure of inner drainage systems led to higher flood damage in 2000 Tokai flood (Ikeda *et al.*, 2007). The average annual economic damage for residential property attributable to pluvial flood damage in Japan was approximately 100 billion yen (about 45% of annual flood damage of same kind) during 1993-2009 (MLIT, 2009). **Figure 1.1** shows the historical total national fluvial and pluvial flood damage for general property in Japan. The figure shows that there is much constant pluvial flood damage in each year than fluvial flooding. The special report of the intergovernmental panel on climate change reported with medium confidence that projected increase in heavy precipitation would contribute to rain-generated local flooding in some region, but still literatures on the impact of climate change on pluvial flood is scarce (Seneviratne *et al.*, 2012). Due to higher concentration of property and population, a small changes in rainfall intensity can led to rapid increase in flood damage in urban areas (Bouwer, 2013).

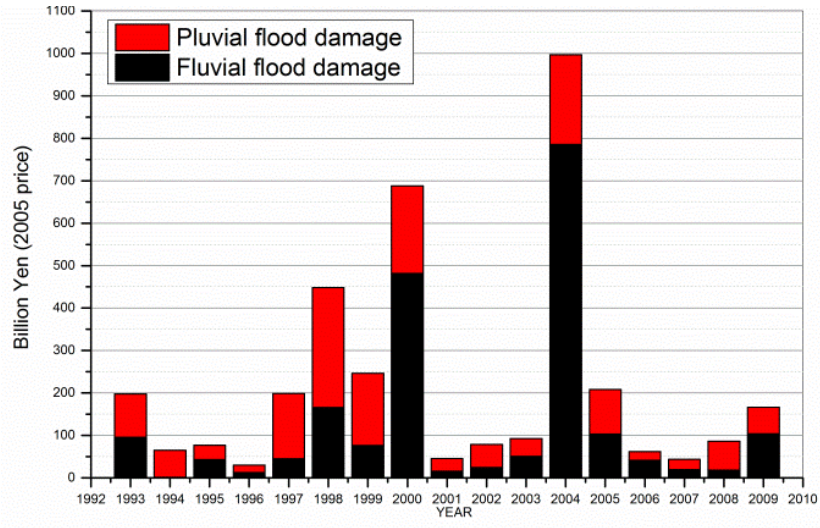

Fig. 1.1 Historical general property damage for Japan from 1993-2009

In regard to the above discussion, a proper way of calculating flood damage amount for each hazard event and thereby assessing its risk in local to global scale for present and future is a demanding task for scientific communities. Risk assessment is one starting point, within the broader risk governance framework, for adaptation to climate change and disaster risk reduction (Lavell *et al.*, 2012). Proper estimate of economic damage is now indispensable for decision makers so that economic viability of proposed infrastructure development, mitigation and/or adaptation plan for flood defense could be justified. Flood risk mapping is an essential element of flood risk management strategies (Merz *et al.*, 2010). A wide range of methodologies have been developed and applied for assessing damage risk over the last few years but still these models possess a number of limitations due to a large uncertainty in methodology and data unavailability. There are still many technical challenges in developing a robust risk assessment and damage costing model (Handmer *et al.*, 2012, Bouwer, 2013). There is still a need of better understanding of the processes lending to damage so that they can be modeled appropriately (Meyer *et al.*, 2013). IPCC (2012) focused the need of more empirical and conceptual efforts to develop a robust risk assessment methodology.

As a result, this research is motivated toward a development of a simple but robust statistical model for pluvial flood damage assessment in Japan and expands it to the

world, developing robust relationship between hazard, exposure and vulnerability in terms of pluvial flooding and its impact on residential property damage and also predicts the future scenario of pluvial flood damage.

1.2 Research Approaches

To date various flood damage assessment models have been developed and used by various organization in the world with diverse approaches. Many conceptual models which provide the different vulnerability or risk indices for spatial comparison were developed for local to global scale. Some popularly known indices are event based disaster risk index (DRI) (UNDP, 2004), Hazard index for Mega cities (HIM) (Munich Re, 2004), Prevalent vulnerability Index (PVI) (Inter-American Development Bank, 2007), Discharge probability index (DPI) (Yoshimura *et al.*, 2008), Flood vulnerability index (FVI) (Hara *et al.*, 2009) and Advance flood risk index (AFRI) (Okazawa *et al.*, 2011). Each index has their own criteria and spatial resolution (local, catchment, national to global scale) for calculating indices for risk or vulnerabilities. Some conceptual models for damage assessment were also available for example: Pelling and Uitto (2001), Birkmann (2007) and Hinkel (2011). The index based approach might be suitable for assessing the relative risk distribution; however a decision maker requires proper estimate of economic damage in absolute monetary term so that economic viability of proposed infrastructure development plan for flood defense could be justified.

The direct flood damage estimating models so far developed basically utilize integration of two different sub-models: first, to estimate hydrological parameters (e.g. flood velocity, flood duration and flood depth) based on some physically based hydrologic modelling techniques (Hydrological models) and second, to estimate absolute damage or relative damage amount based on susceptibility functions usually derived from empirical analysis (loss models) which relate a hydrological parameter to the damage amount as shown in **Fig. 1.2** below.

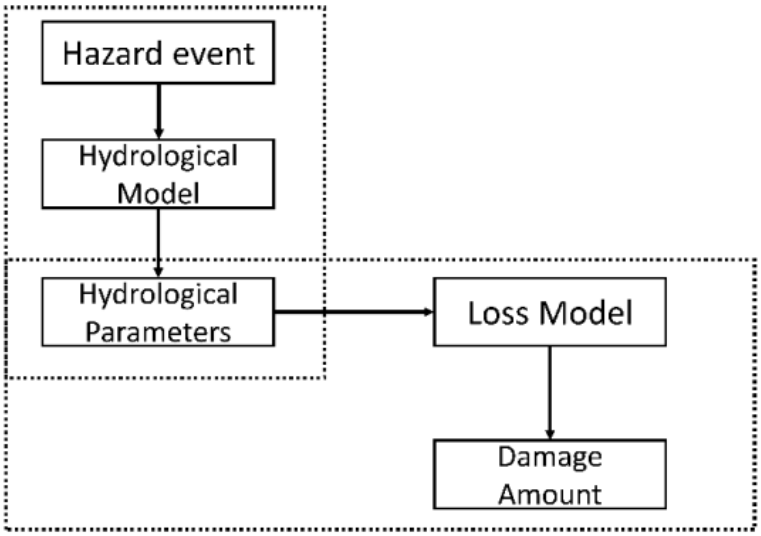

Fig. 1.2 Schematic diagram of integrated damage modeling approach

The hydrological models or sometimes referred as hazard models so far used, varying in its complexity from simple liner interpolation technique to 1D/2D hydraulic model to a Saint-Venant 2D zero-inertia hyperbolic hydraulic models (Apel *et al.*, 2009) and to full-fledged distributed hydrologic models (e.g. Dutta *et al.*, (2003)). The basic features of a hydrological model are to estimate hydrological parameters for a hazard event generally defined by its exceedance probability (Return period). However, these hydrological models possess a number of uncertainties regarding extreme value statistics used, stationary and homogeneity of data series, consideration of proper physical properties of a location (e.g. dikes) and calibration and validation of the model output etc. (Apel *et al.*, 2009).

On the other hand, a loss model is a central idea for flood damage estimation (Merz *et al.*, 2004) and the most common way of estimating direct damage amount so far is the use of depth-damage functions often termed as susceptibility function or vulnerability function (Smith, 1994, Dutta *et al.*, 2003, Kelman and Spence, 2004, Kazama *et al.*, 2009, Kreibich *et al.*, 2010, Jongman, *et al.*, 2012a). Many loss models used single hazard parameter especially flood depth for example: MURL (2000), ICPR (2001), and Glade (2003). Some loss models were multi-parameter models based on several hazard parameters (flood depth, flow velocity, contamination etc.) and resistance

parameters (flood prone object type and/or size, mitigation measures etc.) for example: HAZUS-MH (FEMA, 2003), Model of multi coloured manual (Penning-Rowsell *et al.*, 2005), FLEMOps (Apel *et al.*, 2009), and FLEMOcs (Kreibich *et al.*, 2010).

Recently integrated approaches for developing complete flood damage models in single study were much popular. Few example of integrated approach which combines both hydrological models and loss models are Dutta *et al.* (2003); Hall *et al.* (2005); Rodda (2005); Schmidt-Thomé *et al.* (2006); Kazama *et al.* (2009) and Ward *et al.* (2013).

Further, flood risk quantification depends on the defined spatial boundary (Apel *et al.*, 2009). To date several studies had been done from very local municipal level to global scale. The **Table 1.1** shows few examples of flood damage assessment studies in different spatial scales.

Table 1.1 Studies on flood damage assessment with different spatial scale

Spatial Scale	Studies
Municipality	Baddiley (2003), Grünthal *et al.* (2006)
Catchment	ICPR (2001), Dutta *et al.* (2003), Dutta *et al.* (2006)
National	Hall *et al.* (2005), Rodda (2005), Kazama *et al.* (2009)
Regional	Schmidt-Thomé *et al.* (2006)
Global	Jongman, *et al.* (2012b), Ward *et al.* (2013)

Most of the damage assessment models so far discussed were primarily developed for fluvial flood; however a loss model could be a common component for both fluvial and pluvial flooding. Few studies on pluvial flood and its associated damage were also reported. Zhou *et al.* (2012) described a framework for economic pluvial flood risk assessment considering future climate change which quantifies flood risk in monetary terms as expected annual damage in different return period of rainfall. Escuder-Bueno *et al.* (2012) presented a methodology for assessing pluvial flood risk using two different curves; one for societal risk and other for the economic risk, however both were limited to a local scale.

The flood damage assessment models to dates contain a number of uncertainties both in hazard and vulnerability parts. The largest source of uncertainties in damage modelling were associated with prescribed depth-damage functions (Merz *et al.*, 2004, 2010, Hall *et al.*, 2005, Apel *et al.*, 2009, Moel and Aerts, 2010, Jongman, *et al.*, 2012a). The reason for the uncertainties regarding loss models is its crude assumption of relationship of damage with flood depth. Moreover, these models generally developed for some specific location using past record of floods and its validation are always a critical issue for its temporal and spatial transferability. Uncertainty related with the property types and their total values are also critical in many cases and it is a fact that there is almost no study for pluvial flood damage assessment in national and global scales.

1.3 Research Objectives

With regard to the current challenges in flood damage assessment methodology especially for pluvial flood as described in previous sections, this study aims to develop a statistical model as integral of both hazard and vulnerability based on historical database in Japan for pluvial flood damage. Furthermore the objective are extended to assess the pluvial flood scenario in future climate and extended the methodology to the world. An overall methodology with its broad objective is shown in **Fig. 1.3** below.

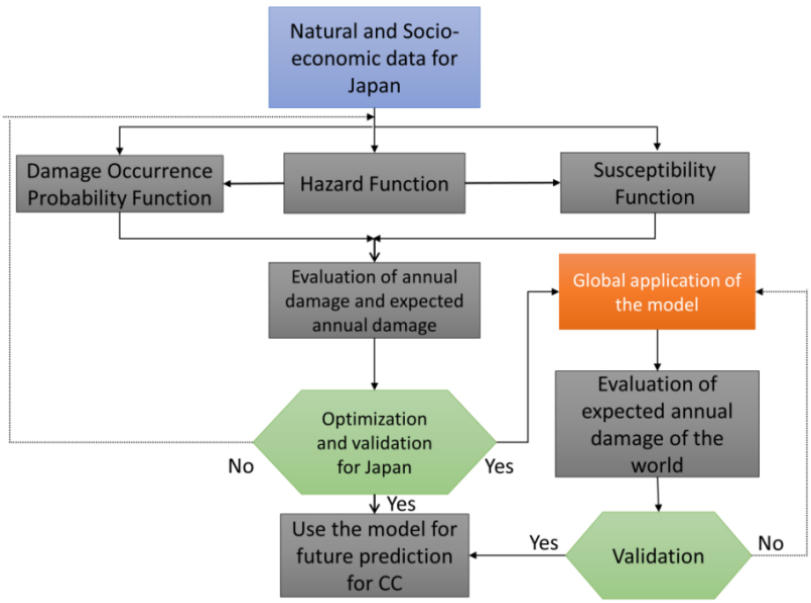

Fig. 1.3 Overview of the research objective

In the broad objective of developing a statistical pluvial flood risk assessment model and study of pluvial flood risk in Japan and in the world, some specific objectives of this study have been listed as:

1) To develop a simple but robust statistical model based on Japanese historical database for pluvial flood risk assessment.
2) To formulate both hazard function and susceptibility function for pluvial flood general property damage assessment in Japan within present flood risk assessment framework.
3) To evaluate the relationship between social and topographical characteristics of a location and pluvial flood damage.
4) To formulate general empirical relationship between damage occurrence probability and vulnerability of a location in relation with hazard, topography and socio-economic dimensions.
5) To evaluate the developed model in Japan along with the evaluation of model uncertainty.
6) To predict the future pluvial flood damage in Japan with different climate scenarios.
7) To expand the model into global scale for calculating pluvial flood damage in the world and its validation.
8) To widen the applicability of the model with intensive validation technique for different nations.
9) To estimate the pluvial flood for different countries in the world.
10) To predict the future pluvial flood damage in the world in different climate scenarios.

1.4 Outline of the Dissertation

The research objectives enumerated above were pursued with the broad review of current state-of-the-art in flood risk assessment methodologies and conceptualizing a robust methodology of pluvial flood. The model was developed based on the Japanese statistical datasets and intensively evaluated the parameters with calibration and validation techniques. The model was further used to estimate future scenario of pluvial flood damage in Japan and also attempted to apply it at global scale in present

condition. Chapter 2 reviews the risk assessment and damage modeling techniques for different flood types, damage types and limitations in current damage modeling techniques. Different terminologies in flood risk assessment framework are defined. Reviews in the work of future climate and socio-economic scenarios are also discussed in this chapter. Chapter 3 describes the formulation of the pluvial flood assessment model with detailed description of data and methodology applied. Each formulation is described in this chapter along with the uncertainty related to it. Chapter 4 describes the application of the model for future assessment of pluvial flood in Japan under different climate scenarios. Chapter 5 deals a way of widening the model for global assessment and evaluates the results based on current global database. The final section concludes the study with recommendations.

2. Review of Risk Assessment/Damage modelling

2.1 General Concepts

Precipitation and runoff are important components of hydrological cycle; a continuous circulation of water in the complex land-ocean-atmosphere system of the earth. The importance of hydrological cycle is not only limited to human beings, every living creatures in the globe sustain their life and advanced to present state basically due to various forms of water. Historically, the most well-known human civilizations were started along the rivers, confirms the vast relationship between people and water. However, relationship of this natural resources and people sometimes becomes much antagonistic due to their extreme nature. The situation of low availability of water (drought) and very high amount than normal condition (floods) are often results harsh condition to people. Millions of people lost their life due to these extreme events in the past and unfortunately continue in the present. The assessment of the available water resources and their temporal and spatial distribution, as well as the analysis of flood and drought risk are of great importance for the health of human societies and environmental systems (Lehner *et al.*, 2006). A special report of intergovernmental panel on climate change, often called IPCC SREX (IPCC, 2012) defines floods as "the overflowing of the normal confines of a stream or other body of water, or the accumulation of water over areas that are normally unsubmerged". The increase of flood extreme due to climate change phenomena on one hand and increment of population and assets in flood prone areas lead the flood risks in future too. Obviously, the interaction of hazard events, exposure and vulnerability of a location produces risk. The basic concept of risk and its components are described in the following sub-sections.

2.1.1 General definition of risk

To this end, various definition of risk can be found in different literatures. Going back to the 1990s, Morgan and Henrion (1990) defined risk as an exposure to a chance of injury or loss. Smith (1996) defined the risk simply as a probability of a specific hazard occurrence. Davidson (1997) further elaborated the risk as the product of hazard, exposure, vulnerability, capacity and measures. Hall *et al.* (2005) specifically

defined flood risk as the product of the probability of flooding and the consequential damage, summed over all possible flood events. As per the definition of United Nation International Strategy for Disaster Reduction (UNISDR) (UNISDR, 2009), disaster risk is a product of hazard, vulnerability and exposure and hence can be simply written as:

$Risk = Hazard\ x\ Vulnerability\ x\ Exposure$ ---------- (1)

The definition as given in equation (1) is widely used to define risk; even the formulation of each component is different in different study. IPCC (2012) broadly defined the disaster risk as the likelihood over a specified time period of severe alternations in the normal functioning of a community or society due to hazardous physical events interacting with vulnerable social condition, leading to wide spread adverse human, material, economic, or environmental effects that require immediate emergency response to satisfy critical human needs and that may require external support for recovery. The **Fig. 2.1** below shows the schematic representation of risk as an interaction of hazard, exposure and vulnerability.

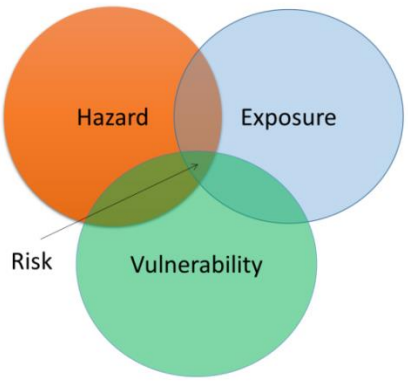

Fig. 2.1 Schematic representation of risk as an interaction of hazard, exposure, and vulnerability

2.1.2 Flood risk and its components

Risk assessment is a starting point, within the broader risk governance framework, for adaptation to climate change and disaster risk reduction (Lavell *et al.*, 2012). Flood risk mapping is an essential element of floor risk management strategy (Merz *et al.*, 2010). Flood risk cannot be completely eliminated and there will always remain residual risk (Escuder-Bueno *et al.*, 2012). IPCC (2012) defined the disaster risk management as the processes for designing, implementing, and evaluating strategies,

policies, and measures to improve the understanding of disaster risk, foster disaster risk reduction and transfer, and promote continuous improvement in disaster preparedness, response, and recovery practices, with the explicit purpose of increasing human security, well-being, quality of life, and sustainable development. In particular, a key aspect of effective flood risk management is the evaluation of the current situation and the effect of implementing new measures (Escuder-Bueno *et al.*, 2012). Whatever be the scale of flood risk study, the flood risk is a complex interaction of hazard and different natural and social components. To form a robust risk assessment model, a clear understanding of all components in it is essential. The following sub-section will describe the definition of each component in flood risk assessment and their inter-relationships.

As increase in population thereby land use change and economic development can led to changes in natural systems (Handmer *et al.*, 2012). Human induced climate change condition also led to the changes in natural hazard events in various ways in future. It is likely that the frequency of heavy precipitation or the proportion of total rainfall from heavy rainfall will increase in the 21st century over many areas of the globe (Seneviratne *et al.*, 2012). The various anthropogenic drivers as a factor for the flood risk changes can be well understood from the **Fig. 2.2**.

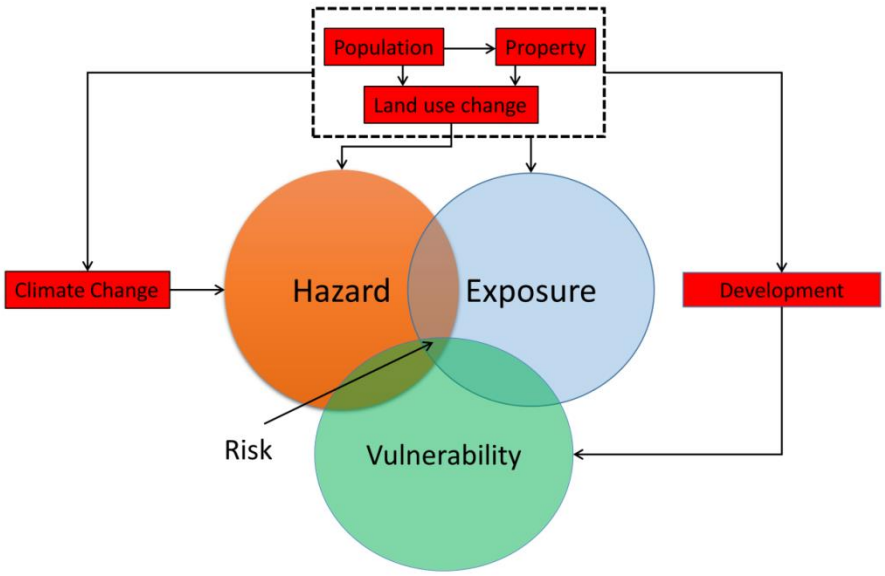

Fig. 2.2 Anthropogenic drivers of changes in flood risk.

All three main components of flood risk are briefly described in following sub-sections.

2.1.3 Hazard

The special report of the intergovernmental panel on climate change (IPCC, 2012) defined hazard as the potential occurrence of a natural or human induced physical event that may cause loss of life, injury, or other health impacts, as well as damage and loss to property, infrastructure, livelihood, service provision, and environmental resources. Apel *et al.* (2009) defined flood hazard more exclusively as "The physical and statistical aspects of the actual flooding e.g. return period of the flood, extent and depth of inundation." In general, it is a probability and extent of flooding. The characteristics of terrestrial/hydrological systems play a pivotal part in driving flood risk, e.g. catchment size, geology, landscape, topography and soils by altering the hazard characteristics, which is very strongly alter by human intervention (Kundzewicz *et al.*, 2013). The anthropogenic climate change also alters the hazard event by changing its frequency and /or amount thereby changes the flood risk.

2.1.4 Vulnerability

As revealed by Lavell *et al.* (2012), the concept of vulnerability has been developed as a theme in disaster work since 1970s. However, the definition of vulnerability is often confusing with the definition of risk itself. Blaikie *et al.* (1994) defined vulnerability as the characteristics of a person or group in terms of their capacity to anticipate, cope with, resist, and recover from the impact of a natural hazard. Similarly, IPCC (2001) defined vulnerability as the degree to which a system is susceptible to, or unable to cope with, adverse effect of climate change, including climate variability and extremes. Allen (2006) separated the term vulnerability from hazard, defining vulnerability as a state that exists within a system before it encounters a hazard event. Allen (2006) further clarified that vulnerability is something that exists within systems independently of external hazards. UNISDR (2009) defined vulnerability as the characteristics and circumstances, system or assets that make it susceptible to the damaging effect of a hazard. It is a characteristic of the elements of interest (community, system or asset) which is independent of its

exposure. Vulnerability is the result of diverse historical, social, economic, political, cultural, institutional, natural resources, and environmental conditions and processes (Lavell *et al.*, 2012). Different levels of vulnerability leads to the different levels of damage under similar conditions of exposure to physical events of a given magnitude (Lavell *et al.*, 2012). As discussed, vulnerability is a key factor in disaster losses, yet it is not well accounted for (Handmer *et al.*, 2012). In this study, vulnerability is defined by degree of damage and quantified by damage amount with respect to total property for a hazard event and will be described in detail in later chapter.

2.1.5 Exposure

UNISDR (2009) defined exposure as people, property, system, or other elements present in hazard zones that are thereby subject to potential losses. IPCC (2012) more clearly defined exposure as the presence of people, livelihoods, environmental services and infrastructures, or economic, social, or cultural assets in a place that could be adversely affected by physical events and which, thereby, are subject to potential future harm, loss, or damage. Often exposure is termed as necessary but not sufficient condition for some impact (Handmer *et al.*, 2012).

As stated in IPCC (2012), vulnerability and exposure both are dynamic in nature, varying across temporal and spatial scale, and depend on economic, social, geographic, demographic, cultural, institutional, governance, and environmental factors. Higher exposure and vulnerability led to higher damage at a location. These two are often associated with skew development processes (Handmer *et al.*, 2012) for example development with environmental degradation, rapid and unplanned urbanization etc.

2.2 Classification of floods and flood damage

The previous sections describes broadly flood risks and its components, however to understand floods and its associated risk, the various form of floods and its associated damage type need to be understood. The following sub-sections describe the various types of floods as per their occurrence, extent, and causes. Various flood impact and flood resistant parameters are also described in the following sub-sections.

2.2.1 Types of flooding

Flooding related to rainfall can be broadly divided into large-scale floods due to high discharge in rivers and streams, and local or urban floods that occur due to excessive rainfall that overwhelms local drainage capacity (Bouwer, 2013). Based on the flooding sources and/or causes, floods can be specifically classified into five categories as shown in **Fig. 2.3**.

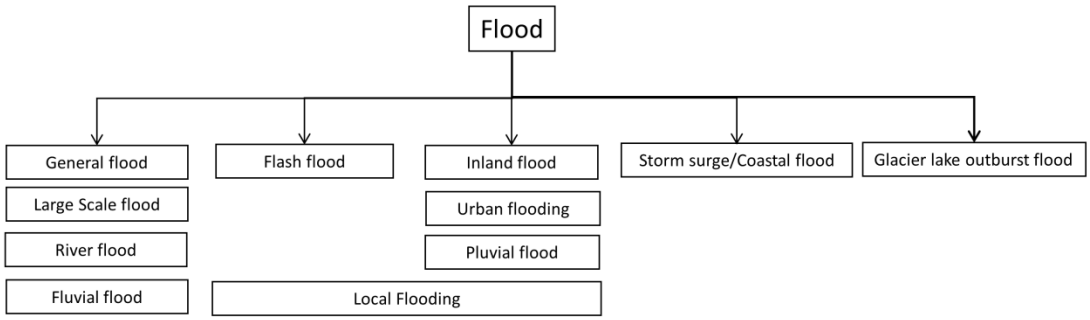

Fig. 2.3 Types of floods based on its source and cause

General floods also referred as large scale floods (river floods or fluvial floods) are the floods caused by overflow of water from the bank of rivers, lake and/or any other water bodies. Very large and devastating in term of people casualties and physical property losses were associated with this type of flood in the past. The 2011 Thai-flood of this kind was an example which has the largest impact on property damage (Haraguchi and Lall, 2013). The total economic damage was estimated about 46.5 billion USD due to this flooding event. Most of the flood damage assessment models so far developed are for general flood damage.

Flash floods are mainly associated with heavy localized rainfall in steep topography. Due to the rapid development of floods in rivers, and hence less time for evacuation, this type of floods often led to high human casualties along with high physical damages. Cross (2001) revealed that small communities are often at high risk in terms of community-wide destruction by flash flood. Flash flood also sometimes occurs after the collapse of natural or artificial reservoir of water. One of the worst examples of this type of flooding was Seti flash flood on 5th May, 2012 in middle Nepal. This

flash flood lasts for only 70 minutes, but killed more than 70 people and had more than 82 million rupees (about 1 million USD) physical losses.

Inland floods often termed as urban flood or pluvial flood occur due to excessive rainfall and overwhelms local drainage capacity (Bouwer, 2013) in relatively flatter slopes. With rapid urbanization with poor drainage facilities led to increase this type of flooding and hence associated with larger physical losses (Kundzewicz *et al.*, 2013). The flood damage in Kochi, Japan in September 1998 (Yamamoto *et al.*, 1999) was largely due to pluvial flood and also the failure of inner drainage system lead to the higher flood damage in 2000 Tokai flood (Ikeda *et al.*, 2007). Many major cities in the world often suffer from this type of flooding. The floods associated with flash flood and inland flooding sometimes combined as local flooding.

Coastal flood is on the coast and lake shores induced by wind. Flood risk in deltaic areas increases because of population growth, economic development, land subsidence, and climatic change impact such as sea-level rise (Moel *et al.*, 2011). There will be a rising threat to potential sea-level rise to the coastal flooding and storm surge in future too (Nicholls, 2004, IPCC, 2012).

Even the nature of glacier lake outburst flood is same as flash flood; the main reason for this type of flooding is breaching of natural glacial lake. Many mountainous regions in the world have threat to glacier lake outburst flood (IPCC, 2012) including Andes, the Caucasus and Central Asia, the Himalayas, North America and the European Alps.

2.2.2 Types of flood damage

Flood damages can be broadly divided into two types: a) direct damage, and b) indirect damage. Direct damages are those which occur due to the physical contact of flood water with humans, property or any other object (Merz *et al.*, 2004); whereas indirect damages are damages which are induced by the direct impacts and may occur in space and time outside the flood event (Merz *et al.*, 2004). Direct damage includes the damage to buildings, economic goods and dykes, loss of crops and livestock in

agriculture, loss of human life, immediate health impact, and contamination of ecological systems (Messner and Meyer, 2005). The costs of direct damages are generally easier to quantify than that of indirect damages. Indirect damages may have impacts on larger time scale also (Merz *et al.*, 2004). Both direct and indirect damages further can be divided into two sub groups: (i) Tangible damage, and (ii) Intangible damage. The broad classification of different types of flood damages is shown in **Fig. 2.4**. Tangible damages are damage to manmade capital or resources flows which can be easily specified in monetary term, whereas intangible damage is the damage to assests which are not traded in a market and are difficult to transfer to monetary values (Merz *et al.*, 2010).

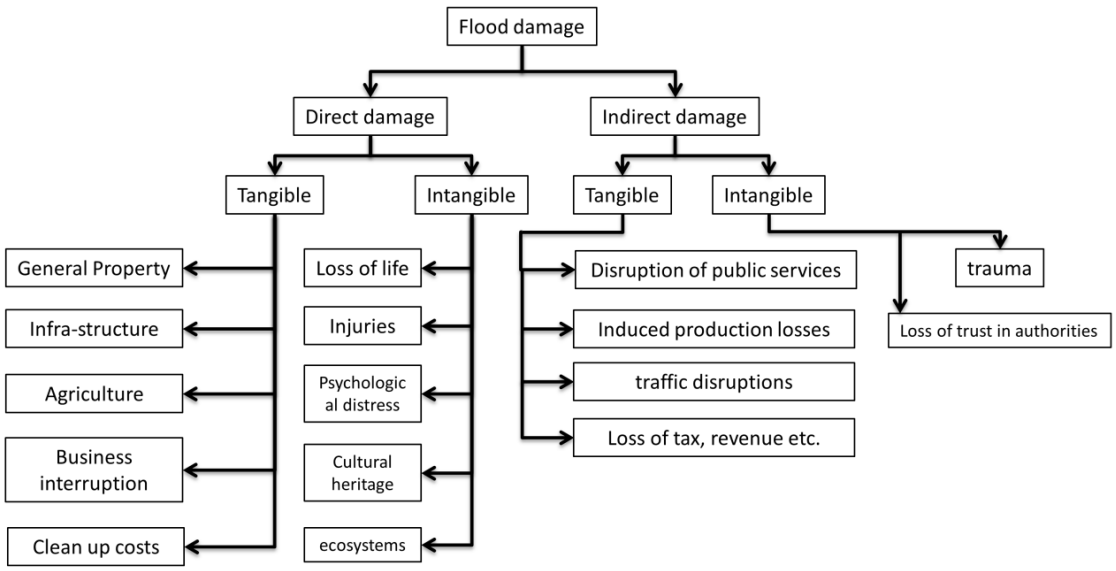

Fig. 2.4 Types of flood damages

Most of the study in damage assessment focuses so far for the estimation of direct tangible damage; hence loss estimates are sometimes referred as lower-bound estimate (Handmer *et al.*, 2012) because other impacts like loss of human lives, cultural heritage, and ecosystem services, are difficult to value and monetized, and thus poorly reflected in estimates of losses (Handmer *et al.*, 2012). However, Bouwer (2013) revealed that the direct tangible economic damage is one of the most important indicators of the intensity of natural hazards and also these costs are most easily quantifiable (Meyer *et al.*, 2013) than other types of damages.

Direct tangible damage can further be classified as per the nature of property: general property damage, infra-structure damage, agricultural damage, business interruption damage, and cleanup costs. Most of the current damage estimating models focuses on general properties (household properties) since current methodologies for estimating infrastructure damage are not well developed (Merz *et al.*, 2010, Jongman, *et al.*, 2012a). Damage to the agricultural sector are frequently much lower than those in urban areas and are neglected in most of the researches (Merz *et al.*, 2010). Business interruption damage cost occur in the area of flooding due to the work interrupted in some business (manufacturing or commercial) houses and also occur if industrial or agricultural production is reduced due to water scarcity (Meyer *et al.*, 2013). The clean-up costs explained the cost incurred in cleaning of debris etc. after the flooding events. The costs for evacuation and rescue operations and reconstruction of flood defenses might be included in cleanup costs.

On the other hand, indirect tangible damages are the damage caused by disruption of different public services, production loss inside the flooded regions, traffic disruptions, and loss of taxes and revenues. Merz *et al.* (2010) revealed that most indirect economic damages at the regional level disappear in a national and even international setting since regional production losses are compensated by production gain in regions outside the flooded area or even outside watershed and hence can be neglected for the national or even larger scale damage assessment.

Even indirect damages are given less attentions, there were few studies reported in this regards as cited in Merz *et al.* (2004) were: the estimation of loss of life (Brown and Graham, 1988, Dekay and Mcclellandl, 1993); psychological damage and stress (Green and Penning-Rowsell, 1988), and indirect monetary damage (Montz, 1992, FEMA, 1998, Olsen *et al.*, 1998).

2.2.3 Sector-wise classification of flood damage

The economic damage also can be divided into different economic sectors since the damage characteristics and its impact are quite different to each other. The

methodologies adopted to assess the damage are also different in each sector of damage. **Figure 2.5** below shows the different economic sectors of damages due to flooding.

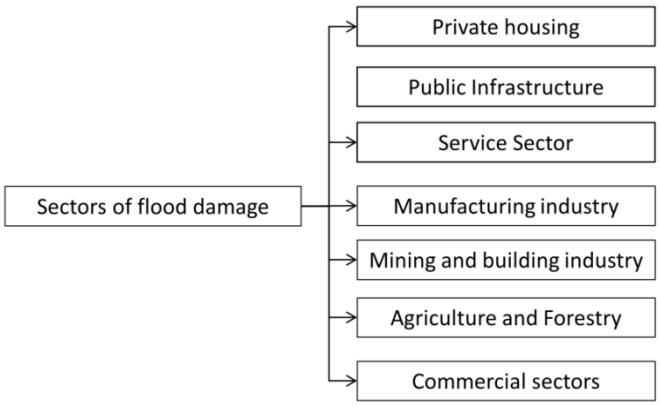

Fig. 2.5 Sector wise classification of economic flood damage

2.2.4 Flood impact and Resistance parameters

Flood damage is largely associated with the characteristics of flood itself usually expressed by its depth, its extent and flow velocity and the object that affected by flood. The former usually termed as flood impact parameters and the latter flood resistant parameters. The impact parameters reflect the specific characteristics of a flood event for the object under study e.g. water depth, duration of flooding, flow velocity, sediment concentration, sediment size, wave and wind action and contamination etc. The resistance parameter depicts the capability or incapability of an object to resist the flood impact, which depend on characteristics of the flood prone object i.e. object size, and type of structure etc. (Merz *et al.*, 2010).

Flood damage to residential building is strongly dependent on the water depth of flood, whereas for damage to agriculture crops, the time of flooding and the duration of the flood are decisive (Förster *et al.*, 2008, Merz *et al.*, 2010). However, most of the damage influencing factors are neglected in damage modelling, since they are very heterogeneous in space and time, difficult to predict, and there is limited information

on their effect (Merz *et al.*, 2010). Still the impact parameter most commonly used for loss estimation is flood depth.

In a broad sense, flood damage and flood risk are dependent on various social and natural factors. Topographical and/or hydrological characteristics (Kundzewicz *et al.*, 2013). Socio-economic factors (Moel *et al.*, 2011, Okazawa *et al.*, 2011, Feyen *et al.*, 2012) play a vital role in driving flood and thereby flood damage as described in the previous sections.

2.3 Previous research on flood risk assessment

A wide range of methodology has been developed and applied for assessing flood damage amount over the last few years. As discussed in chapter 1, direct flood damage estimating models so far developed basically utilizes integration of two different sub-models; first hydrological models to estimate hydrological parameters (e.g. flood velocity, flood duration and flood depth); and second loss models to estimate damage amount in relation to hydrological parameters (Fig 1.1). Following sub-sections briefly describe some widely used hydrological models and loss models.

2.3.1 Hydrological models

There are numerous physical hydrological models exist to estimate different flood parameters, using simple linear interpolation techniques to complex three-dimensional solution of the Saint-Venant equations. A physical based hydrological model normally consists of major hydrologic processes (interception, evapotranspiration, river flow, over land flow, unsaturated zone flow and saturated zone flow) and the governing equations for flow propagation are solved with different numeric techniques (e.g. finite difference methods). Dutta *et al.* (2003) and Kazama *et al.*, (2009) were good examples of flood risk assessment which used distributed hydrological models to estimate different hydrological parameters as an integrated approach. However, these models often suffer from a lack of distributed data to parameterize and validation (Moel *et al.*, 2011, Feyen *et al.*, 2012) and hence often limited to micro scale study. To date a few high resolution inundation models are also available for example Catchment-based Macro-scale Floodplain Model (CaMa-Flood) (Yamazaki *et al.*, 2011) which could be a better tool for meso- to macro-scale flood risk assessment.

Moreover, all hydrological parameters are estimated for a hazard event generally defined by its exceedance probability (return period) with some extreme value statistics. Apel *et al.* (2009) described the various uncertainties in these hydrological models ranging from underlying assumption of the extreme value statistics, various physical properties of the location to calibration and validation of the models.

The detail description of hydrological models are out of scope of the present study and in this study the use of a hydrological model is purposefully eliminated and a statistical relationship between hazard frequency and damage occurrence probability of a location is adopted to evaluate damage risk of a location which will be described in detail on chapter 3.

2.3.2 Loss models

Loss models often termed as vulnerability or susceptibility functions is a central idea for flood damage estimation (Merz *et al.*, 2004). The hydrological parameters (e.g. flood depth) are often relating to the absolute (or relative) damage amount through the use of these loss models. These loss models are generally derived from two ways: (i) based on damage data of past flood records; (ii) based on hypothetical analysis from land cover and land use pattern, types of object and questionnaire survey of residents. As described earlier, the loss models developed so far varies in many senses; with their scale (micro, meso, and macro); with sectors (e.g. residential, commercial, agricultural etc.) and also use of single hazard parameter or multi-hazard parameters. A few studies that use flood depth to evaluate damage with their depth-damage relationship typically for residential building are tabulated in **Table 2.1**.

Other impact parameters are also used, to relate with damage at a location in some studies. Flow velocity which could be a cause of direct damage to building, crops etc. is used in some studies to evaluate damage for example in Kreibich *et al.* (2009), and Pistrika and Jonkman (2009). Some studies include duration of inundation, contamination, debris or sediments concentrations, and frequency of inundation and timing of inundation in their loss model. Damage due to floods not only depends on impact parameters but also to the resistance parameters.

Table 2.1 Loss models that relate damage with single hazard parameter (depth) for residential building

Study	Depth-Damage Relationship	Variables	Scale	Regions
MURL, (2000)	$D = 0.02\ h$	*D*: damage ratio, *h*: water depth in *meter.*	Meso	Germany
Hydrotec, (2001)	$D = 27\sqrt{h}\ /100$	*D*: damage ratio, *h*: water depth in *meter*	Meso	Germany
ICPR, (2001)	$D = (2h^2 + 2h)/100$	*D*: damage ratio, *h*: water depth in *meter*	Meso	Germany
Dutta *et al.*, (2003)	Average depth-damage function for wooden, RCC buidling and residential property seperately	Damage in % and depth in *meter*	Meso	Japan

Few example of loss model that considered different resistant parameters are tabulated in **Table 2.2** (adopted from Merz et al., 2010).

Some loss models uses both multi-hazard and resistant parameters, for example, Flood Loss Estimation Model for the private sectors (FLEMOps) (Apel *et al.*, 2009) calculates the damage ratio at buildings for five classes of inundation depths, three distinct building types and two categories of building quality and can be used in both micro and meso scale.

Since, all above discussed models are generally derived from some past flood events in local scale (usually in municipality level), their temporal and spatial transferability are always questionable. There is still a wide room for improving above loss models so that the uncertainty related to their temporal and spatial transferability can be reduced. The various uncertainties related to both hydrological and loss models are briefly described in the later sections.

Table 2.2 Example of Resistance parameters considering in different flood damage assessments (Adopted from Merz et al., 2010)

Resistance parameter	Selected References
Business sector/use of building	MURL, (2000) ICPR, (2001) FEMA, (2003) Penning-Rowsell *et al.*, (2005) Scawthorn *et al.*, (2006)
Building type	Penning-Rowsell *et al.*, (2005) Büchele *et al.*, (2006) Kreibich and Thieken, (2008)
Building material	Nicholas *et al.*, (2001)
Precaution	Kreibich *et al.*, (2005) Büchele *et al.*, (2006) Kreibich and Thieken, (2008)
Early warning	NRE, (2000) Penning-Rowsell *et al.*, (2005)

2.3.3 Spatial scale of flood damage modeling

The choice of flood risk quantification methodology and their results depend largely on the defined spatial boundary (Apel *et al.*, 2009). As per the size of study area (spatial scale), the flood damage modeling technique can be divided into three categories. (i) Micro scale; (ii) Meso Scale; (iii) Macro-Scale (Messner and Meyer, 2005). As described in Kreibich *et al.*, (2010), in micro-scale analysis, losses are evaluated on an object level, e.g. production sites. In contrast, meso-scale approaches are based on land-use categories, which are connected to particular economic sectors (section 2.1.3) and macro scale approaches are done for national or even bigger spatial scale. The characteristics of each approach are tabulated in **Table 2.3** as described in Messner and Meyer, (2005).

To date, most of the flood damage assessments were reported for micro or meso scale analysis i.e. local municipal level to catchment level. Few examples of these types of models are: ICPR, (2001); Dutta *et al.*, (2003); Glade, (2003); FEMA, (2003); Kelman and Spence, (2004); FLEMOps (Apel *et al.*, 2009); and FLEMOcs (Kreibich *et al.*, 2010).

Table 2.3 Characteristics of micro, meso, and macro scale approaches of flood assessment (Adopted from Messner and Meyer, 2005)

Scale	Research Area	Management Level	Demands on accuracy	Amount of resources required per unit area	Amount of input data required
Micro	Local	Single protection measures	High	High	High
Meso	Regional	Large-scale flood mitigation strategies	Medium	Medium	medium
Macro	(inter)-national	Comprehensive flood mitigation policies	Low	Low	Low

As a macro level study, Hall *et al.* (2005) reported a national scale flood risk assessment methodology with the use of some vulnerability indices to estimate expected annual damage (EAD) in England and Wales. Total damage cost for different return periods across Japan was reported by Kazama *et al.* (2009), which incorporated flood damage data using a physical flood model, and the damage rate was calculated using a national average unit rate method for different land uses. Global scale flood damage assessment models were formulated recently by many researchers. Jongman *et al.* (2012b) calculated the exposed assets as per inundation grid number with specified return period, and Ward *et al.* (2013) calculated flood damage on the basis of stage-damage function and estimated expected annual damage from integral of the area under exceedance probability-impact curve. Winsemius *et al.* (2013) also provided a framework for global river flood risk assessment. Due to the increasing need of national scale and even larger scale flood risk assessment (Winsemius *et al.*, 2013), a macro-scale study will be better choice in this regard. The need of global scale assessment are to compare risks from region to region in order to decide which region deserves the most commitment to the development of risk reduction measures or mitigation processes in present and also to future climate change scenario (Winsemius *et al.*, 2013).

2.3.4 Flood damage assessment for future climate

As discussed earlier, globally flood damages have been increased from a few billion USD per year in 1980s to more than 20 billion USD in 2011 (Kundzewicz *et al.*, 2013). IPCC (2012) also revealed, with high confidence that the economic losses from weather- and climate- related disasters have increased. However, most of the observed

upward trend in flood damage can be attributed to socio-economic factors, such as increase in population and wealth in flood prone areas, as well as the changes in the terrestrial system, such as urbanization and deforestation (Feyen *et al.*, 2012).

IPCC (2012) also focused that future changes in exposure, vulnerability, and climate extremes resulting from natural climate variability, anthropogenic climate change, and socio-economic development can alter the impacts of climate extremes on natural and human system and potential for disaster. To date, there are numerous literatures, regarding the impact of future socio-economic changes and climate changes have been reported. Many of these studies prevailed that due to the warming climate flood risk is expected to increase in many parts of the world (Hirabayashi *et al.*, 2008, 2013). It is likely that the frequency of heavy precipitation or proportional of total rainfall from heavy rainfalls will increase in 21st century over many areas of the globe (Seneviratne *et al.*, 2012), which eventually lead to the higher flood damages. Even with the medium confidence IPCC (2012) mentioned that the projected increase in heavy precipitation would contribute to rain-generated local flooding in some catchments or regions.

Various studies as summarized in Bouwer (2013) had shown that the median increase of projected flood losses is 83% by the year 2040 as compared with the base year 2000. The same study also revealed that smaller scale flood events in urban areas create potentially the largest changes in losses. In Europe, annual damage (6.4 billion Euro) and number of people exposed (200,000) in 1961-1990 are expected to increase about two fold by the 2080s under SREX B2 scenario and about three fold under SREX A2 scenario (Feyen *et al.*, 2012).

From above discussion, we come to know that there is an increasing need of flood risk assessment in current and future, however there are many technical challenges in developing robust risk assessment and damage costing models (Handmer *et al.*, 2012). The quantification of potential future losses is mainly hindered by the lack of a common analytical framework for estimating of natural hazard risk over time (Bouwer, 2013), damage data and its validation technique. The **Table 2.4** below

summarizes the different studies in local, national, continental to global scale for future flood risk so far.

Table 2.4 Studies on future flood risk assessment in different spatial scale

Local Scale Study	Region
1. Schreider *et al.*, (2000)	Australia
2. Morita, (2011)	Japan
3. Pall *et al.*, (2011)	England
4. te Linde *et al.*, (2011)	Rhine basin
5. Ranger *et al.*, (2011)	Mumbai
National scale study	**Country**
1. Choi and Fisher, (2003)	USA
2. Hall *et al.*, (2005)	UK
3. Kazama *et al.*, (2009)	Japan
4. Maaskant *et al.*, (2009)	Netherland
5. Bouwer *et al.*, (2010)	Netherland
6. Mouri *et al.*, (2013)	Japan
Continental scale study	**Region**
1. Lehner *et al.*, (2006)	Europe
2. Douglas, (2009)	Asia
3. Di Baldassarre *et al.*, (2010)	Africa
4. Feyen *et al.*, (2012)	Europe
5. Jongman *et al.*, (2014)	Europe
Global scale study	
1. Hirabayashi *et al.*, (2008)	
2. Okazawa *et al.*, (2011)	
3. Jongman *et al.*, (2012b)	
4. Hirabayashi *et al.*, (2013)	
5. Ward *et al.*, (2013)	

2.4 Uncertainty and limitation of previous flood damage modeling techniques

Uncertainty related to a model outputs can be broadly divided into two types: epistemic uncertainty and aleatory uncertainty. The former is a result of incomplete knowledge of the object of investigation and is related to our ability to understand, measure, and describe the system under study (Apel *et al.*, 2009) and the latter refers to quantities that are inherently variable over time, space, or population of individuals or objects. The flood damage modelling technique so far possesses both type of uncertainties.

IPCC (2012) also revealed that there is a large uncertainty in present flood risk assessment models which limit its use for future projections. The level of uncertainty in risk estimation is largely depend on available information especially flood damage data (Escuder-Bueno *et al.*, 2012). There is a huge scarcity of flood damage data in the world, which always limit the model's calibration and validation in different temporal and spatial scale. Moreover, the present damage recording technique doesn't hold uniform definition of loss components and hence to better understand trend and amount of flood losses, these international loss database should have to be standardized (Handmer *et al.*, 2012). There is a huge gap between damage amount in the existing international damage database and national level database (even found in some developed countries). The total annual national damage records in national damage database are often much larger than that on the international damage database. Not only damage data, but also assets values of a location are not well documented in present. The use replacement value instead of depreciated values of assets in flood damage often produces high variation in true economic damage estimation (ICPR, (2001); Jongman, *et al.*, (2012a)).

The different methodological approaches used in different risk assessment models hinder the understanding of the real cause and effect of flooding. Moreover, current damage models often use single impact factors or resistance factors to estimate the entire damage amount; however damage is a complex outcome of all associated factors and largely depends not only on hazard characteristics but also on many socio-economic dimensions. Meyer *et al.* (2013) focused on use of multi-parameter damage

models that capture the variety of damage influencing parameters, including resistance parameters. Hence, there is a need of huge effort to improve the current understanding of damage modelling approach.

As discussed earlier, the current flood damage assessment models contain a large uncertainty both in hydrological model and loss model. A hydrological model possess uncertainties regarding the extreme value statistics used, stationary and homogeneity of data series, consideration of proper physical properties (e.g. dikes and drainage systems) of the location and calibration and validation of model outputs etc. (Apel *et al.*, 2009). On the other hand, the loss models possess the largest source of uncertainty in the construction of damage curves, the assets values connected to these curves and the larger methodological framework (Merz *et al.*, 2004, Hall *et al.*, 2005, Apel *et al.*, 2009, Moel and Aerts, 2010, Jongman, *et al.*, 2012a). Jongman, *et al.*, (2012a) revealed that the quantitative results of the model outcomes are very sensitive to uncertainty in both depth-damage curve and asset values.

The quantification of potential future losses are hindered more importantly by the lack of a common analytical framework for estimate of natural hazard risk over time (Bouwer, 2013). Due to the largest uncertainties remain in the output of different climate models (GCMs and RCMs), there is large uncertainty in the projected changes in the magnitude and frequency of floods (Kundzewicz *et al.*, 2013) in future and thereby the projected flood damage estimates.

Moreover, most of the studies so far discussed are deterministic in nature but the nature of flood occurrence and its associated damage are rather probabilistic. Wind *et al.* (1999) revealed that most comparable flooding events in terms of flooding volume and inundation area could produce different damage even at a same location. The historical damage record in Japan shows that all low frequency events (larger rainfall) didn't necessarily produce damage, whereas many high frequency events (smaller rainfall) exhibit damages. Mouri *et al.* (2013) showed the change of damage occurrence probability due to hazard frequency and its further dependency on population size of a location. Fukubayashi (2012) calculated expected annual pluvial

flood damage over Japan using a damage occurrence probability function and a damage rate, however proper relation of hazard, vulnerability and exposure could not be well established, and hence not flexible for temporal and spatial transferability.

Because of such large uncertainties and limitations in the present damage modelling technique, their temporal and spatial expansion rarely performed; however there is increasing need of meso to macro scale (global scale) damage assessment of flood risk in current and future condition (Winsemius *et al.*, 2013). Regional and global risk sharing approaches is necessary not only for present but also for future due to the globalization of the world. A large devastating event in a place now widely affects the entire global economy and hinders the whole development process of the world. A robust macro scale flood risk assessment is now indispensable for us for the well beings of all human creatures.

Hence this research is motivated towards the development of macro scale pluvial flood risk assessment model and its application for future climate as well.

3. Development of a Statistical Model for pluvial flood damage assessment

3.1 Introduction

In this study, a novel statistical model for assessment of pluvial flood general property damage has been developed based on the recorded damage data in Japan that are archived in the Ministry of Land, Infrastructure, Transport and Tourism (MLIT) of Government of Japan. The new model can be used for all locations irrespective of their individual characteristics of pluvial flooding, vulnerability and assets values and thereby estimate the area averaged annual damage amount. The most remarkable achievement of this study is the formulation of two functions namely damaged occurrence probability function and damage cost function of a location, which will be further used for assessing the damage amount of a location due a rainfall event. The former function represents the relationship of exceedance probability of rainfall and its corresponding damage probability, and the latter represents the relationship of exceedance probability of rainfall to relative damage cost of a particular location. The new model largely reduces the use of sophisticated hydrological models on one hand and present micro-scale loss models on other hand and hence the model can be a very light and robust tool for decision makers to estimate annual damage for short term planning and to estimate expected annual damage for long term planning with reasonable level of confidence. The new model reduces many uncertainties associated with current state of the art methodologies and can be used in macro level studies in a national level and also can be expanded on to global level. Moreover, this new statistical model considers all daily rainfall events in a year and thereby calculates annual damage, many of which are often neglected by previous models. The previous models often calculate damage using some high return period rainfall values. The limitations regarding previous deterministic approach are eliminated by using the probabilistic approach of damage occurrence. As a macro level study, some readily available data, including population density, elevation, and national gross domestic product (GDP) were used which make this model more flexible to use for future climate scenarios and also extendable to the global scale.

It should be noted that the model is optimized to estimate only general property damage which includes housing, household appliances, depreciable business property, business inventory property, depreciable agriculture/fisheries property, agriculture/fisheries inventory properties. ("Flood damage" or sometimes referred as only "damage").

Following sections describe the model structures, the cascade procedure of damage calculations, model forcing data, calculation of different components of the model, the model outputs and the uncertainty associated with data and methodologies.

3.2 Model structures

The overall model structure can be well explained as in **Fig. 3.1**. Each daily rainfall is characterized by it exceedance probability. In general, an exceedance probability is a probability that an event of specified magnitude will be equaled or exceeded in any defined period of time, on average and generally calculated and expressed as 1 in year.

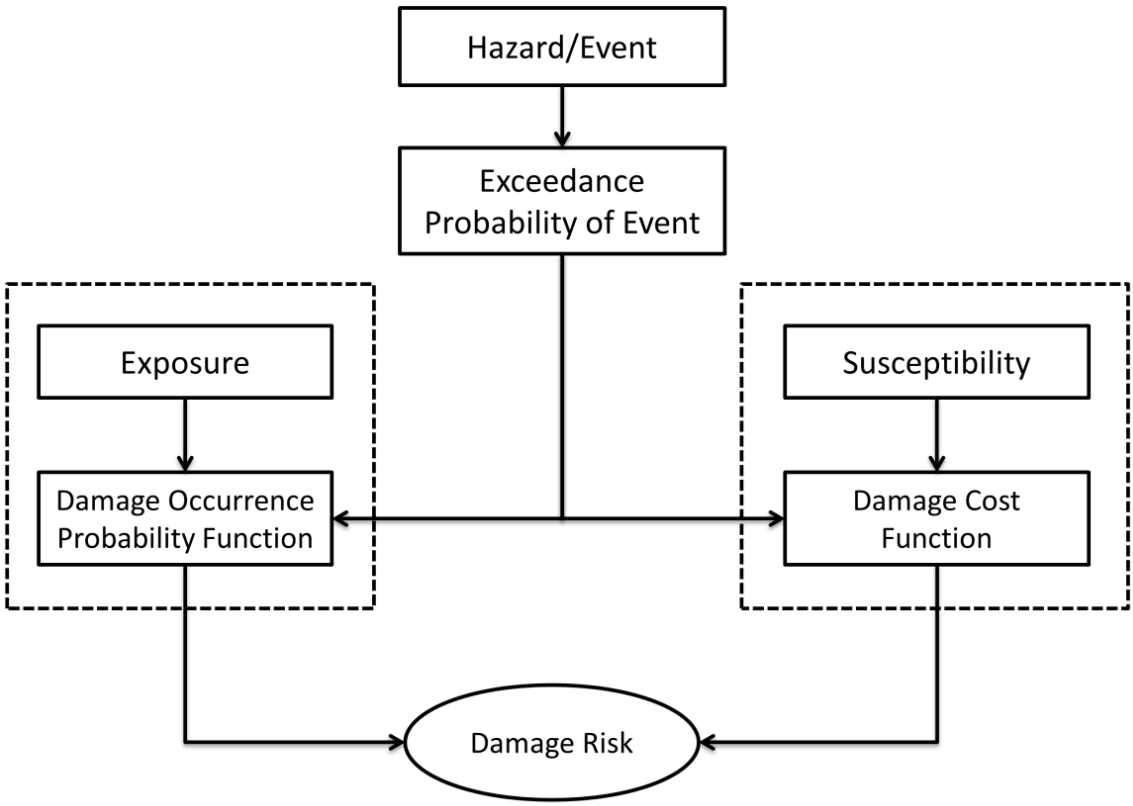

Fig. 3.1 Conceptual model structure

The exceedance probability gives the probability of the daily rainfall of certain amount or higher at a location. Its value is expands from zero to one. The higher value shows high frequency (light in amount) and lower value shows the lower frequency (large in amount) daily rainfall amount at a location. These exceedance probabilities are further relate with the probability of damage occurrence at a location in one hand (referred as damage occurrence probability) and average cost of damage due to this event on the other hand (referred as damage cost function). The division of total risk into two components enhances to judge the contributing factors of risk by defining each risk components independently. The probable cost of damage is then obtained with the product of these two components. The natural and socio-economic dependence of these two components are also evaluated which shows the damage occurrence probability of a location is much dependent on its exposure and average damage cost is dependent on the susceptibility (or vulnerability) of the location.

3.3 Model cascade

The overview of the model cascade or steps of calculation of different components and parameters are shown in **Fig. 3.2**.

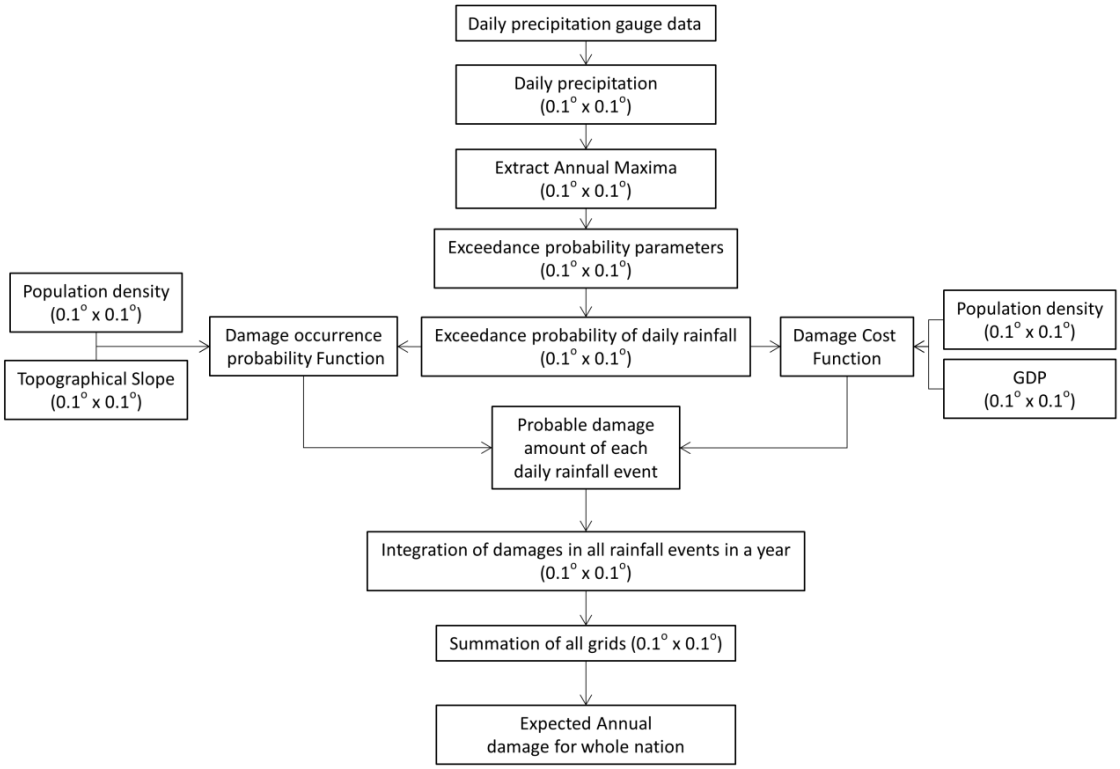

Fig. 3.2 Flowchart showing the main flow of data and models used in this study

The model starts from the preparation of gridded daily precipitation data from point observation and then calculates the exceedance probability parameters for each grid using Gumbel distribution extreme value theory. The newly developed damage occurrence probability function and damage cost function are used to calculate probable damage amount due to daily rainfall at a location based on its population density, topographical slope and GDP. Total national annual damage is then estimated by the summation of all grids for all rainy days in a year. The descriptions of each data and theory related to each steps are described in more details in following sections.

3.4 Model forcing data

Precipitation data is a major external loading dataset used in this model, whereas digital elevation model (DEM) was used as topographical dataset; population and national gross domestic product were used as socio-economic data set to compute various components and sub-models. The damage data of city scale were used from MLIT database. All these data were further converted onto 0.1-deg spatial resolution. A summary of model forcing data is tabulated in **Table 3.1** and briefly described in following sub-sections.

Table 3.1 Summary of model forcing data

Data	Spatial Resolution	Temporal Resolution	Time Span	Source of data	Final Spatial Resolution
Rainfall	Station data	Daily	1976 - 2009	AMeDAS	0.1° x 0.1°
Population	0.5° x 0.5°	Yearly	1993 - 2009	GPWv3	0.1° x 0.1°
Damage	City data	Daily	1993 - 2009	MLIT	0.1° x 0.1°
GDP	National	Yearly	1993 - 2009	IMF	0.1° x 0.1°
Elevation	30 ″ x 30 ″	-	-	GTOPO30	Ave. Max. Slope 0.1° x 0.1°

3.4.1 Precipitation data

Daily precipitation data were used as an external forcing for hazard in this study since it is a strong external loading for pluvial flood (Zhou *et al.*, 2012). Daily precipitation data were obtained from the Auto Meteorological Data Acquisition System (AMeDAS), which covers all areas of Japan at an interval of about 20km on average. Each station of AMeDAS records precipitation and other meteorological data such as temperature, wind velocity etc at every hour. The high density of observation stations and having longer observation period lead us to use AMeDAS dataset. Daily precipitation data for the period 1976-2009 were utilized. Approximately 1300 Japan Meteorological Agency (JMA) rain gauges were sampled, and data were interpolated using the inverse distance method for its simplicity and much appropriate for relatively dense gauge network (Dirks *et al.*, 1998, Yoshimura *et al.*, 2008, Mouri *et al.*, 2013) to assign a value to each grid point on a $0.1^{o} \times 0.1^{o}$ grid. For each 0.1^{o} grid, the surrounding rain gauges were averaged with a weighting of $1/d^2$, where d is the distance from the center of the grid to the rain gauge. The annual maximum daily precipitation data were computed from daily precipitation data for each grid and thereby calculated the exceedance probability of annual maximum daily rainfall, which will be explained in later section. The spatial distribution of annual maximum daily precipitation data for the year 2003 is shown in **Fig. 3.3** as an example.

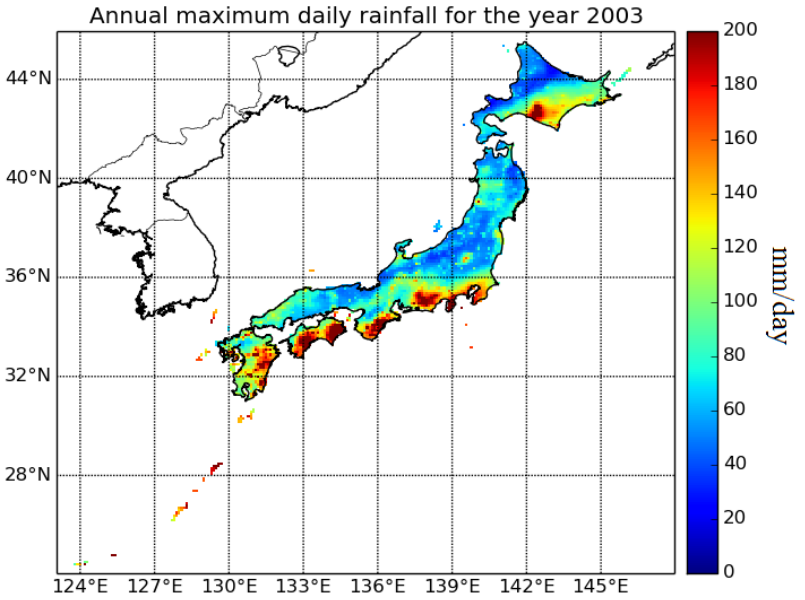

Fig. 3.3 Annual maximum daily rainfall distribution in Japan for the year 2003 in each 0.1˚ grid.

3.4.2 Population density data

Population size of a location has strong influence to flood risk (Kundzewicz *et al.*, 2013). Increasing population in a flood prone zone increases exposure and thereby total damage amount increases with increasing population (Moel *et al.*, 2011, Morita, 2011). The case of Japan is even more serious as a large number of population live in relatively small flood prone area (Kundzewicz *et al.*, 2013). However, population size is not a sole component for determining flood risk. Resident of small cities or towns are often far more vulnerable to disaster than residents of megacities (Cross, 2001). Three population density classes (Low: 0-250 per km^2, Medium: 250-2000 per km^2, and High (>2000 per km^2) were prepared to analyze the damage occurrence and vulnerability in different population density. For this purpose, annual population data for 1993–2009 were used from the Gridded Population of the World, version 3 (GPWv3), and these data were interpolated onto a 0.1º × 0.1º grid. The global data were adjusted based on the Japan national census so that the population of each prefecture was properly given. The prefectural population data were taken from the Statistics Bureau, Ministry of Internal Affairs and Communications (MIC), Government of Japan. Spatial distribution of population in Japan for the year 2003 is shown in **Fig 3.4** as an example.

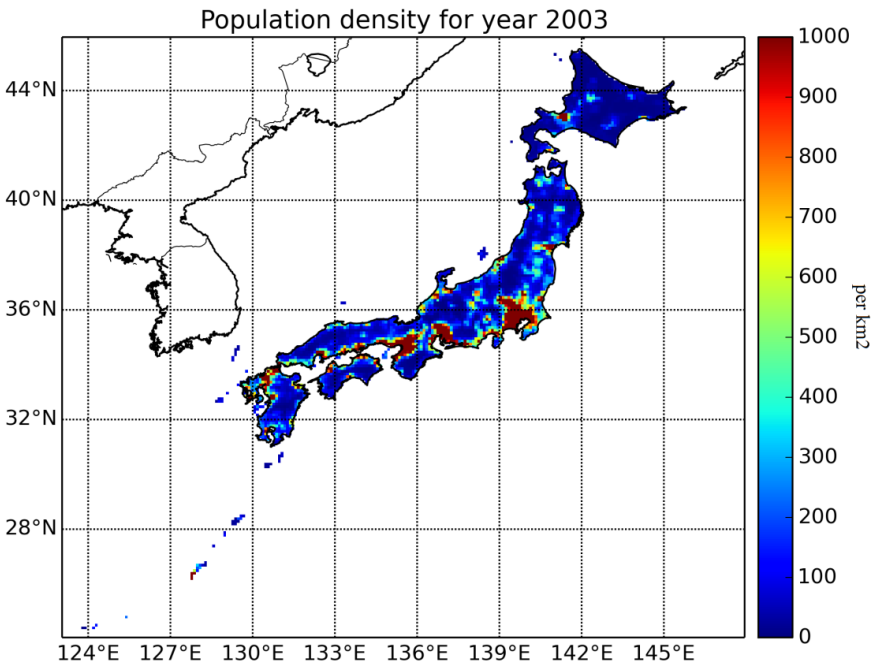

Fig. 3.4 Population density distribution in Japan for the year 2003 in grid of 0.1˚.

3.4.3 Damage data

Damage data are always a critical issue in risk assessment. Lacking of reliable, consistent and comparable data is a major obstacle (Handmer, 2003, Hall *et al.*, 2005, Merz *et al.*, 2010, Handmer *et al.*, 2012, Kundzewicz *et al.*, 2013, Meyer *et al.*, 2013) to formulate a robust methodology and to validate it. Moreover the level of uncertainties in risk estimation will mainly depend on available data (Handmer, 2003, Escuder-Bueno *et al.*, 2012). There are several international flood damage database which archive the flood damage data from all over the world along with duration (start and end date) and location for example EM-DAT, Dartmouth flood observatory, Munich Re and Swiss Re etc. Since all databases have their own criteria of damage recording, local scale small damages (Meyer *et al.*, 2013) and in some cases big damages often were not recorded hence total annual damage recorded in these database are much smaller than that recorded in respective national damage database. An example for the annual total flood damage data recorded in EM-DAT, Dartmouth flood observatory and national database in Japan for the year 1993-2005 are shown in **Fig. 3.5**, which reveals that many small damages were not archived in these international data sources. However such national level damage databases are only available for some developed countries.

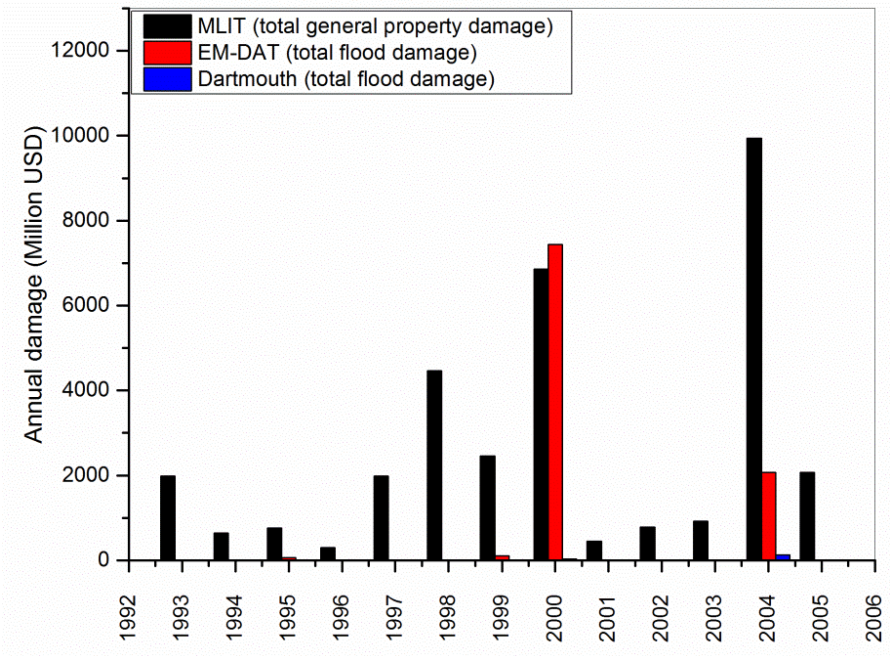

Fig. 3.5 A comparison of total flood damage recording in different databases for Japan

In this study, daily damage data due to pluvial flood for the period 1993–2009 based on economic damage to tangible general property (housing, household appliances, depreciable business property, business inventory property, depreciable agriculture/fisheries property, agriculture/fisheries inventory property) from MLIT's flood disaster statistics were used. The various characteristics of this database are well described in Mouri *et al.*, (2013) and **Table 3.2** which is adopted from Mouri *et al.*, (2013) shows some typical selected flood disaster with other details of floods that archived in MLIT database as an example of database recording methods. These data include the name of the city or town where a disaster happened, type of disaster (Fluvial or Pluvial), type of damaged assets, date of start and end of flooding, and total damage amount.

Table 3.2 MLIT records of floods for some selected events (Adopted from Mouri et al., (2013))

Year	Date of event onset	End of event	Extreme weather event	Region	Cause of flood disaster
1976	7/9/1976	14/9/1976	T7617, heavy rain	Handa-shi, Aichi	Dyke break
1976	7/9/1976	14/9/1976	T7617, heavy rain	Agui-cho, Aichi	Dyke break
1976	7/9/1976	14/9/1976	T7617, heavy rain	Isshiki-cho, Aichi	Inland flooding
1976	7/9/1976	14/9/1976	T7617, heavy rain	Tokoname-shi, Aichi	Overflow stream divided with levee
1976	7/9/1976	14/9/1976	T7617, heavy rain	Miham-cho, Aichi	Overflow stream divided with levee
1976	18/10/1976	21/10/1976	Heavy rain, ocean waves, wind gusts	Noboribetsu-shi, Hokkaido	Overflow stream divided with levee
1976	18/10/1976	21/10/1976	Heavy rain, ocean waves, wind gusts	Monbetsu-cho, Hokkaido	Overflow stream without a levee
1976	19/5/1976	21/5/1976	T7609, heavy rain	Ago-cho Mie	Inland flooding
1976	1/8/1976	16/8/1976	Heavy rain	Yamagata city-owned wholesale market, Yamagata	Flood inundation without a levee

Further disaggregation of these data into temporal and spatial resolution was really a big challenge. For this study, the first day of damage onset was considered the

damage day and total recorded damage amount was given to that single day. These damage data were further interpolated onto the $0.1^{o} \times 0.1^{o}$ grid based on the geometric center of the city (Yoshimura *et al.*, 2008, Mouri *et al.*, 2013). The geometric center of each city was calculated using an address-matching service developed by the Centre for Spatial Information Science, The University of Tokyo (CSIS UT, 2013). Obviously above assumptions for spatial and temporal breakdown of damage data produces some uncertainty. Yoshimura et al. (2008) examined the various criteria of spatial and temporal breakdown of the recorded damage data and found that the above consideration works better for simulating daily damage amount for Japan. Better damage data recording techniques for both spatial and temporal scale are indispensable for developing a robust damage model. Nevertheless area-averaged annual national damages were well calculated by the proposed methodology showing the capability of the proposed model. The total recorded annual pluvial flood general property damage for year in 2003 with gridded distribution is shown in **Fig. 3.6** and **Fig. 3.7** shows the average annual damage recorded for the period 1993-2009 in Japan.

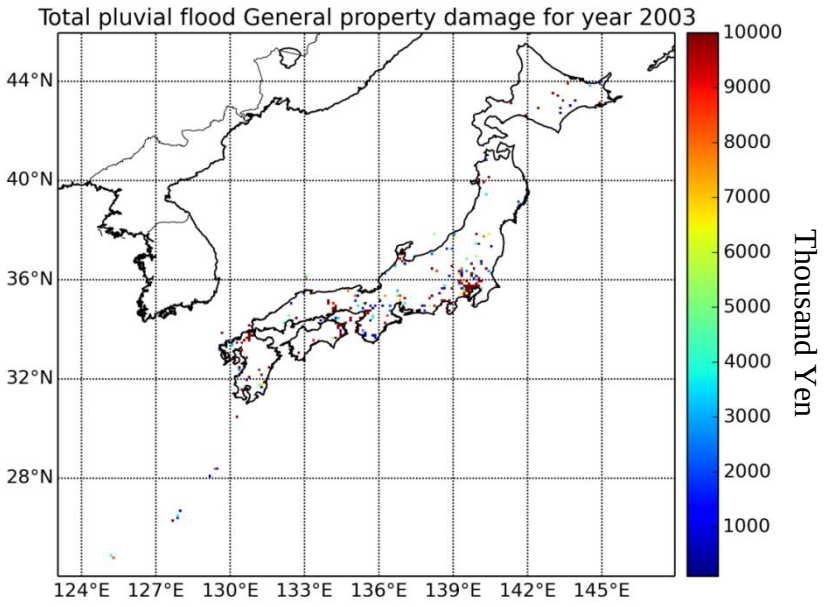

Fig. 3.6 Recorded total pluvial flood damage distribution for the year 2003 in Japan in each grid of 0.1˚

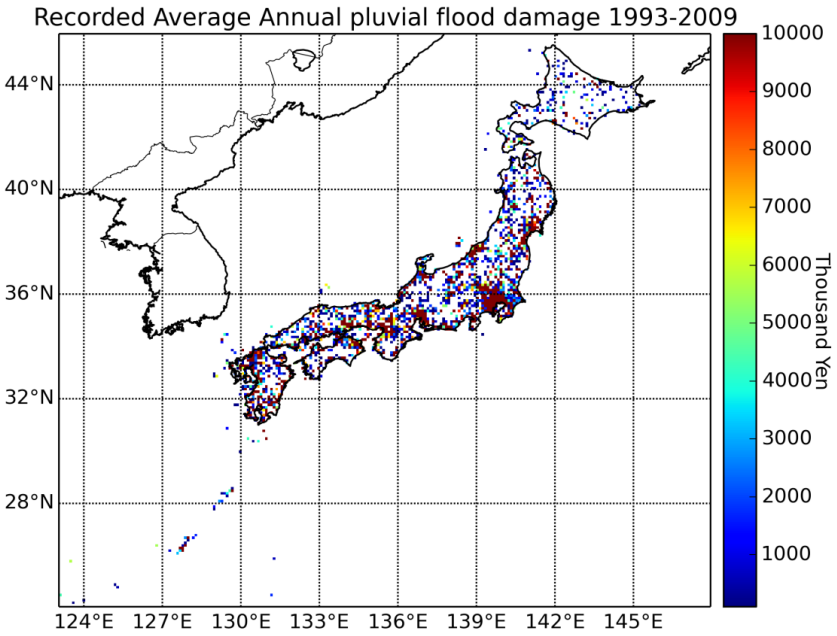

Fig. 3.7 Recorded average annual pluvial flood damage in Japan in each grid of 0.1˚. [1993-2009]

3.4.4 Gross Domestic Product (GDP) data

Assets value is an important component of economic damage assessment. Current models for economic flood damage estimation possess high uncertainties regarding the assets value used (Moel and Aerts, 2010, Jongman, *et al.*, 2012a). For regionalization of a model, integrated assets value which has a uniform definition for all regions is essential. Gross Domestic Product (GDP) can be a powerful candidate in this regard as it can be related with asset value (Jongman, *et al.*, 2012a) of a location.

World Bank defined gross domestic product (GDP) as the measure of the total output of goods and services for final use occurring within the domestic territory of a given country, regardless of the allocation to domestic and foreign claims. More elaborately it is the sum of value added by all resident producers plus any product taxes (less subsidies) not included in the valuation of output. GDP is now very popularly used by all nations, along with major international organization as a value of total products for a specified time period (usually annual) of a nation and regarded as a flux of total assets value of a country.

As a macro-scale study, an aggregated asset value is more appropriate to make it flexible (Merz *et al.*, 2010). GDP data were used as an asset value and macro-economic vulnerability is defined as the ratio of damage to GDP at a location which will be more described in later section. National annual GDP data for 1993–2009 were taken from the International Monetary Fund (IMF) world economic outlook database of April 2012. Prefectural GDP data were taken from the statistics bureau, ministry of internal affairs and communications (MIC), government of Japan. These data, shown in **Fig. 3.8**, reveal that the GDP of each prefecture is approximately proportional to the population (these data are for 2003, but the trend was similar in other years).

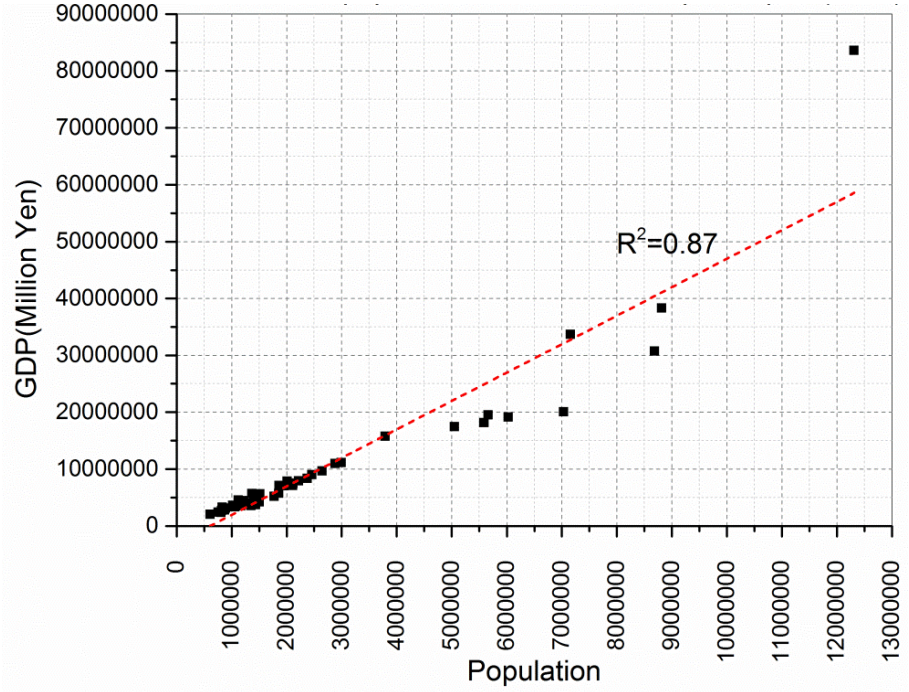

Fig. 3.8 GDP as a function of prefectural population in Japan for the year 2003

The national level annual GDP was hence distributed onto each grid proportional to the grid population (Chan *et al.*, 1998, Jongman, *et al.*, 2012b, Ward *et al.*, 2013) as given in equation (3.1).

$$GDP_{grid} = GDP_{nation} * \frac{Population_{grid}}{Population_{nation}} . \quad \text{..... (3.1)}$$

Figure 3.9 shows the distribution of annual GDP onto each grid of 0.1° x 0.1° for the year 2003.

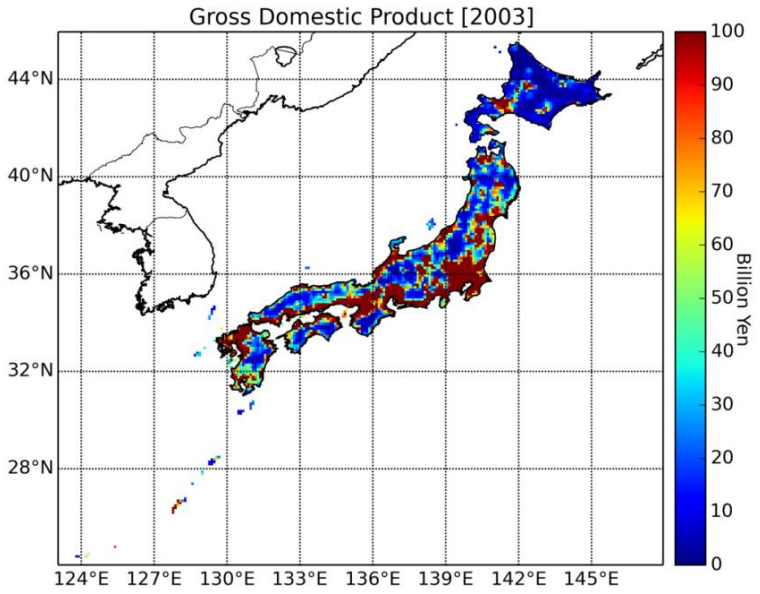

Fig. 3.9 Distribution of gross domestic product in each 0.1˚grid in Japan for the year 2003

3.4.5 Slope Data

Many geological and topographical characteristics contribute to the flood risk (Kundzewicz *et al.*, 2013). Topographical characteristic fundamentally determines the flooding extent, its depth and velocity which ultimately govern flooding impact at a location. In most of the reported methodology (Dutta *et al.*, 2003, Kazama *et al.*, 2009, Zhou *et al.*, 2012) topographical slope was implicitly used in their hydrological model. In some model direct elevation data were also used to evaluate flood water depth as in Feyen et al. (2012). We also evaluated the topographical dependency in damage occurrence at a location. To preserve topographical characteristics in flooding, we use slope as one of the parameter in our damage occurrence probability function which will be described later.

Topographical slope data were prepared based on GTOPO30 datasets (USGS, 1996). GTOPO30 is a global digital elevation model (DEM) with horizontal grid spacing of 30 arc seconds (approximately 1 km). The maximum slope at each grid point was compared with the slope in the surrounding eight grids, and the mean of the maximum slopes in each grid was used for the 0.1-degree grid data. **Figure 3.10** shows the sequence of preparation of average maximum slope data in each 0.1˚ grid from 30 arc

second GTOPO DEM data. First the slope of a 30 arc second grid was computed based on all eight surrounding grids and maximum of all were adopted as a slope of that particular grid (S_{max}) using the relation 3.2.

$$S_{max} = max\left[\frac{E-E_i}{d_i}\ x\ 100\ \%\right] \text{ ---------- (3.2)}$$

Where, E: Elevation of particular grid of concern

E_i: Elevation of surrounding grids (i=1 to 8)

d_i: horizontal distance between each grids centers.

S_{max} : Maximum slope expressed in percentage

The average of all maximum slopes within 0.1° grid was taken for the average maximum slope ($SMAX_{ave}$) for a particular 0.1° grid.

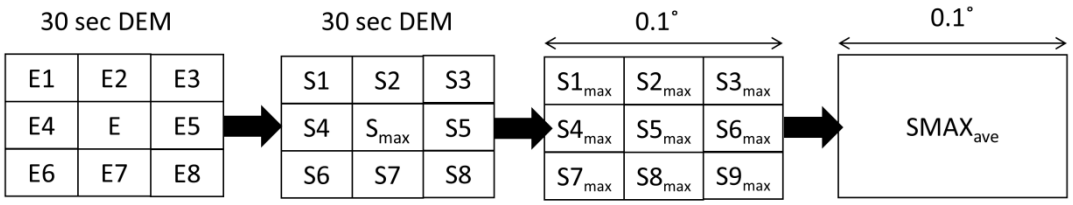

Fig. 3.10 Sequence of average maximum slope calculation

Figure 3.11 shows the slope variations in Japan computed from method described above and used in this study as a topographical slope.

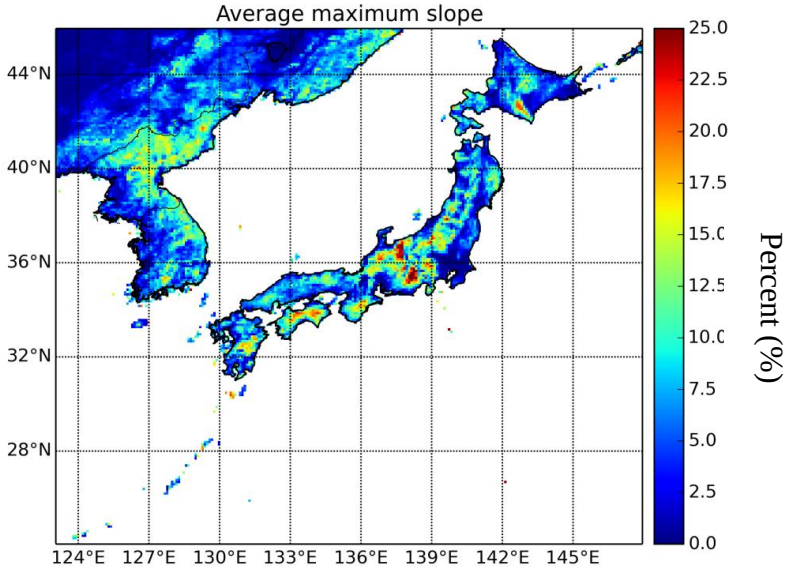

Fig. 3.11 Topographical slope for each 0.1° grid derived from GTOPO30 dataset

3.5 Calculation of model components

This section describes the major components of the statistical models. The hazard function as defined by its exceedance probability, the damage occurrence probability and the damage cost function will be defined and calculation procedure of each will be explained in details in the following sub-sections.

3.5.1 Exceedance Probability of rainfall (w)

The annual maximum daily rainfall was assumed to follow a Gumbel distribution. The annual maximum daily rainfall data for the period 1976-2009 were used to calculate the Gumbel parameters. Gumbel distribution is one of the extreme value statistical distributions which were widely adapted for hydrological events (Yoshimura *et al.*, 2008, Hirabayashi *et al.*, 2013, Mouri *et al.*, 2013, Ward *et al.*, 2013). Mouri *et al.* (2013) showed the applicability of Gumbel distribution for AMeDAS daily precipitation for entire Japan using standard least-square criterion (SLSC). The goodness of fit of Gumbel distribution to annual maximum daily rainfall was evaluated using the Probability Plot Correlation Coefficient (PPCC) (Vogel, 1986, Hirabayashi *et al.*, 2013) test which revealed that about 94% of grids as shown in **Fig. 3.12** have PPCC value greater than the critical PPCC (0.95532 for 34 samples) corresponding to 5% significance level prevailing its applicability.

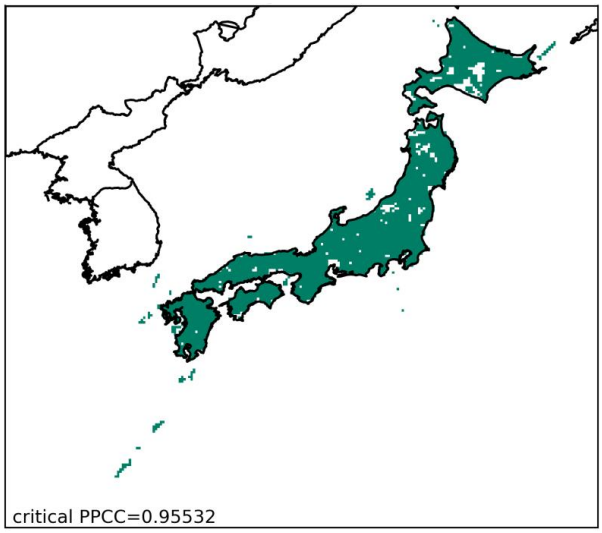

Fig. 3.12 The colors grids showing the goodness of fit for Gumbel distribution for AMeDAS precipitation dataset for Japan using Propbability Plot Correlation Coefficient at 5 % significance level

Based on Gumbel distribution extreme value theory, the cumulative distribution function for the annual maximum daily precipitation, *x*, can be written as:

$F(x) = e^{-exp(-a(x-b))}$ ---------- (3.3)

where *a* and *b* are the Gumbel parameters, calculated based on the annual maximum daily precipitation value from 34 years (1976-2009) precipitation data set for each grid point. The parameters '*a'* is a scale parameter, and was calculated using the relation 3.4. The calculated value of '*a' for* each 0.1° is shown in **Fig. 3.13.**

$a = \frac{\sqrt{6\pi}}{6\sigma}$ ---------- (3.4)

Where, σ is the standard deviation of the annual maximum daily precipitation rate. The unit of parameter *a* is the inverse of precipitation (*day/mm* in our case). The parameter *b* is a location parameter and was calculated using the relation 3.5. Calculated value of *b* for each 0.1° is shown in **Fig. 3.14.**

$b = \mu - \frac{0.5772}{a}$ ---------- (3.5)

Where, μ is the mean annual maximum daily precipitation rate, and *0.5772* is Euler's constant. The unit of parameter *b* is same as precipitation (*mm/day* in our case). The parameters, *a* and *b* are also termed as *Euler-Masheroni* constant.

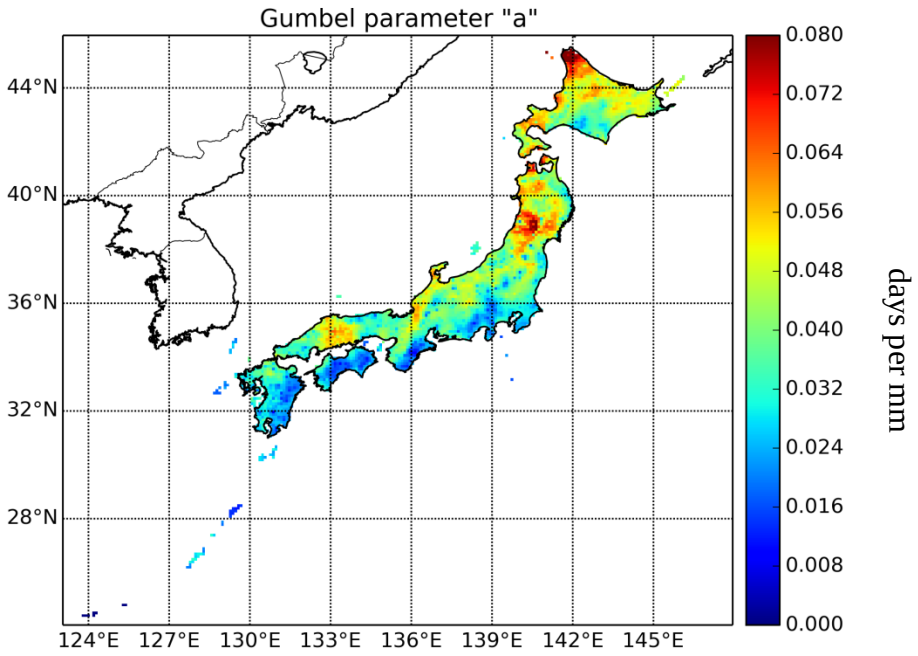

Fig. 3.13 Gumbel parameter "a" in each 0.1° grid over Japan

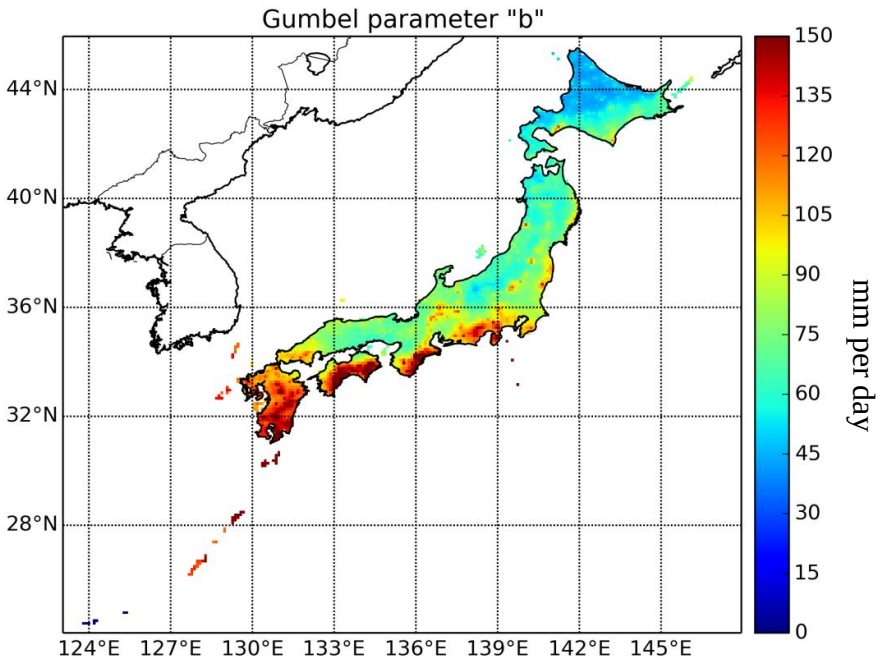

Fig. 3.14 Gumbel parameter "b" in each 0.1˚grid over Japan

The exceedance probability (*w)* of each daily precipitation can be written as equation 3.6.

$w = 1 - F(x)$ ---------- (3.6)

The return period or recurrence interval can be defined by the reciprocal of the exceedance probability and has unit of year as given in equation

$Return\ period\ (T_R) = \frac{1}{w}$ ---------- (3.7)

In this study, all daily rainfall is characterized by its exceedance probability using equation 3.6 hence each grid possesses different amount of daily rainfall with same return period. Defining rainfall by its exceedance probability makes the homogenous condition of rainfall events to every location i.e. grid. **Figure 3.15** shows an example of 50 years return period rainfall in each grid over Japan.

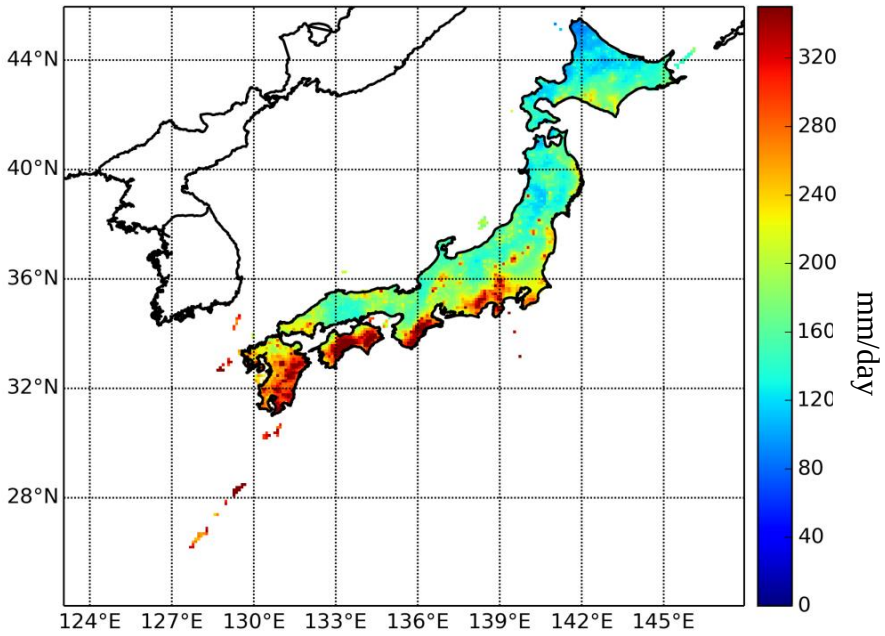

Fig. 3.15 Rainfall of 50 years return period in each grid over Japan

3.5.2 Damage Occurrence Probability (DOP)

The damage occurrence probability (DOP) is the probability of damage at a given location (i.e., grid point) in response to a rainfall event. To evaluate the damage occurrence probability at each location, first some "bins" of exceedance probability bin were prepared. The width of each bins were fixed as per their sensitivity regarding number of daily rainfall events and number of damaging events. Several trials were performed to fix the bin size especially for lower exceedance probability bin. The numbers of damaging events for each bin for three population density classes are shown in **Fig. 3.16.** The figure prevails that the number of damaging events were very few in smaller exceedance probability bin (i.e. higher return period), however the number of damaging events in higher exceedance probability bin (i.e. smaller return period) were surprisingly higher. The higher damaging events irrespective of higher damage amount in frequent rainfall events are often neglected in recent damage modelling methodology however these damages had with as equal cumulative damage amount as the high return period had.

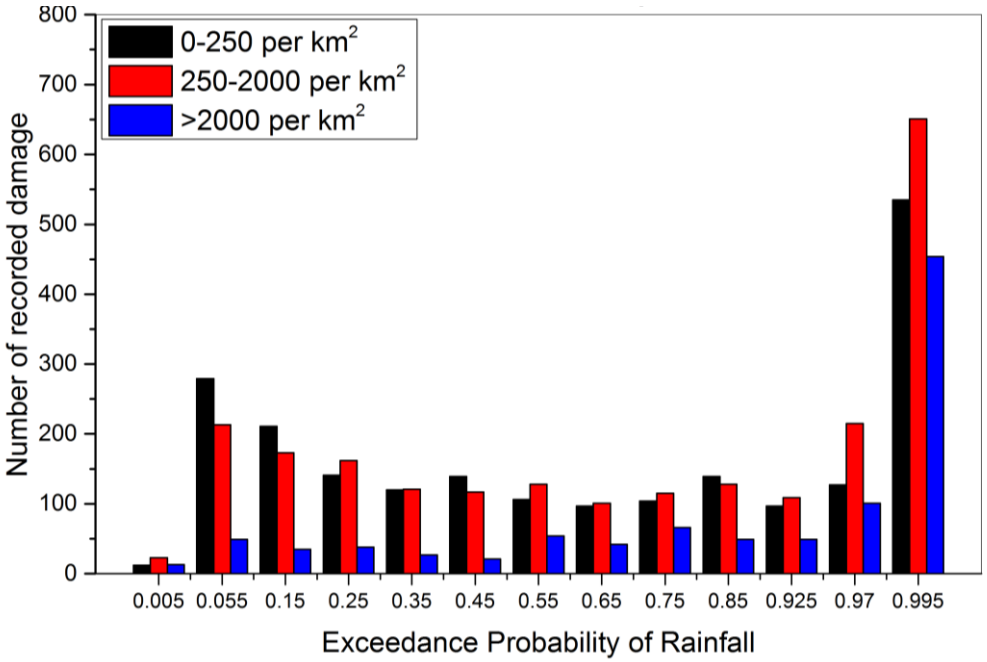

Fig. 3.16 Number of recorded damaging events in each exceedance probability bin for the period 1993-2002 for Japan

The DOP was calculated as a ratio of damaging events (n) in relation to the total number of events (N) within a specified exceedance probability "bins" using recorded damage data as in relation (3.7) below.

$DOP = \frac{n}{N}$ ---------- (3.7)

3.5.2.1 Damage occurrence probability in different population density class

Three population density classes (Low: 0-250 per km^2, Medium: 250-2000 per km^2, and High: > 2000 per km^2) were prepared to evaluate the dependency of population density and damage occurrence probability at a location due to a daily rainfall event using relation 3.7. The recorded damage at each grid for the years 1993-2002 were used to evaluate damage occurrence probability. The calculated damage occurrence probability in all exceedance probability bins along with the total number of events and total damaging events for population density greater than 2000/km^2 is shown in **Table 3.3**. For other population density classes, please refer to annexes.

Table 3.3 Calculation of DOP for population density > 2000 km^{-2}

Exceedance probability bins		Mean Value	Dam Day	Total event days	*DOP*
0	0.01	0.005	**13**	**17**	0.76470588
0.010	0.1	0.055	**49**	**99**	0.49494949
0.1	0.2	0.15	**35**	**125**	0.28000000
0.2	0.3	0.25	**38**	**123**	0.30894309
0.3	0.4	0.35	**27**	**122**	0.22131148
0.4	0.5	0.45	**21**	**176**	0.11931818
0.5	0.6	0.55	**54**	**266**	0.20300752
0.6	0.7	0.65	**42**	**330**	0.12727273
0.7	0.8	0.75	**66**	**597**	0.11055276
0.8	0.9	0.85	**49**	**1076**	0.04553903
0.9	0.95	0.925	**49**	**1305**	0.03754789
0.95	0.99	0.97	**101**	**3795**	0.02661397
0.99	1	0.995	**454**	**83182**	0.00545791

The Damage Occurrence Probability as a function of exceedance probability of daily rainfall for all three population density class is shown in **Fig. 3.17.** The figure prevailed that the higher population density had higher damage occurrence probability and smaller population density area had smaller damage occurrence probability. Obviously, lower exceedance probability (i.e. high return period) had larger damage occurrence probability than higher exceedance probability had. The figure clearly shows the dependency of damage occurrence probability on the exposure of a location.

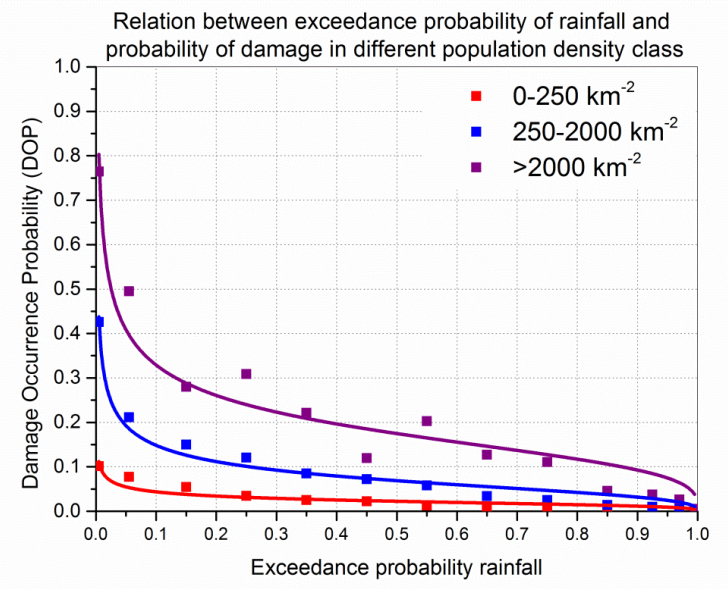

Fig. 3.17 The damage occurrence probability as a function of the exceedance probability of rainfall for different population density

3.5.2.2 Damage occurrence probability in different topographical slopes

Since topographical slopes have strong influence on drainage of water from a location and it can contributes to the pluvial flooding. The relationship of damage occurrence probability and topographical slopes were analysed for all population density classes based on the damage recording data for the period 1993-2002 in each grid. For this at least three topographical slope sub-classes were prepared based on the available data. Different slope sub-classes for each population density class were prepared to manage the number of damaging event. For example, high population density class was subdivided into three slope sub-classes (0-0.5%), (0.5-1%) and (1-25%) which belong only 8 (out of 9), 3 (out of 5), and 2 (out of 5) number of damaging events produces DOP of 0.889, 0.600, and 0.400 respectively. Some uncertainties related to small number of data remains especially for this bin. The size of lower exceedance probability bin was optimized so that it produced better results in both calibration and validation period. **Figure 3.18** shows an example topographical dependency for high population density class with different slope sub-classes. The figure prevail that lower topographical slope exhibits higher damage occurrence probability perhaps due to the poor natural drainage of water. For slopes with gradients greater than 25%, no damage was recorded (even in populated areas), perhaps due to the higher gradients, no pluvial flooding occurs at least for the evaluation periods.

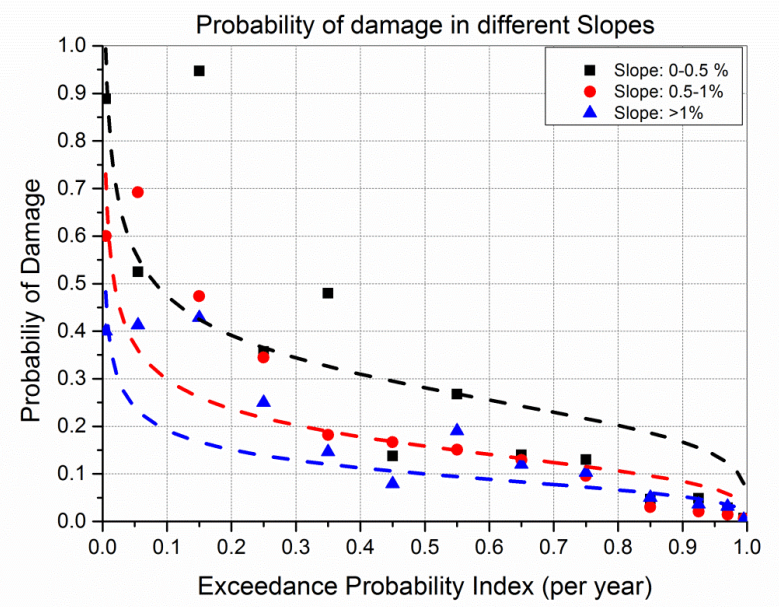

Fig. 3.18 The damage occurrence probability as a function of the exceedance probability of rainfall for different topographical slope classes for population density > 2000 km^{-2}

3.5.2.3 Functions for damage occurrence probability

We implemented a multi-regression fitting algorithm for the damage occurrence probability as a function of exceedance probability (w) and the topographical slope (S) for different population density classes to produce an equation for damage occurrence probability as given in equation (3.8). For slope higher than 25%, no probability of damage presumed.

$$\left.\begin{aligned} DOP(w,S) &= e^{c\,ln\left(\frac{1}{w}-1\right)+d*(S\ in\ \%)+d'} \quad for\ S<25\ \% \\ DOP(w,S) &= 0 \quad for\ S \geq 25\ \% \end{aligned}\right\} \text{---------- (3.8)}$$

The parameters c, d, and d' in the above relationship were computed for all population density classes using damage data for the period 1993-2002 and equation (3.8). The calibration of these parameters was performed to produce the reasonable national annual damage during 1993-2002. The calibrated parameter values are tabulated in **Table 3.4**. The range of DOP is obviously from zero to one as a probability of an event.

Table 3.4 Damage occurrence parameter values for Japan in all population density classes

Parameter value for the DOP functions for Japan					
Level	Population Density	c	d	d'	R^2
Low Population density	0-250 km^{-2}	0.55	-0.01100	-4.1218	0.56
Medium Pop. Density	250-2000 km^{-2}	0.52	-0.01194	-2.8861	0.54
High Pop. Density	> 2000 km^{-2}	0.40	-0.04374	-1.7125	0.72

3.5.3 Damage Cost Function

The damage cost function describes the degree of damage associated with each daily rainfall event in this study and hence also can be termed as vulnerability. As described earlier the most common way of estimating direct damage amount so far was the use of depth-damage functions. The depth-damage function shows the relationship between flood depth and relative damage associated with it, but total damage amount due to a flood event is not only depended on water depth but also other factors like flow velocity, duration of inundation, sediment concentration etc. (Merz *et al.*, 2004, Kundzewicz *et al.*, 2013). The resistance parameters (type, size, shape and property of objects) (Kreibich *et al.*, 2010) and level of preparedness of the society (Merz *et al.*,

2004) also determines the degree of damage. Another main issue related to depth-damage function is its spatial and temporal non-transferability especially for national level and global level risk assessment, because they were often developed from local municipality level or catchment level. Also the asset value at a location always creates a large uncertainty and largely depends upon various building characteristic. In this study, we introduce a damage cost function which relates the exceedance probability of rainfall to the average damage per GDP (DpG) in each population density class. The GDP was taken as asset value which indicates assets irrespective of the individual characteristics of a location and hence widen its application to all regions.

For this we prepared exceedance probability bins and mean DpG in each bin with different damaging events were evaluated for period 1993-2002 and for all population classes. Damage per GDP value in each bin showed large biases with each other as seen as box plot in **Fig. 3.19** for low population density class. The lower and higher end of box gives the 25th and 75th percentile value of data, whereas red bar within each box shows the median value of the data series within each bin. The larger deviation in each bin is shown by whisker plots (dotted line) which shows the range of 1.5 times of inner quartile. The green line joins the mean value of DpG in each bin.

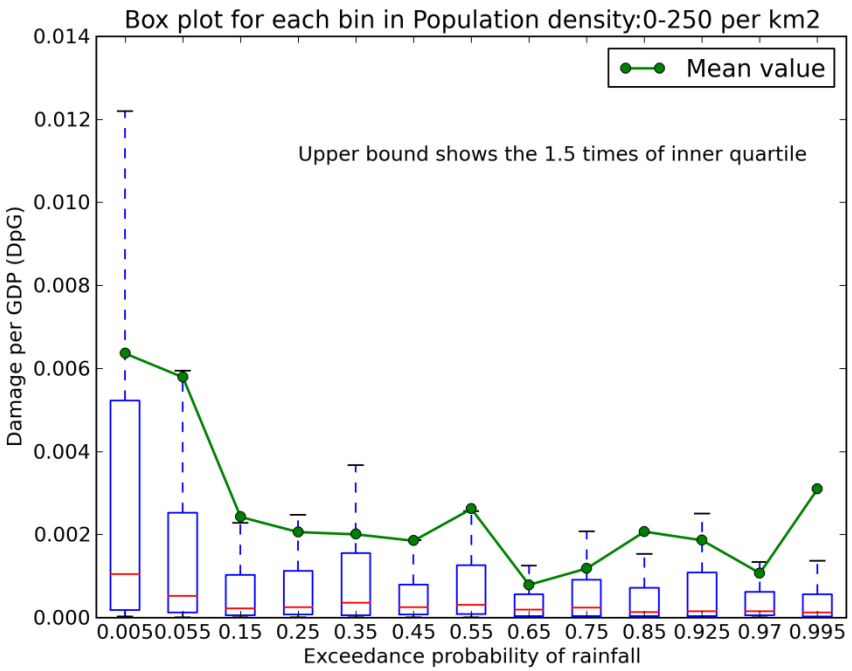

Fig. 3.19 Distribution of DpG in each exceedance probability bin for low population density class.

The **Fig 3.19** prevailed that there is a large deviation of damaging value with respect to its property even with similar hazard events. This uncertainty is partly due to the size of the bins itself (i.e. methodological biases), which constitute a large variation of hazard frequency, and partly due to the large uncertainty in damage amount even with same hazard event at a location practically. Moreover, the mean value of damage per GDP is evaluated very high than its corresponding median value showing that these as more affected by the largest few damaging events. The similar relationship for medium population density and high population density class is shown in **Fig. 3.20.** The mean DpG values for all population density class in each exceedance probability bin are tabulated in **Table 3.5.**

Table 3.5 Mean DpG values in each exceedance probability bin for all three populations density classes.

Exceedance Probability bins		Mean Value	Mean DpG in different population density class		
			Low	Medium	High
0	0.01	0.005	0.00636400	0.00272500	0.00475900
0.01	0.1	0.055	0.00579000	0.00147600	0.00042400
0.1	0.2	0.15	0.00242638	0.00401447	0.00021910
0.2	0.3	0.25	0.00206100	0.00056600	0.00032900
0.3	0.4	0.35	0.00200800	0.00090900	0.00008700
0.4	0.5	0.45	0.00185200	0.00037400	0.00005600
0.5	0.6	0.55	0.00262100	0.00126400	0.00007100
0.6	0.7	0.65	0.00079100	0.00044300	0.00004000
0.7	0.8	0.75	0.00118500	0.00049400	0.00007900
0.8	0.9	0.85	0.00207200	0.00040000	0.00004800
0.9	0.95	0.925	0.00186400	0.00048000	0.00024600
0.95	0.99	0.97	0.00107300	0.00069000	0.00021400
0.99	1	0.995	0.00309800	0.00037600	0.00010500

We adopted inverse power law to relate exceedance probability of rainfall (w) and damage per GDP (DpG) for mean, 90th percentile and 10th percentile DpG for each population density class as given in relation (3.9).

$DpG = p * w^{-q}$ ---------- (3.9)

Where, the parameters p and q are computed from historical data [1993-2002] for all three (mean, 90th, and 10th percentile) with least square curve fitting technique and tabulated in **Table 3.6**. The relation of exceedance probability to the mean DpG is shown in **Fig. 3.21**.

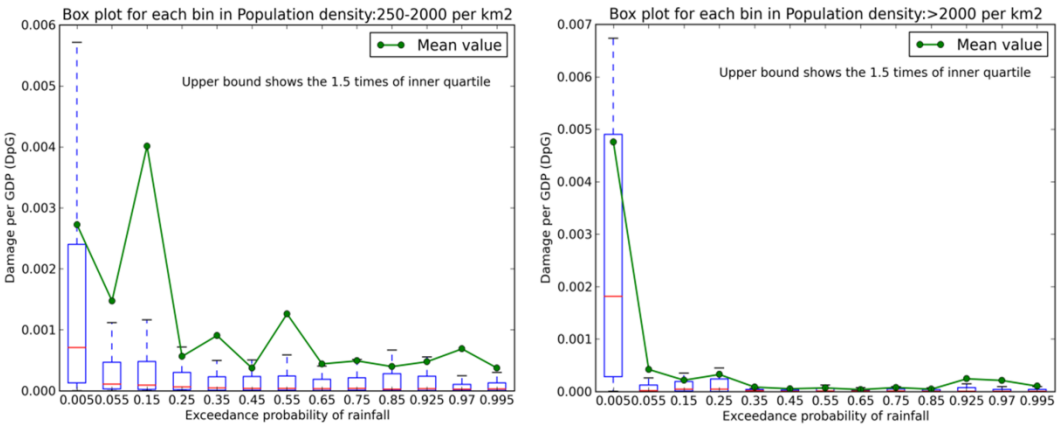

Fig. 3.20 Distribution of DpG in each exceedance probability bin for medium population density class (left) and high population density class (right)

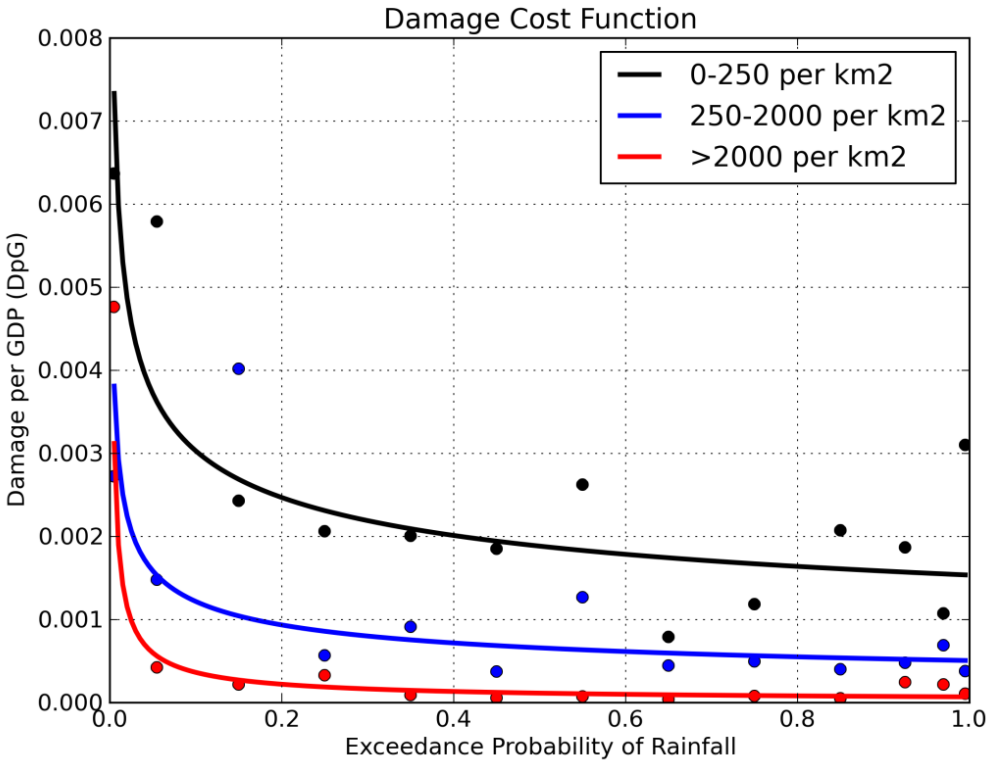

Fig. 3.21 The damage cost function for different population density classes as a function of the exceedance probability of rainfall derived by using mean *DpG*

Table 3.6 The value of damage cost function parameters for different population density class in Japan

Population density	p			q			R^2		
percentile	90th	Mean	10th	90th	Mean	10th	90th	Mean	**10th**
0-250 km^{-2}	0.002400	0.001535	0.000012873	0.409	0.295	0.355	0.85	0.56	**0.85**
250-2000 km^{-2}	0.0006074	0.000510	0.000002465	0.483	0.381	0.473	0.93	0.54	**0.93**
>2000 km^{-2}	0.0001642	0.000070	0.000000377	0.586	0.720	0.968	0.61	0.72	**0.70**

3.6 Annual damage and expected annual damage

The annual damage is calculated from the sum of the daily damage value due to each daily rainfall event in a year, as simply shown in relation (3.10).

$$Annual\ loss\ of\ each\ grid\ = \sum_{1}^{365} DOP(w_i,S)\ DpG(w_i)\ GDP \text{ ------- (3.10)}$$

The DOP and DpG (mean) for each rainfall event are calculated using equations (3.8) and (3.9) for each grid, and the summation of the damage from all daily rainfall events during one year is taken as the annual loss for the grid point as in equation (3.10). The summation of damage from all grids over Japan gives the annual national damage due to pluvial flood inundation. Since, the damage varies temporally and spatially, and stochastic nature of the damage at a location due to same type of hazard, Expected Annual Damage (EAD) seems to be a more appropriate representative value. An EAD is simply an average value of an annual series for a period. Moreover use of 90th percentile and 10th percentile DpG gives the highest and lowest limit of the annual damage which provides 80% probable range of estimated annual damage.

3.7 Calibration and Validation of the model

The parameters in the DOP and the damage cost function were first computed using the damage data for 1993–2002. Damage data for 2003–2009 were used for validation purpose. Only DOP parameters were calibrated during the fine tuning process to evaluate better annual damage variation and expected damage during the period. The average annual damage and the annual distribution were observed for calibration of the DOP parameters.

3.8 Evaluation of the model in Japan

3.8.1 Annual variation of pluvial flood damage

The results of proposed model is evaluated by its capability to produce the annual total national damage and expected annual damage in both calibration and validation period using damage occurrence probability functions and damage cost function with mean DpG. Along with total national damage, total annual damage for all three population density classes are also evaluated. **Figure 3.22 (a), (b),** and **(c)** shows the annual variation of total calculated damage within low, medium and high population density class respectively along with recorded damage variation. Whereas; **Fig. 3.22 (d)** shows the annual variation of total national pluvial flood damage (recorded and calculated). The figures also show the highest and lowest range of estimated damage by the use of 90^{th} and 10^{th} percentile DpG parameters respectively by shaded area. The annual variation in the calculated damage compared with the actual variation in damage shows good agreement in most years, except for 1997 (in low population density) and 1998 (medium population density class). As parameter values are generated using spatial and temporal averaging, the large localised damage in some grids may have been underestimated.

The largest recorded damage in 1998 (as shown in figure 3.22 (b) and (d)) was due to the Kochi flood on 24 September 1998; however, as Iwasada *et al.* (1999) pointed out, the inundation of the Kochi flood resulted from overflowing water from a part of the Kasumi Levee (a traditional Japanese discontinuous levee) along the Kokubu river. This means that this particular inundation was unexpected, given the existing flood-mitigation measures. Thus, some of the recorded damage in pluvial flooding may be from river flooding and may therefore be over-recorded. The annual variation in the total damage during the validation period shows good agreement with the recorded data, which may be due to the absence of any event causing extensive damage in this time period in a particular grid. However, maximum three calculated annual damage were outside the 80 % probable range in all four cases in 17 years period, which justified the result statistically.

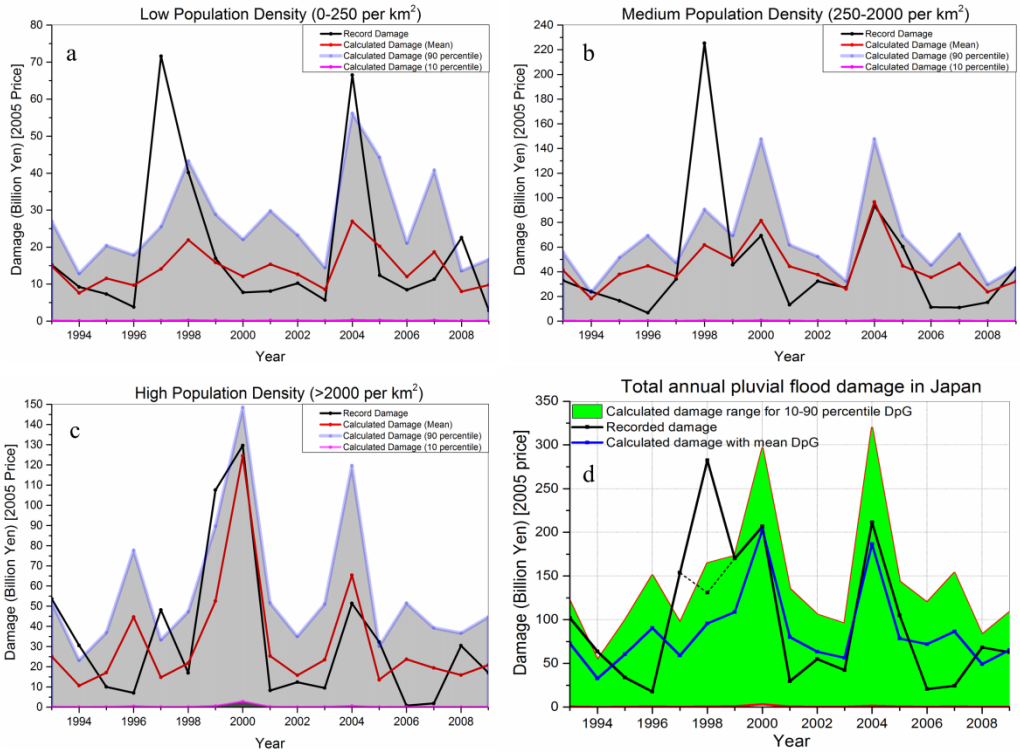

Fig. 3.22 Total annual pluvial flood damage variation in (a) low population density class, (b) medium population density class, (c) high population density class, and (d) whole nation. The period 1993-2002 was used for calibration, and 2003-2009 for validation. The dotted line for 1997-1999 in (d) shows the highest recorded damage excluding the Kochi flood in 1998. The shaded area shows the 80% probable range of damage estimation. The data were normalized to 2005 levels.

3.8.2 Expected Annual Damage (EAD)

Expected annual damage is an average annual damage for a period, which is usually taken as a single value to estimate flood damage due to large uncertainty of annual flood damage. This value is generally used for comparison of flood damage intensity of various periods and also helpful for decision makers to make a decision of flood defense planning. Proper estimate of this value is also an important task in flood damage assessment. We evaluated proposed model output by comparing expected annual damage and recorded average annual damage in both calibration and validation period. **Table 3.7** shows a summary of outputs. The computed expected annual national damage (with the financial costs normalised to 2005 levels) during the calibration period 1993–2002 was 94 billion yen, which is slightly lower than the recorded average annual damage over this period (111 billion yen). Computation of

the expected annual damage for 2003–2009 using this method gave 84 billion yen, slightly higher than the recorded average damage in this period (76 billion yen).

Table 3.7 Comparison of calculated and recorded pluvial flood damage for general properties during calibration and validation period

Period	Recorded Average Annual damage (billion yen)	Expected Annual damage (billion yen)	Remarks
1993-2002	111	94	Calibration
2003-2009	76	84	Validation
1993-2009	97	90	Entire

3.8.3 Sensitivity of model output in different horizontal resolution

The sensitivity of model result due to different horizontal resolution input forcing was also evaluated. The annual variation of total national damage due to the use of 20 km and 60 km resolution AMeDAS precipitation data along with 0.1° data are shown in **Fig. 3.23**. The figure reveals that the model has very low sensitivity towards the horizontal resolution. [It should be noted that the final resolution to calculate the national damage is again from the 0.1° horizontal grids, which were prepared with interpolation of 20- and 60 km resolution data.]

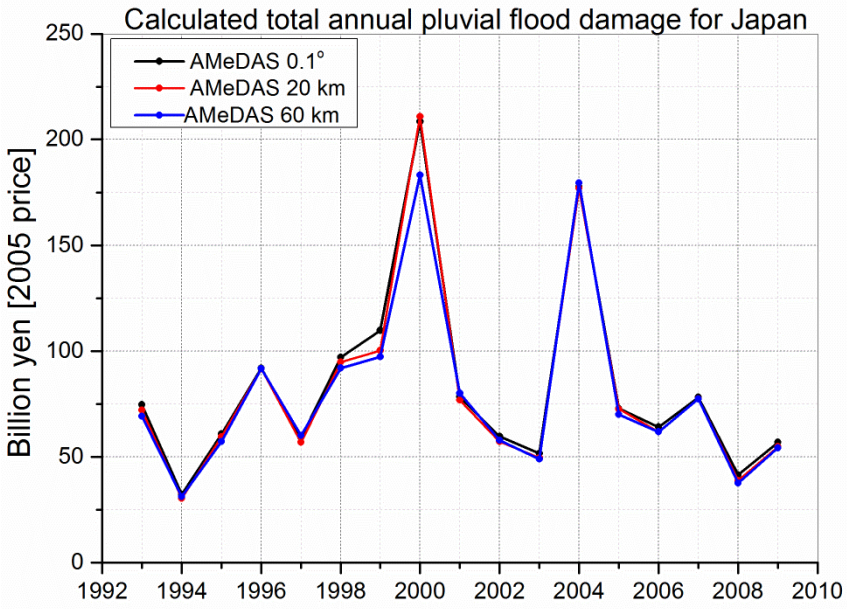

Fig. 3.23 Total national annual damage variation with precipitation forcing of three different horizontal resolutions.

3.8.4 Seasonal variation of pluvial flood damage

Average monthly damage for the period 1993-2009 were calculated and compared with the historical recorded average monthly damage through the same period in Japan. **Figure 3.24** shows the recorded and calculated average monthly pluvial flood damage which shows that the model has nicely captured the variation of average monthly damage though there seems some positive bias with lower values and negative bias with higher values.

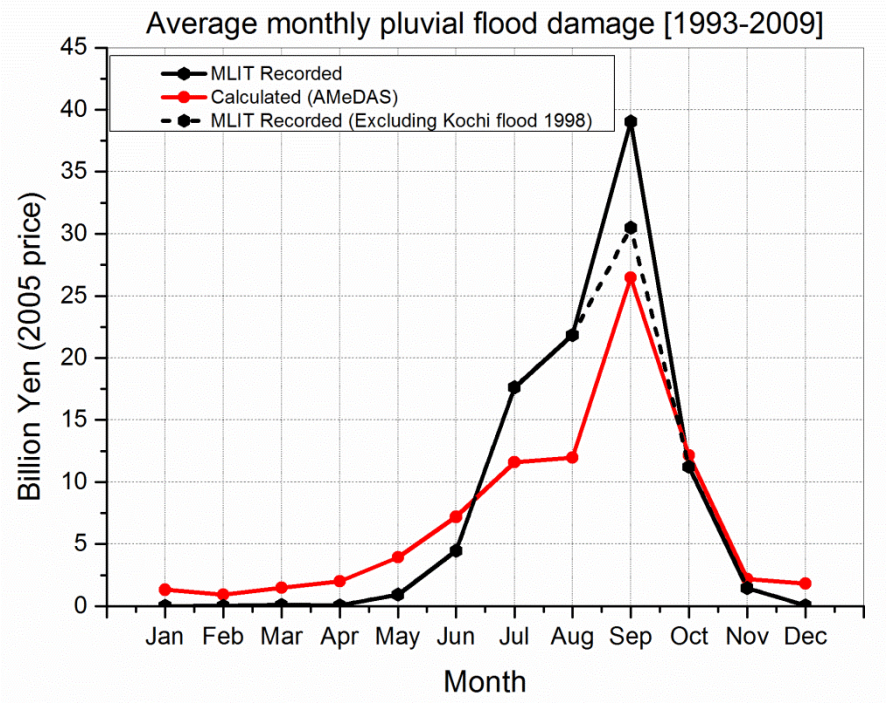

Fig. 3.24 Average monthly pluvial flood damage variation for entire Japan. Estimated average monthly variation well matched with recorded.

The positive bias during the period of low record of damage data is obvious since the model calculated damage for all rainfall events via its probability and accumulate to estimate annual damage for which the model is originally designed. Nevertheless, capability to estimate monthly variation of damage will useful to assess the future seasonal change due to anthropogenic climate change.

3.9 Spatial Distribution pluvial flood damage and damage per GDP in Japan

The formulation of damage occurrence probability function and damage cost function further use to calculate the spatial distribution of the expected annual damage and expected annual damage per GDP for the period 1993–2009, as shown in **Fig. 3.25**

and **Fig. 3.26**, respectively, using equations (3.8), (3.9), and (3.10). The absolute expected annual damage distribution shows very large damage in big city areas, particularly Tokyo, Osaka, Nagoya, and Niigata, which is related to the large population density and hence property concentration in flat land areas. However, the spatial distribution of the average damage per GDP shows an inverse trend. In general, scattered small towns have higher damage per GDP than do big cities, perhaps due to the lower GDP and less preparedness.

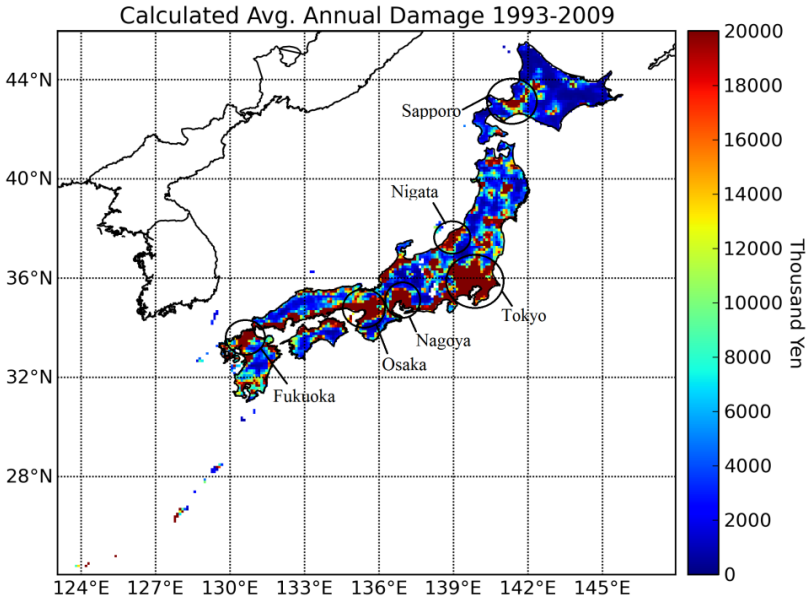

Fig. 3.25 Spatial distribution of expected annual damage per 0.1˚ grid [1993-2009] over Japan. More highly populated areas had higher absolute damage value.

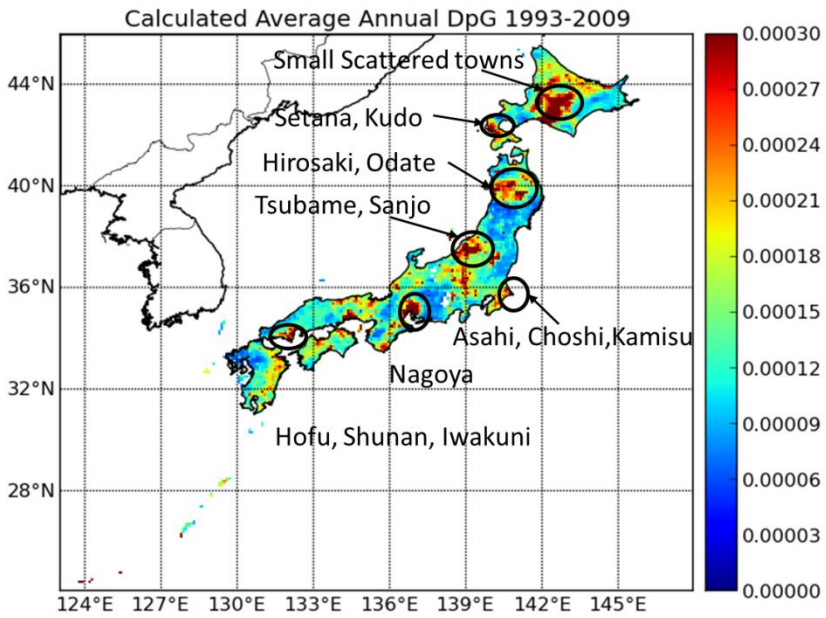

Fig. 3.26 Spatial distribution of expected annual damage per GDP per 0.1˚grid for 1992-2009 in Japan. Many areas with smaller population densities exhibited larger damage per GDP

3.10 Summary

This chapter describes the development process of newly developed statistical model for general property damage estimation due to pluvial flooding. The model structure with all its components are well described and also shows each steps of model execution to calculate total national annual damage by model cascade. The chapter also discusses the different model forcing data used to derive empirical relationship of damage occurrence probability and damage cost function. The model performance to calculate annual damage, average monthly damage and expected annual damage are also discussed.

The newly developed model is very robust tool for estimating annual damage of a location. The damage occurrence probability seems to be higher for higher population density and flatter slope area, where as the vulnerability in less populated area seems to be higher than that in densely populated urban areas. The model is very light tool to calculate seasonal variation of the damage as well as to calculate regional variation of the pluvial flood damage.

4. Application of the model for future pluvial flood damage assessment in Japan

4.1 Introduction

IPCC (2012) reported that changes in future exposure, vulnerability, and climate extremes as a result of anthropogenic climate change phenomena, and socio-economic changes can be the potential for disaster increase in the globe. The frequency of heavy precipitation or the proportion of total rainfall from heavy precipitation is likely to be increase in the 21st century over many parts of the world (Seneviratne *et al.*, 2012), which imply the possible increase of flooding events, and thereby increase in flood damage. Moreover, Seneviratne *et al.* (2012) revealed that moderate to light rainfall (the rainfall that are not extreme statistically) can lead to extreme impacts induced by exposure or vulnerable condition of a location, and can contribute significant amount of total global cost of natural hazard (Bouwer, 2013). Different climate models projected increase in frequency and intensity of heavy rainfall, which should contribute to increase in pluvial flooding (Seneviratne *et al.*, 2012, Bouwer, 2013, Kundzewicz *et al.*, 2013).

A policy report, Climate Change Adaptation Strategies to Cope with Water-related Disaster due to Global Warming, by panel on Infrastructure Development, Ministry of Land, Infrastructure, Transport and Tourism (MLIT, 2008) revealed that future annual precipitation, summer precipitation, and frequency of heavy precipitation will increase in many parts of Japan. The probability of flood damage is also expected to increase in many parts of Japan in future as predicted by Mouri *et al.* (2013). The flood risk described by risk density curve in Morita (2011) has shown a significant increase of flood risk in future in one of the river basin in Japan due to the climate change. Kazama *et al.* (2009) also discussed the change in flood damage over Japan with the increase of precipitation intensity, evaluating flood damage in different return period and its regional distribution over Japan. Owing to the fact of very high concentration of property, and effect of the large increase of hazard extremes, the future estimates of pluvial flood damage in Japan along with its regional distribution are very important for policy makers to formulate future flood defense strategies.

However, future projection of flood risk, are associated with number of uncertainties. The main three sources as discussed by Seneviratne *et al.* (2012) are: the natural variability of climate, uncertainty in climate model parameters and structure, and projection of future emissions. IPCC (2012) further elaborated various depended factors for future projection includes the types of extreme, the region and season, the amount and quality of observational data, the level of understanding of the underlying processes, and reliability of their simulation in models. Due to the lack of common analytical framework for flood risk assessment (Bouwer, 2013), and the associated uncertainties as discussed above, very few studies were reported for future damage estimation especially related to pluvial flooding incorporating anthropogenic climate change (Seneviratne *et al.*, 2012). The methodology as discussed by Morita (2011) for future flood risk and damage assessment is only limited to a basin scale. The need of regional or much larger scale flood risk assessment is difficult to address by these formulation. In this regard, we applied our statistical model to estimate future pluvial flood damage in Japan and also evaluate distribution of future change of pluvial flood damage and its intensity. The uncertainties related to future climate condition were evaluated with the use of different GCM results.

Precipitation outputs of different GCM were utilized in this study, which will be briefly described in following sections. One climate scenario (A1B) from SREX scenarios (IPCC, 2000) and two climate scenarios (RCP2.6 & RCP8.5) from RCP scenarios (Moss *et al.*, 2008, 2010) were taken for future assessment. The uncertainties of future projection in these three scenarios due to different GCM results were evaluated with their ensemble mean and standard deviation. Following assumptions were made while using the developed statistical model for future prediction of pluvial flood damage over Japan in different climate change scenarios:

1) To estimate far-future climate change effect only, the socio-economic conditions in far-future period (2083-2095) were adopted as same as the base period (1993-2005). It means the population density and GDP variation during 2083-2095 is same as the variation in 1993-2005.
2) Future pluvial flood damage from 2006-2099 for two RCP scenarios were conducted taking the base social-economic data same as the year of 2005.

3) The risk curves (damage occurrence probability function and damage cost function) derived from statistical data in present are fitted for the exceedance probability range (0.005-0.995). To minimize any uncertainty due to the extrapolation of these curves beyond these range, all the damage amounts were calculated for the return period below or equal 200 years (w=0.005), and any daily precipitation value with return period above this value is treated as same as 200 years return period value.

4.2 Future climate scenarios

Different climate scenarios were developed and used by researcher to understand the interaction of climate system; ecosystem and human activities (Moss *et al.*, 2010) in future based on future socio-economic development, technological and environmental conditions, emissions of greenhouse gases and aerosols. These scenarios help to evaluate uncertainty in future climate response due to human activities. Three different climate scenarios (A1B, RCP2.6 & RCP8.5) were used for future projection of pluvial flood damage in Japan. A1B, RCP2.6 and RCP8.5 climate scenarios were designed by Intergovernmental Panel on Climate Change (IPCC). A1B is one of the scenario based on the Special Report on Emission Scenarios (SRES) (IPCC, 2000); whereas RCP2.6 and RCP8.5 are newly developed scenario by IPCC, also called Representative Concentration Pathways (RCPs) scenarios (Moss *et al.*, 2008, 2010). Climate projections in the fourth assessment report of IPCC (AR4) were based on SRES scenarios, whereas in the fifth assessment report (AR5), climate projections were based on RCPs scenarios.

A1B scenario considered a future world of very rapid economic growth, global population that peaks in mid-21st century and declines thereafter, and the rapid introduction of new and more efficient technologies (IPCC, 2000). More over this scenario considers convergence among regions, capacity building, and increased cultural and social interactions, with substantial reduction in regional difference in per capita income. A1B scenario considers much balanced use of energy sources (fossil intensive and non-fossil energy sources) in future and based primarily on the future technological development aspect.

The RCP scenarios are based on different scenarios of future radiative forcing, which is the change in the balance between incoming and outgoing radiation to the atmosphere caused by changes in atmospheric constituents, e.g. carbon dioxide (Moss *et al.*, 2010). These scenarios include time paths for emissions and concentrations of the full suite of greenhouse gases (GHGs) aerosols and chemically active gases, as well as land cover (Moss *et al.*, 2008). The RCP2.6 scenario is designed in which radiative forcing peaks at approximately 3 W/m^2 before 2100 and then declines, having about 2.6 W/m^2 at 2100. The greenhouse gas concentration will also peaks at approximately 490 CO_2-eq before 2100 and then declines. On the other hand, RCP8.5 is a high pathway scenario for which radiative forcing reaches >8.5 W/m^2 and greenhouse gas concentration will be 1370 CO_2-eq by 2100 and continues to rise for some time. These two scenarios from RCPs were taken in this study to compare the lower and higher bound of expected pluvial flood damage in Japan, along with A1B scenario from SREX.

4.3 Forcing data

Pluvial flood damage for future in Japan was projected using different Global Circulation Models (GCM) daily precipitation results as forcing for hazard. The daily precipitation data produced by these GCM for historical run were also used to evaluate the GCM results **[Fig. 4.1]**. The precipitation frequency in present was used for future, confirming the same amount of precipitation in present produces same amount of damage in future as well. The socio-economic data were used as same as the historical base period [1993-2005] to compare expected pluvial flood damage in far-future (end of 21st century). The population density, gross domestic product, and topographical slope data were as described in chapter 3 [section 3.4.2, 3.4.4, and 3.4.5 respectively]. The **Table 4.1** shows the different GCM whose daily precipitation results for A1B, RCP2.6 and RCP8.5 scenarios in future were utilized.

Table 4.1 Different General Circulation Model used for future pluvial flood damage estimation in this study

S.N.	A1B Scenario						
	GCM	Spatial Resolution	Convective Scheme	Future SST	Historical period	Future period	Nomenclature used in this study
1	MRI-AGCM	20 km	Yoshimura		1979-2005	2083-2095	MRI-AGCM-SFA-YO-A1B
2	MRI-AGCM	60 km	Yoshimura		1979-2005	2083-2095	MRI-AGCM-HFA-YO-A1B
3	MRI-AGCM	60 km	Yoshimura	Cluster 1	1979-2005	2083-2095	MRI-AGCM-HFA-YO-C1-A1B
4	MRI-AGCM	60 km	Yoshimura	Cluster 2	1979-2005	2083-2095	MRI-AGCM-HFA-YO-C2-A1B
5	MRI-AGCM	60 km	Yoshimura	Cluster 3	1979-2005	2083-2095	MRI-AGCM-HFA-YO-C3-A1B
6	MRI-AGCM	60 km	Arakawa-Schubert		1979-2005	2083-2095	MRI-AGCM-HFA-AS-A1B
7	MRI-AGCM	60 km	Arakawa-Schubert	Cluster 1	1979-2005	2083-2095	MRI-AGCM-HFA-AS-C1-A1B
8	MRI-AGCM	60 km	Arakawa-Schubert	Cluster 2	1979-2005	2083-2095	MRI-AGCM-HFA-AS-C2-A1B
9	MRI-AGCM	60 km	Arakawa-Schubert	Cluster 3	1979-2005	2083-2095	MRI-AGCM-HFA-AS-C3-A1B
10	MRI-AGCM	60 km	Kain-Fritsch		1979-2005	2083-2095	MRI-AGCM-HFA-KF-A1B
11	MRI-AGCM	60 km	Kain-Fritsch	Cluster 1	1979-2005	2083-2095	MRI-AGCM-HFA-KF-C1-A1B
12	MRI-AGCM	60 km	Kain-Fritsch	Cluster 2	1979-2005	2083-2095	MRI-AGCM-HFA-KF-C2-A1B
13	MRI-AGCM	60 km	Kain-Fritsch	Cluster 3	1979-2005	2083-2095	MRI-AGCM-HFA-KF-C3-A1B
S.N.	**RCP2.6 and RCP8.5 Scenario**						
1	MRI-AGCM	60 km	Yoshimura		1979-2005	2083-2095	MRI-AGCM-HFA-YO-RCP26/85
2	MIROC-ESM-CHEM	2.8125˚ (T42)			1971-2005	2006-2099	MIROC-ESM-CHEM-RCP26/85
3	GFDL-ESM2M	2.0˚ x 2.5˚			1971-2005	2006-2099	GFDL-ESM2M-RCP26/85
4	IPSL-CM5A-LR	1.9˚ x 3.75˚ (L39)			1971-2005	2006-2099	IPSL-CM5A-LR-RCP26/85
5	NORESM1-M	2.0˚			1971-2005	2006-2099	NORESM1-M-RCP26/85

*Symbol *"F"* in SFA or HFA is replaced by *"P"* in present case without A1B, RCP2.6 and RCP8.5 at the end.

For SREX A1B scenario, only one GCM (MRI-GCM) with different convective schemes, different future SSTs (Ensemble of three different clusters of CMIP models) and different horizontal resolutions were used for future projection; this will provide a kind of semi-ensemble result for A1B scenario in future. For RCP2.6 and RCP8.5, daily precipitation results from one MRI-AGCM (MRI-AGCM-HFA-YO), MIROC-ESM-CHEM, GFDL-ESM2M, IPSL-CM5A-LR, and NORESM1-M were utilized. A brief description of each GCM is given in the following sub-sections.

4.3.1 MRI-AGCM

For A1B scenario, Meteorological Research Institute-Atmospheric General Circulation Model (MRI-AGCM) daily precipitation results were used. The main features of MRI-AGCM are its high resolution output. In this study, 20- and 60-km mesh was used. For A1B scenario, the precipitation results from only MRI-AGCM were utilized. To assess the uncertainty of the projection, the results from three different cumulus convection schemes Yoshimura-Scheme (Yukimoto *et al.*, 2011); Arakawa Schubert scheme (Arakawa and Schubert, 1974); and the Kain-Fritsch convection scheme (Kain and Fritsch, 1990) mainly for 60 km mesh were used. Moreover, results from four different sea surface temperatures (SST) change pattern based on ensemble of SSTs output of CMIP model clusters with each convective scheme were used and hence total ensemble for A1B to be 13 as shown in **Table 4.1**. For the historical run, the daily precipitation data for the period 1979-2009 were utilized to calculate precipitation parameters, whereas annual pluvial flood damage were calculated for the period 1993-2005 (13 years) and for far-future projection (late 21st century), daily precipitation output for the period 2083-2095 were utilized for A1B scenarios. For RCP scenarios only MRI-AGCM-H-YO was used as an ensemble candidate. All precipitation data were further interpolated onto 0.1° grid in Japan domain.

4.3.2 MIROC-ESM-CHEM

An earth system model (MIROC-ESM) is based on global climate model MIROC (Model for Interdisciplinary Research on Climate), which has been cooperatively developed by the University of Tokyo, NIES, and JAMSTEC (Watanabe *et al.*, 2011),

and MIROC-ESM includes an atmospheric chemistry component (CHASER), a nutrient-phytoplankton-zooplankton-detritus (NPZD) type ocean ecosystem component, and a terrestrial ecosystem component dealing with dynamic vegetation (SEIB-DGVM) (Watanabe *et al.*, 2011). The CHASER-coupled version of MIROC-ESM is termed as MIROC-ESM-CHEM, which considers the detailed photochemistry in troposphere and stratosphere by simulating tracer transport, wet and dry deposition, and emission (Watanabe *et al.*, 2011). The output of daily precipitation data at spatial resolution of 0.5° developed in the framework of the Inter-Sectoral Impact Model Inter-comparison Project (ISI-MIP) (Hempel *et al.*, 2013, Warszawski *et al.*, 2014) were utilized in this study. All precipitation data were further interpolated in Japan domain onto 0.1° grid for further analysis. The historical data for the period [1971-2005] were used to calculate precipitation parameters, whereas historical annual pluvial flood damage data were estimated for 1993-2005 (13 years) and far-future for the period [2083-2095] in both RCP2.6 and RCP8.5 scenarios, based on the similar socio-economic trend as historical run to compare the change of pluvial flood in far-future than in present base period Further, futures run for entire 21st century period from 2006-2099 were also performed with 2005 base socio-economic condition.

4.3.3 GFDL-ESM2M

GFDL-ESM2M is a carbon-climate earth system model developed in the Geophysical Fluid Dynamics Laboratory (GFDL) of National Oceanic and Atmospheric Administration (NOAA) (Dunne *et al.*, 2012, 2013). The detail description of this model can be found in Dunne *et al.*, (2012), and Dunne *et al.*, (2013). The output of daily precipitation data at spatial resolution of 0.5° developed in the framework of the ISI-MIP (Hempel *et al.*, 2013, Warszawski *et al.*, 2014) were utilized. All precipitation data were further interpolated in Japan domain onto 0.1° grid for further analysis. The historical data for the period [1971-2005] were used to calculate precipitation parameters, whereas historical annual pluvial flood damage data were estimated for 1993-2005 (13 years) and future projected damage data for the period [2083-2095] were used in both RCP2.6 and RCP8.5 scenario, based on the similar socioeconomic trend as historical run to compare the change of pluvial flood in far-

future than in present base period. Further, futures run for entire 21st century period from 2006-2099 were also performed with 2005 base socio-economic condition.

4.3.4 IPSL-CM5A-LR

The Institut Pierre Simon Laplace (IPSL) climate modelling center developed IPSL-CM5 earth system model based on the LMDZ atmospheric model, Nemo ocean circulation model, Orchidee surface-vegetation atmosphere transfer and dynamic vegetation model, the Inca model for chemistry and aerosols, and LMDZ-Reprobus coupled chemistry climate model (Hourdin *et al.*, 2012). The output of daily precipitation data at spatial resolution of 0.5° developed in the framework of the ISI-MIP (Hempel *et al.*, 2013, Warszawski *et al.*, 2014) were utilized. All precipitation data were further interpolated in Japan domain onto 0.1° grid for further analysis. The historical data for the period [1971-2005] were used to calculate precipitation parameters, whereas historical annual pluvial flood damage data were estimated for 1993-2005 (13 years) and future projected damage data for the period [2083-2095] were used in both RCP2.6 and RCP8.5 scenario, based on the similar socioeconomic trend as historical run to compare the change of pluvial flood in far-future than in present base period. Further, futures run for entire 21st century from 2006-2099 were also performed with 2005 base socio-economic condition.

4.3.5 NORESM1-M

The Norwegian Earth System Model (NORESM) is developed with the coordinated effort of the research project Reg-Clim, the development of the Bergen Climate Model (BCM) at the Bjerknes Centre for Climate Research in Bergen, and aerosol-cloud-radiation interaction schemes developed in Oslo (Bentsen *et al.*, 2013). Various features of NORESM is well described in Bentsen *et al.* (2013). NORESM is based on the Community Climate System Model version 4 (CCSM4) and utilizes an isopycnic coordinate ocean general circulation model. NORESM1-M is the first version of NORESM with intermediate horizontal resolution of approximately 2° for atmosphere and land components and 1° for ocean and ice components. However, similar to previous GCMs, the output of daily precipitation data at spatial resolution

of 0.5° developed in the framework of the ISI-MIP (Hempel *et al.*, 2013, Warszawski *et al.*, 2014) were utilized, which further interpolated onto 0.1-deg grid. The historical data for the period [1971-2005] were used to calculate precipitation parameters, whereas historical annual pluvial flood damage data were estimated for 1993-2005 (13 years) and future projected damage data for the period [2083-2095] were used in both RCP2.6 and RCP8.5 scenario, based on the similar socioeconomic trend as historical run to compare the change of pluvial flood in far-future than in present base period. Further, futures run for entire 21st century from 2006-2099 were also performed with 2005 base socio-economic condition.

Author believe that the ensemble mean from different climate models should provide better estimate of pluvial flood damage in future climate with different future scenarios and also provide the uncertainty range of future estimate.

4.4 Evaluation of GCM results in historical run

The daily precipitation data produced by each GCM in historical (present base) period were first evaluated with the test of Gumbel distribution fitness for annual daily maximum precipitation data as described earlier in chapter 3 (section: 3.5) with the use of Probability Plot Correlation Coefficient (PPCC) (Vogel, 1986). **Figure 4.1** shows the grids in which PPCC value is greater than critical PPCC, showing the goodness of fit for Gumbel distribution for annual maximum daily precipitation for all GCMs under consideration for SRES and RCP scenarios in 5% significance level. **Table 4.2** shows the percentage of total grids in which Gumbel distribution is fitted well in 5% significance level. It is seen that more than 90% grids are well fitted in Gumbel distribution for all GCM except MRI-AGCM-HPA-KF and NORESM1-M which has only 89.14% and 65.32% grids well fitted for Gumbel distribution respectively. Nevertheless, the PPCC test shows good fitness for Gumbel distribution for annual maximum daily precipitation for all GCM under consideration in Japan.

Table 4.2 Percentage of Grids that fit Gumbel distribution for annual maximum daily rainfall in 5% significance level by different GCMs in historical run

S.N.	GCM	Historical Period	Years	Critical PPCC @ 5% significance level	% of grids above Critical PPCC
1	MRI-AGCM-SPA-YO	1979-2009	31	0.95328	93.27
2	MRI-AGCM-HPA-YO	1979-2009	31	0.95328	95.04
3	MRI-AGCM-HPA-AS	1979-2009	31	0.95328	90.38
4	MRI-AGCM-HPA-KF	1979-2009	31	0.95328	89.14
5	MIROC-ESM-CHEM	1971-2005	35	0.95600	94.97
6	GFDL-ESM2M	1971-2005	35	0.95600	96.32
7	IPSL-CM5A-LR	1971-2005	35	0.95600	95.27
8	NORESM1-M	1971-2005	35	0.95600	65.32

Further, annual pluvial flood damages were calculated for the period 1993-2005 (13years) in present [base period] with all GCMs daily precipitation data. The expected annual damage (mean) and standard deviation of inter-annual damage variation were estimated in the base period using the statistical empirical relationship developed as given in relation (3.8), (3.9), and (3.10) with mean DpG parameter value which estimate total annual damage and finally expected annual damage for the base period. **Table 4.3** shows the mean and inter-annual standard deviation in base period from daily precipitation with all eight GCMs. The table also shows the mean and standard deviation of recorded total national damage by MLIT, estimated annual damage from AMeDAS precipitation dataset and percentage change of each GCM output from the MLIT recorded. From the table it is revealed that expected annual damage for the period is quite comparable with the recorded average value.

There is both positive and negative bias in estimation of expected annual damage. Most GCM shows negative bias up to 51%. Some large record in MLIT dataset in some years produces such large negative bias in estimation. However, most of the expected annual total national damage estimated is within 30% of recorded damage. The range of expected annual damage estimated from different GCM is 56 to 117 billion yen. Calculated standard deviation of inter-annual variation has both positive and negative bias with MLIT recorded annual damage variation. The ensemble mean damage from all GCM (87 billion yen) with ensemble standard deviation (84 billion yen) is quite comparable to recorded (mean: 113 billion yen & Std. dev: 84 billion yen) damage and also with the damage calculated from AMeDAS precipitation

dataset (mean: 97 billion yen & Std. dev.: 52 billion yen) where the model was optimized. Underestimation of damage value in most of the GCM is also partly caused by some missing grids during the process of re-gridding from high resolution to low resolution.

This led to the use of the statistical model and GCM produced daily precipitation data for future prediction of pluvial flood damage in Japan.

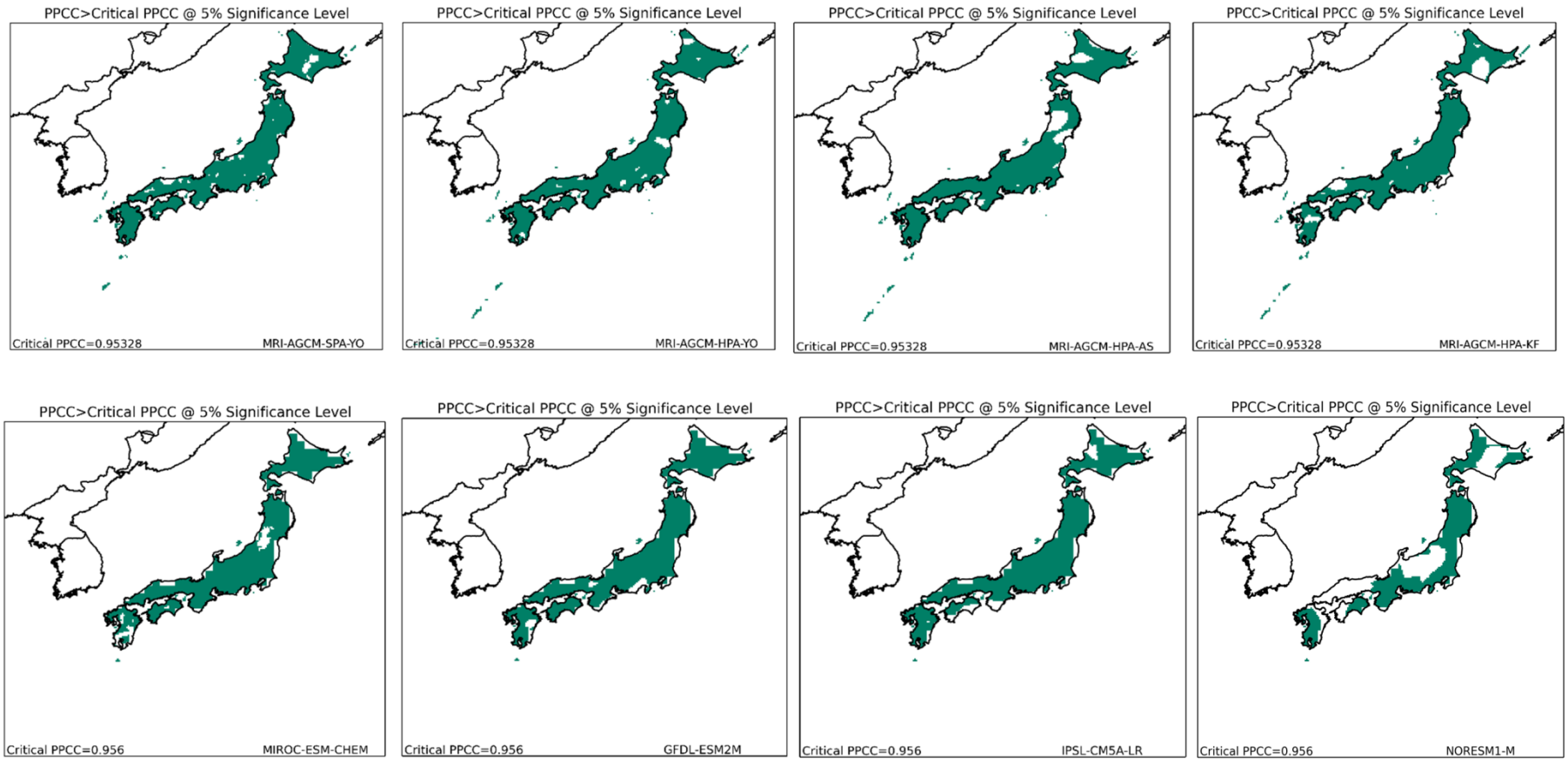

Fig. 4.1 Grids which shows PPCC value greater than critical PPCC in 5% significance level showing fitness of Gumbel distribution for all GCMs under used for future prediction of pluvial flood damage in Japan.

Table 4.3 A comparison of recorded average annual damage and standard deviation of annual variation of recorded damage with expected annual damage estimated from AMeDAS precipitation and precipitation from different GCMs using our model.

S.N.	GCM	Present base period of damage estimation	Years	Mean damage (billion yen, 2005 price)	Standard deviation of annual variation of damage (billion yen, 2005 price)	% change from MLIT recorded mean damage	% change from MLIT standard deviation
1	MLIT recorded	1993-2005	13	113.35	84.37	0.00	0.00
2	AMeDAS precipitation	1993-2005	13	97.44	51.97	-14.04	-38.40
3	MRI-AGCM-SPA-YO	1993-2005	13	100.92	52.84	-10.96	-37.38
4	MRI-AGCM-HPA-YO	1993-2005	13	55.58	28.43	-50.96	-66.31
5	MRI-AGCM-HPA-AS	1993-2005	13	93.85	85.50	-17.20	1.33
6	MRI-AGCM-HPA-KF	1993-2005	13	106.75	100.43	-5.82	19.03
7	MIROC-ESM-CHEM	1993-2005	13	74.08	81.63	-34.65	-3.25
8	GFDL-ESM2M	1993-2005	13	69.18	51.15	-38.97	-39.37
9	IPSL-CM5A-LR	1993-2005	13	78.73	104.88	-30.54	24.31
10	NORESM1-M	1993-2005	13	117.15	167.63	+3.36	98.68

4.5 Future projection of pluvial flood damage

The pluvial flood damage in late 21st century [2083-2095] (referred as far-future) were estimated using newly developed statistical model with mean DpG and the use of daily precipitation output from different GCM as describe in **Table 4.1** for all three future scenarios. The mean change of pluvial flood damage for entire Japan from present base period [1993-2005] was calculated along with their inter-annual variability. It is believed that the ensemble of GCMs will provide better estimate of total national expected annual damage in far-future. Average monthly damage for present and far-future in RCP2.6 and RCP8.5 were also estimated to examine the seasonal change of pluvial flood damage in Japan.

4.5.1 A1B Scenario

Calculated future total national expected annual damage by different GCMs and its percentage change from present for A1B scenario is tabulated in **Table 4.4**. The table reveals that the range of total national expected annual damage in far- future will be from 124 billion yen to 262 billion yen giving ensemble mean value of 177 billion yen. The ensemble of expected annual damage in late 21st century seems to be more than double (105% increase) than present base period for A1B scenario as shown in **Fig 4.2** below.

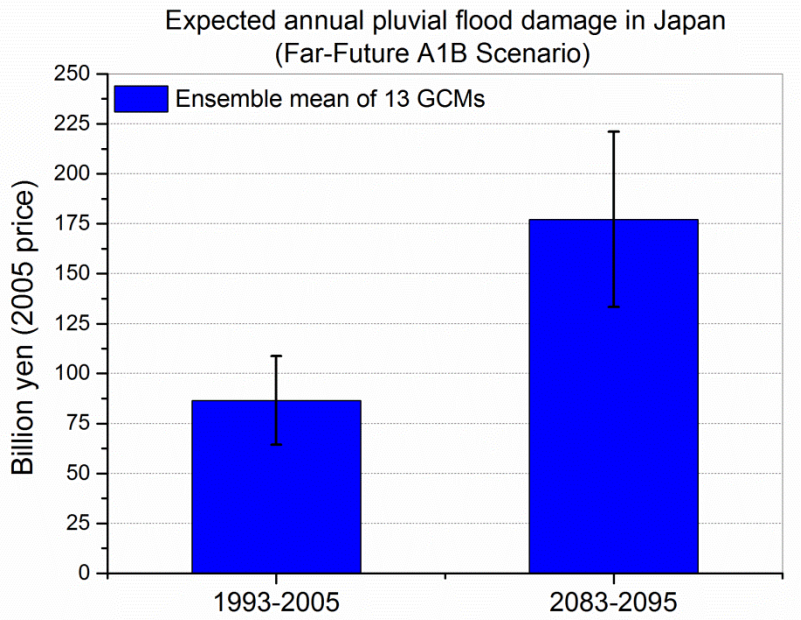

Fig. 4.2 Expected annual pluvial flood damage as an ensemble of candidate GCMs for A1B scenario in future. The error bar shows the standard deviation of ensemble.

The annual variation of GCM output in present and far-future for A1B scenario are shown in **Fig. 4.3**, which shows a clear increase in the mean value. The shaded green area shows the higher (90^{th} percentile) and lower (10^{th} percentile) value of 13 GCM outputs in each year. The uncertainty range of GCM output in future seems larger than that of present base period. The standard deviation of inter-annual variation in present and far-future for A1B scenario are tabulated in **Table 4.5,** which shows large variation in inter-annual damage in future as the standard deviation calculated are higher than present base period. However, the coefficient of variability (CV), which is ratio of standard deviation to its corresponding mean value usually expressed in percentage (as given in relation 4.1), shows that the inter-annual variability is not changed significantly in all GCM for A1B scenario in future.

$$CV = \frac{Standard\ deviation}{Mean} x\ 100\ \% \text{ -------- (4.1)}$$

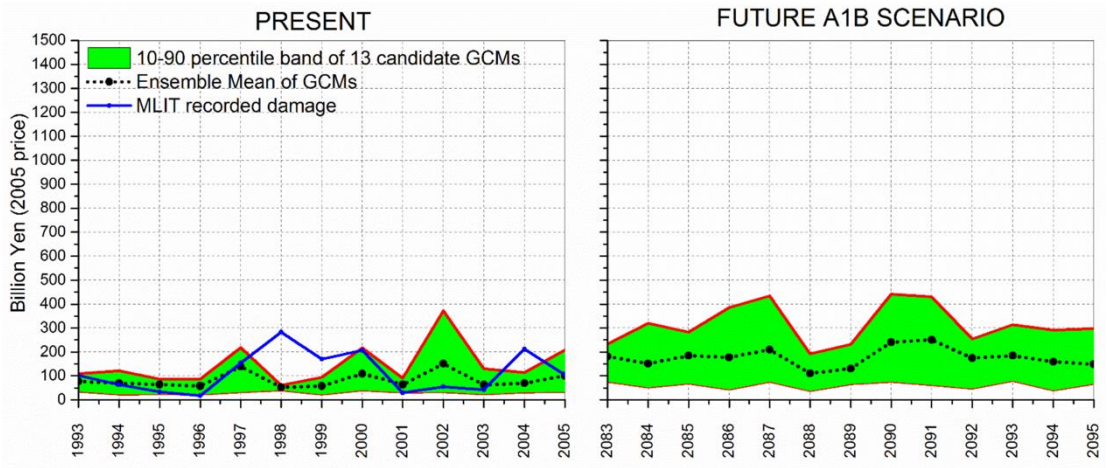

Fig. 4.3 Annual variation of total national pluvial flood damage in present and future estimated by mean DpG for A1B scenario. The shaded green area shows the annual GCM uncertainty range with 10^{th} to 90^{th} percentile. The dotted black line shows the ensemble damage and blue line shows MLIT recorded damage in present.

4.5.2 RCP2.6 and RCP8.5 Scenarios

The calculated far-future total national expected annual pluvial flood damage by different GCM (**Table 4.1**) and its percentage change from present for RCP2.6 and RCP8.5 scenario are tabulated in **Table 4.6** and **Table 4.7** respectively. The table shows that the range of total national expected annual damage in far-future is from 99

billion yen to 134 billion yen giving the ensemble mean value of 116 billion yen for RCP2.6, whereas RCP8.5 scenario will have ensemble mean damage of 274 billion yen, with the range having 152 billion yen to 388 billion yen. The ensemble of expected annual damage in late 21st century seems to be more than triple (247% increase) from present base period for RCP8.5 scenario, whereas RCP2.6 shows increase of about 47% than that of present base period. **Figure 4.4** below shows a comparison for far-future pluvial flood total national damage in both RCP scenarios.

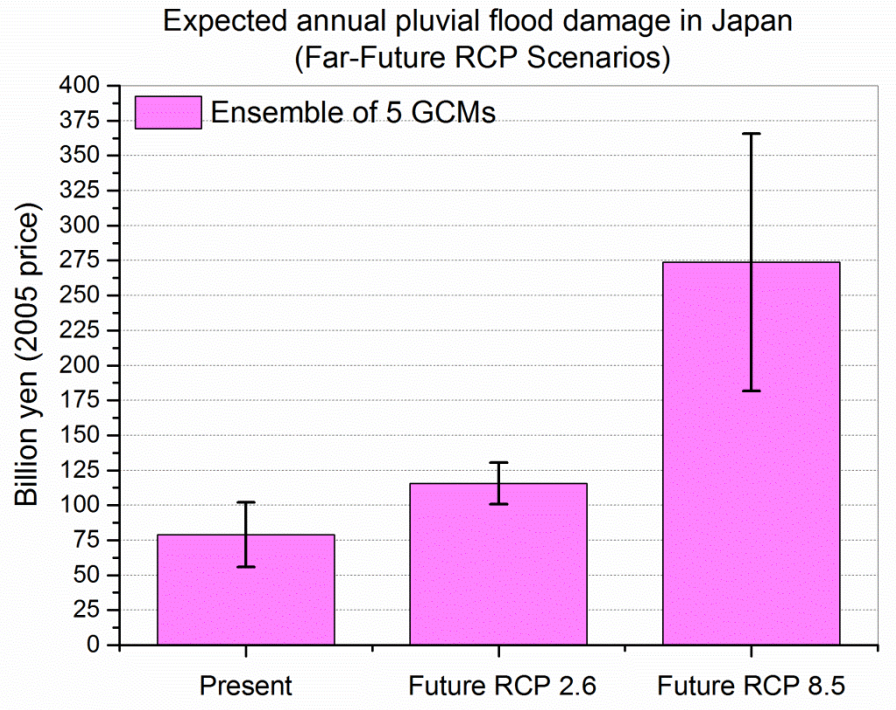

Fig. 4.4 Expected annual damage in present and far-future due to RCP2.6 and RCP8.5 scenarios in future. The error bar shows standard deviation of ensembles

Annual variation of GCM outputs in present and far-future for RCP2.6 and RCP8.5 are shown in shown in **Fig. 4.5** and **Fig. 4.6** respectively. In the far future (late 21st century), the annual variation and annual range from different GCMs seems almost similar to present in RCP2.6 scenario, though the ensemble mean increase of 47% revealed. Whereas, for RCP8.5 shows a clear change in mean and large variation in GCM annual estimate. The shaded green area shows higher (90th percentile) and lower value (10th percentile) of candidate GCMs output in each year. The standard deviation of inter-annual variation in present and future for RCP2.6 and RCP8.5 scenario are

tabulated in **Table 4.8** and **Table 4.9,** which shows a comparable variation in inter-annual damage in future for RCP2.6 as the standard deviation and coefficient of variability calculated are similar in present and future. On the other hand, the standard deviation of inter-annual damage variation in far-future for RCP8.5 scenario is significantly larger than present. However, the coefficient of variability (CV) shows that the inter-annual variability is not changed significantly in all GCM.

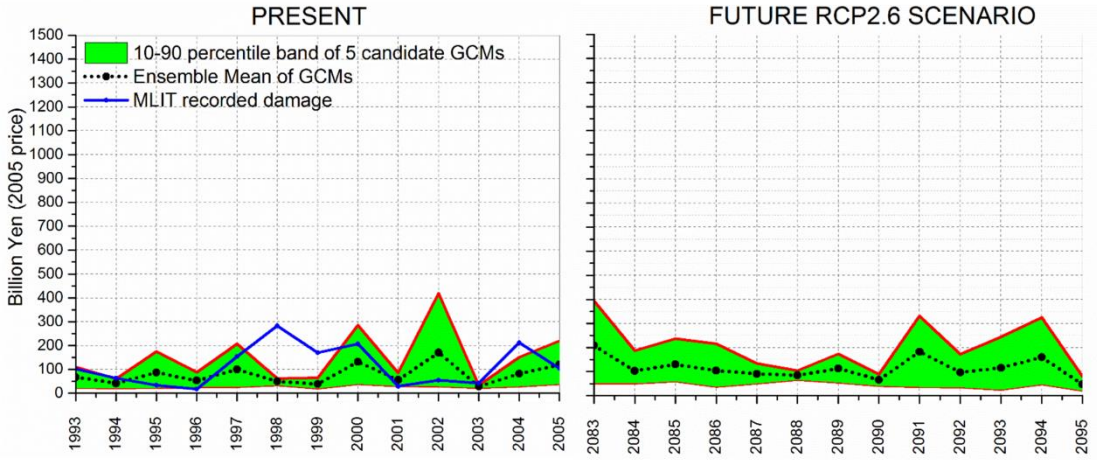

Fig. 4.5 Annual variation of total national pluvial flood damage in present and future estimated by mean DpG for RCP2.6 scenario. The shaded green area shows the annual GCM uncertainty range with 10th and 90th percentile. The dotted line shows annual ensemble mean damage. The blue line shows the MLIT recorded pluvial flood damage in present.

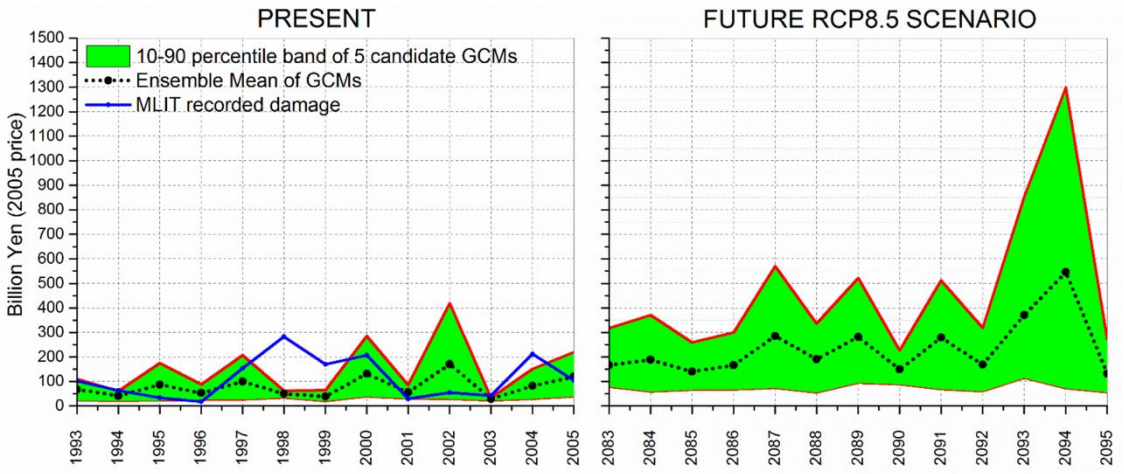

Fig 4.6 Annual variation of total national pluvial flood damage in present and future estimated by mean DpG for RCP8.5 scenario. The shaded green area shows the annual GCM uncertainty range with 10th and 90th percentile. The dotted line shows annual ensemble mean damage. The blue line shows the MLIT recorded pluvial flood damage in present.

Table 4.4 Present and far-future expected annual damage by different GCM, their ensemble mean for A1B scenario

S.N.	GCM	Present expected annual damage (billion yen, 2005 price) [1993-2005]	Present ensemble mean damage (billion yen, 2005 price)	Future expected annual damage (billion yen, 2005 price) [2083-2095]	Future ensemble mean damage (billion yen, 2005 price)	Ensembles mean increase in damage (%)
1	MRI-AGCM-SFA-YO-A1B	100.92	86.59	136.51	177.18	104.63
2	MRI-AGCM-HFA-YO-A1B	55.58		192.08		
3	MRI-AGCM-HFA-YO-C1-A1B	55.58		249.56		
4	MRI-AGCM-HFA-YO-C2-A1B	55.58		123.60		
5	MRI-AGCM-HFA-YO-C3-A1B	55.58		179.93		
6	MRI-AGCM-HFA-AS-A1B	93.85		198.99		
7	MRI-AGCM-HFA-AS-C1-A1B	93.85		262.26		
8	MRI-AGCM-HFA-AS-C2-A1B	93.85		160.26		
9	MRI-AGCM-HFA-AS-C3-A1B	93.85		140.55		
10	MRI-AGCM-HFA-KF-A1B	106.75		184.29		
11	MRI-AGCM-HFA-KF-C1-A1B	106.75		200.12		
12	MRI-AGCM-HFA-KF-C2-A1B	106.75		135.74		
13	MRI-AGCM-HFA-KF-C3-A1B	106.75		139.44		

Table 4.5 Standard deviation and coefficient of variability of estimated annual damage in present and future for A1B scenario

S.N.	GCM	Present Standard deviation of annual variation of damage (billion yen, 2005 price)	Coefficient of variation in present annual damage in %	Future expected annual damage (billion yen, 2005 price)	Coefficient of variance in future annual damage in %
1	MRI-AGCM-SFA-YO-A1B	52.84	52.36	62.40	45.71
2	MRI-AGCM-HFA-YO-A1B	52.84	95.07	138.53	72.12
3	MRI-AGCM-HFA-YO-C1-A1B	52.84	95.07	235.11	94.21
4	MRI-AGCM-HFA-YO-C2-A1B	52.84	95.07	71.57	57.90
5	MRI-AGCM-HFA-YO-C3-A1B	52.84	95.07	119.64	66.49
6	MRI-AGCM-HFA-AS-A1B	28.43	30.29	159.50	80.16
7	MRI-AGCM-HFA-AS-C1-A1B	28.43	30.29	151.97	57.95
8	MRI-AGCM-HFA-AS-C2-A1B	28.43	30.29	169.52	105.78
9	MRI-AGCM-HFA-AS-C3-A1B	28.43	30.29	88.01	62.62
10	MRI-AGCM-HFA-KF-A1B	85.50	80.09	228.61	124.05
11	MRI-AGCM-HFA-KF-C1-A1B	85.50	80.09	118.94	59.43
12	MRI-AGCM-HFA-KF-C2-A1B	85.50	80.09	133.59	98.42
13	MRI-AGCM-HFA-KF-C3-A1B	85.50	80.09	79.40	56.94

Table 4.6 Present and Future expected annual damage by different 5 GCMs, their ensemble mean for RCP2.6 scenario in future

S.N.	GCM	Present expected annual damage (billion yen, 2005 price) [1993-2005]	Present ensemble mean damage (billion yen, 2005 price)	Future expected annual damage (billion yen, 2005 price) [2083-2095]	Future ensemble mean damage (billion yen, 2005 price)	Ensembles mean increase in damage (%)
1	MRI-AGCM-HFA-YO-RCP26	55.58	78.94	132.66	115.65	46.50
2	MIROC-ESM-CHEM-RCP26	74.08		133.99		
3	GFDL-ESM2M-RCP26	69.18		110.48		
4	IPSL-CM5A-LR-RCP26	78.73		102.26		
5	NORESM1-M-RCP26	117.15		98.85		

Table 4.7 Present and Far-future expected annual damage by different GCMs, their ensemble mean for RCP8.5 scenario in future

S.N.	GCM	Present expected annual damage (billion yen, 2005 price) [1993-2005]	Present ensemble mean damage (billion yen, 2005 price)	Future expected annual damage (billion yen, 2005 price) [2083-2095]	Future ensemble mean damage (billion yen, 2005 price)	Ensembles mean increase in damage (%)
1	MRI-AGCM-HFA-YO-RCP85	55.58	78.94	152.41	273.61	246.59
2	MIROC-ESM-CHEM-RCP85	74.08		319.22		
3	GFDL-ESM2M-RCP85	69.18		294.76		
4	IPSL-CM5A-LR-RCP85	78.73		388.03		
5	NORESM1-M-RCP85	117.15		213.61		

Table 4.8 Standard deviation and coefficient of variability of estimated annual damage in present and future for RCP2.6 scenario

S.N.	GCM	Present Standard deviation of annual variation of damage (billion yen, 2005 price)	Coefficient of variance in present annual damage in %	Future expected annual damage (billion yen, 2005 price)	Coefficient of variance in future annual damage in %
1	MRI-AGCM-HFA-YO-RCP26	52.84	95.07	116.07	87.50
2	MIROC-ESM-CHEM-RCP26	81.63	110.20	103.28	77.08
3	GFDL-ESM2M-RCP26	51.15	73.95	94.54	85.57
4	IPSL-CM5A-LR-RCP26	104.88	133.21	111.20	108.75
5	NORESM1-M-RCP26	167.63	143.09	92.63	93.70

Table 4. 9 Standard deviation and coefficient of variability of estimated annual damage in present and future for RCP8.5 scenario

S.N.	GCM	Present Standard deviation of annual variation of damage (billion yen, 2005 price)	Coefficient of variance in present annual damage in %	Future expected annual damage (billion yen, 2005 price)	Coefficient of variance in future annual damage in %
1	MRI-AGCM-HFA-YO-RCP26	52.84	95.07	277.48	182.06
2	MIROC-ESM-CHEM-RCP26	81.63	110.20	106.33	33.31
3	GFDL-ESM2M-RCP26	51.15	73.95	88.39	29.99
4	IPSL-CM5A-LR-RCP26	104.88	133.21	227.25	58.57
5	NORESM1-M-RCP26	167.63	143.09	420.23	196.73

4.6 Regional distribution of future pluvial flood damage over Japan

Expected annual damage in each 0.1° grid was estimated using the model over Japan. In fact the total annual national damage is the sum of annual damage in all grids due to every daily rainfall event. **Figure 4.7** shows the distribution of expected annual damage (ensemble mean) (left) and expected annual damage per GDP (right) over Japan for A1B scenario in far-future [2083-2095].

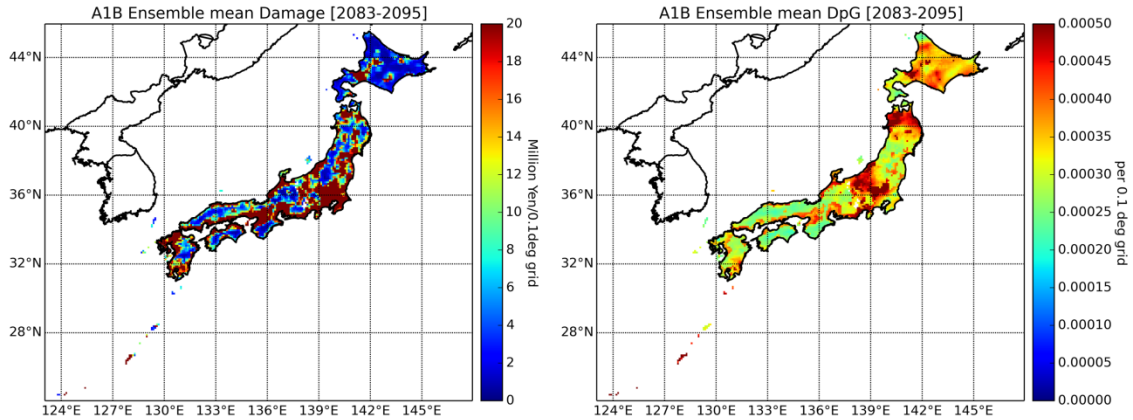

Fig. 4.7 Distribution of expected annual pluvial flood damage (left) and expected annual pluvial flood DpG (right) over Japan in far-future for A1B scenario.

Distribution of absolute pluvial flood damage is quite similar to the present; it is because absolute damage is mainly governed by population density and GDP concentration, which is considered same as present in future too. However, vulnerability in terms of damage per GDP seems to be more concentrated in center and northern part of main inland. The ensemble mean change of damage (DpG) in far-future from the present is shown in **Fig. 4.8**, which reveals that there will be large change of damage is expected in the central and northern part of main inland (Kyushu region) under A1B scenario, showing more than 200% increment of pluvial flood damage.

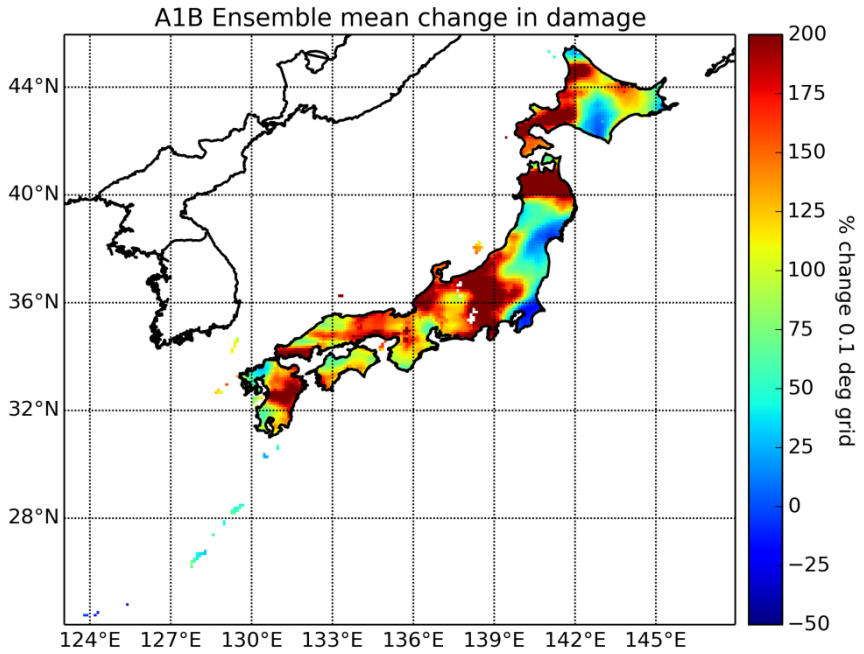

Fig. 4.8 Percentage change in absolute damage amount or DpG in each grid from the present period to far-future in A1B scenario.

Similarly, for both RCPs scenario, the ensemble mean damages (expected annual damage) for far-future [2083-2099] are shown in **Fig. 4.9.**

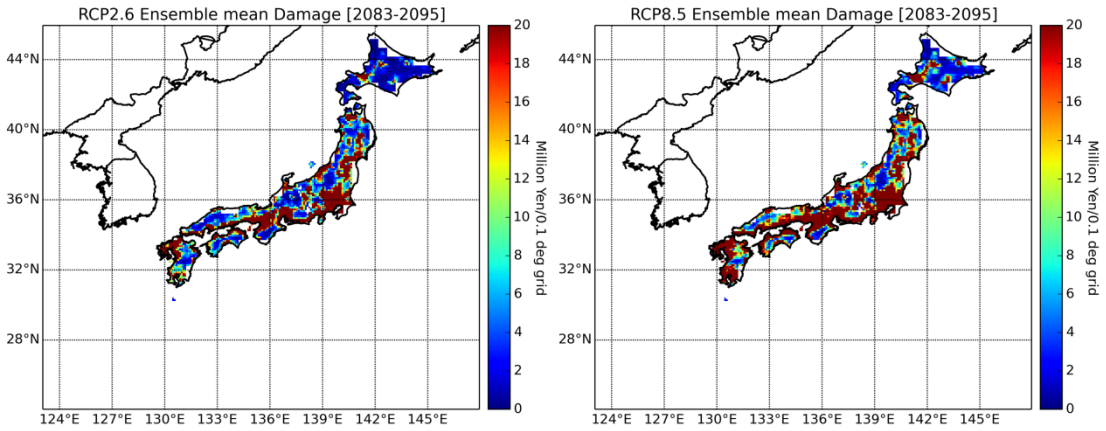

Fig. 4.9 Ensemble mean damage in far-future for RCP2.6 (left) and RCP8.5 (right)

Distribution of damage for far-future is quite similar to each other, though widening of some area in RCP8.5 is noticeable than RCP2.6. **Figure 4.10** shows the distribution of expected damage per GDP (vulnerability) in each grid during far-future. The figure reveals that vulnerability in RCP8.5 scenario will be significantly larger than in

RCP2.6 scenario. RCP8.5 scenario shows that vulnerability in the western Japan will increase significantly if present socio-economic condition prevails in far-future too.

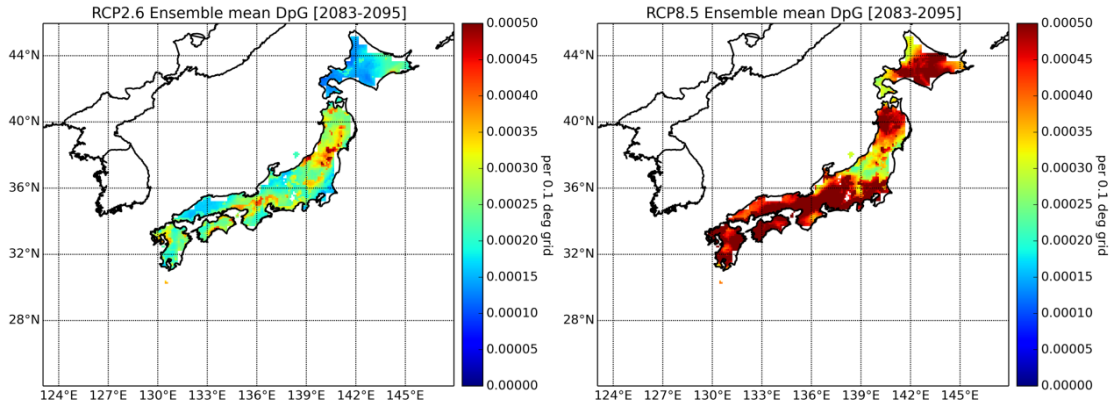

Fig. 4.10 Distribution of damage intensity (DpG) over Japan in far-future with RCP2.6 (left) and RCP8.5 (right) scenario.

Ensemble mean changes of absolute damage for both RCP scenarios are shown in **Fig. 4.11**. The ensemble mean change in RCP8.5 is much larger than RCP2.6 scenario in most grids. Most of the grids show that mean change of damage is larger than 200% in RCP8.5 scenario. The western, central and northern main inland attributed to higher change in damage in RCP8.5 than in RCP2.6 scenario.

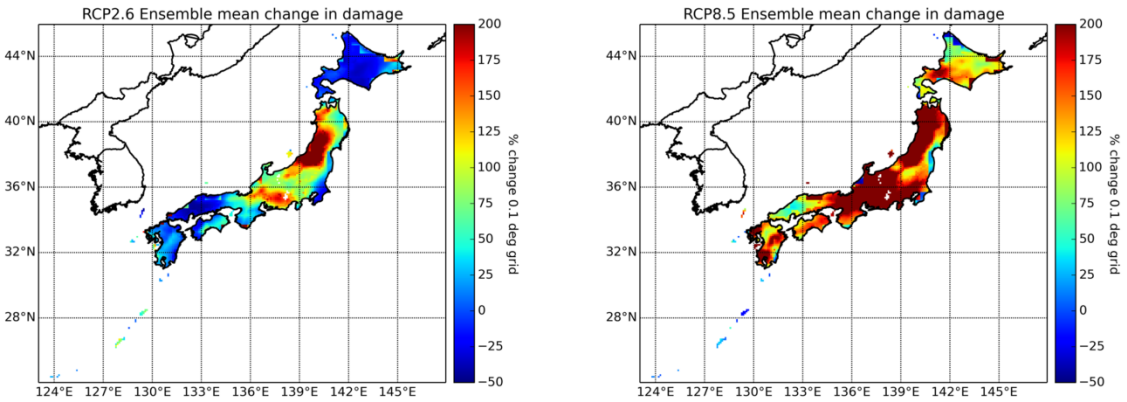

Fig 4.11 Percentage change of absolute damage amount for RCP2.6 (left) and RCP8.5 (right)

4.7 Expected monthly damage in far-future

Average monthly far-future pluvial flood damage in RCP2.6 and RCP8.5 scenarios were estimated and compared with the model estimated present seasonal variations.

Average monthly pluvial flood damage in present and in the future with each candidate GCMs in RCP2.6 and RCP8.5 are shown in **Fig. 4.12**.

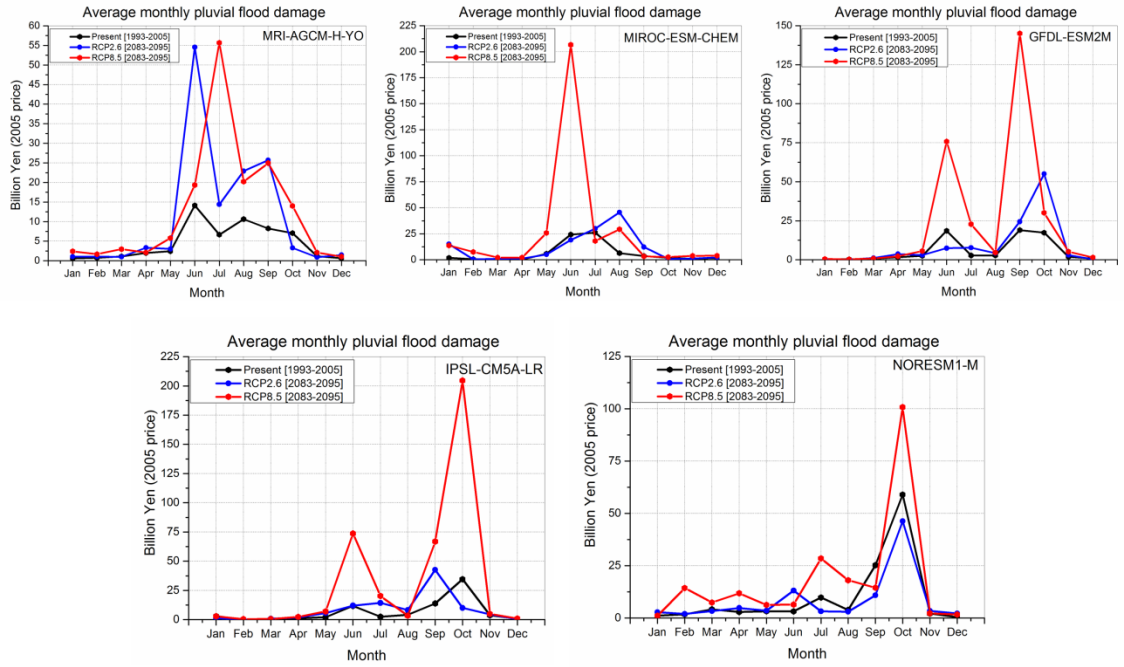

Fig 4.12 Present and Far-future average monthly pluvial flood damage in RCP2.6 and RCP8.5 scenarios

From the figure, it can be concluded that seasonal variation of damage largely depended on the GCMs. First two GCMs (MRI-AGCM and MIROC-ESM-CHEM) show a large increment of damage during June-July (East Asian monsoon season), whereas latter three GCMs (GFDL-ESM2M, IPSL-CM5A-LR, and NORESM1-M) showing larger increment during September-October (Typhoon season). However, comparing with present variation, similar trend in present will conserved in future with higher values in each GCMs, indicating that large daily precipitation (extremes) becomes even larger in future climate change condition. The ensemble average monthly damage is shown in **Fig. 4.13**. The figure shows there will be large increment (about three times) on pluvial flood damage over Japan in both rainfall seasons.

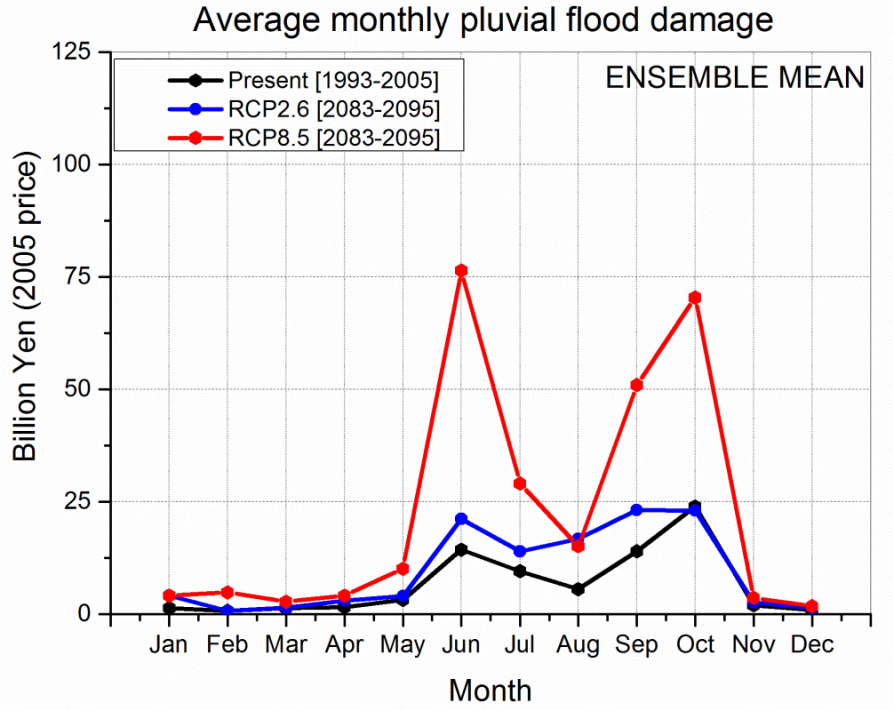

Fig. 4.13 Expected monthly pluvial flood damage (ensemble mean) in present and far-future, showing large increment of damage during rainy seasons in RCP8.5 scenario

4.8 Future trend of total national pluvial annual flood damage in Japan

To assess future long term trend of total annual pluvial flood damage over Japan, the daily precipitation output of the four GCMs (MIROC-ESM-CHEM, GFDL-ESM2M, IPSL-CM5A-LR, and NORESM1-M) were used. As described earlier, socio-economic condition (Population densities, and GDP) were kept constant to the year 2005, and conducted future simulation for 2006-2099. The robustness of the newly developed model prevail the long term trend of pluvial flood damage as shown in **Fig. 4.14** (linear scale) and **Fig. 4.15** (log scale).

The figure reveals that there is increasing trend of pluvial flood damage in RCP8.5 scenario; however rate of increment will rapidly increase after 2060s. Upto 2060s both RCP2.6 and RCP8.5 have similar trend, and almost similar to present as seen from ensemble mean value. The impact of climate change due to pluvial flooding for RCP2.6 will not noticeable, whereas impact in RCP8.5 will be much severe during late 21st century.

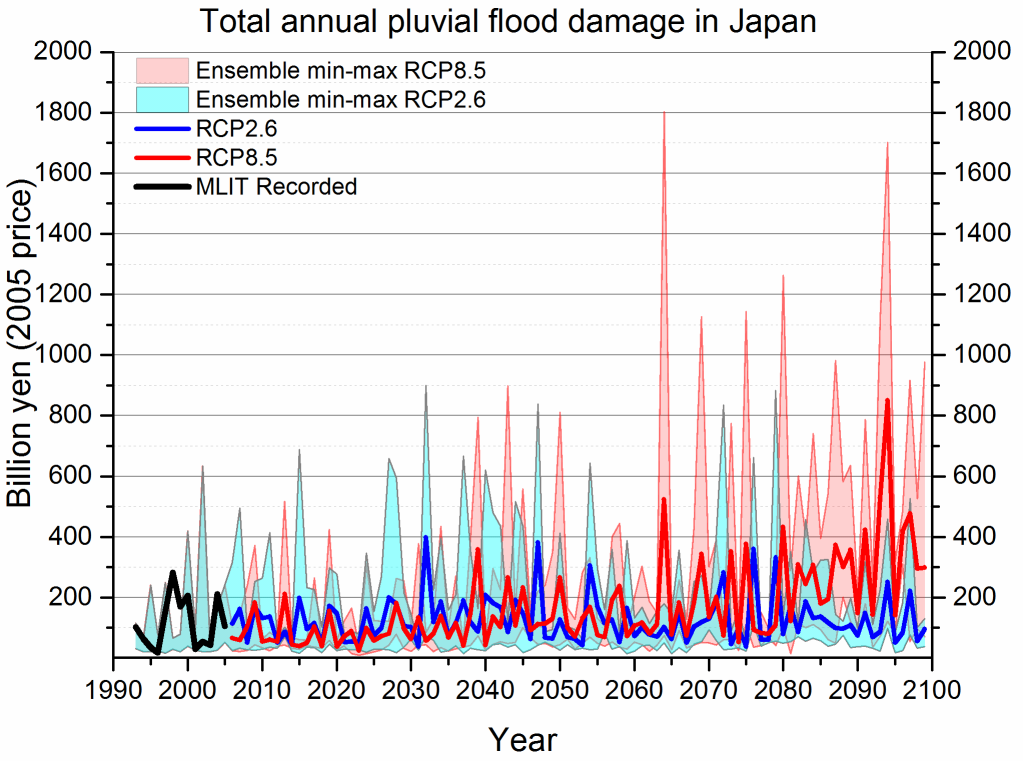

Fig. 4.14 Future trend of total national annual pluvial flood damage over Japan

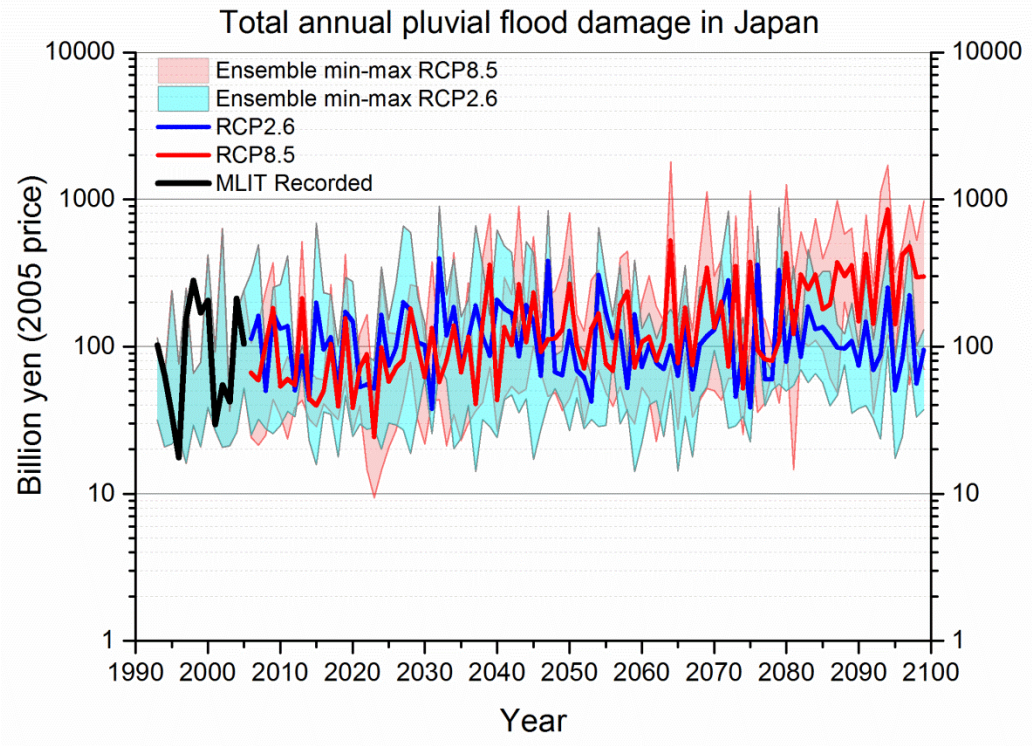

Fig. 4.15 Future trend of total national annual pluvial flood damage over Japan

4.9 Summary

This chapter dealt with the application of the statistical model in future projection of pluvial flood damage over Japan. The flexibility of the proposed model and its high capability to produce annual damage and expected annual damage very close to observation in historical simulation led us to use the model for future prediction of pluvial flood damage over Japan. The expected annual national damage in late 21st century was predicted and compared with the present observed value for two climate one SRES scenarios (A1B) and two RCP scenarios (RCP2.6 and RCP8.5) using different GCM precipitation output for future. The ensemble expected annual damage was estimated to be 177 billion yen for A1B scenario in far-future, showing increment of 105% from present base period. On the hand, the ensemble expected annual damage in RCP2.6 and RCP8.5 for far-future will be 116 billion yen and 274 billion yen in late 21st century, which was only about 80 billion yen in present base period. The results show that there will be about 47% increase in total national pluvial flood damage for RCP2.6 scenario and about 247% increase for RCP8.5 scenario, if the socio-economic condition and technological development in regard to the flood defense remains same as in present condition. The regional distribution of future pluvial flood damage and damage per GDP was also predicted by the use of proposed model. The percentage change of damage shows many parts of Japan will have more than 200% increment in damage especially for RCP8.5 scenario. The damage intensity also rises significantly in most part of the country. The ensemble average monthly damage in far-future will be increased by three fold in both rainy season (Jun-July, and Sep-Oct). However, the long-term future prediction of pluvial flood damage reveals that the increment of pluvial flood damage will be much severe after 2060s, particularly for RCP8.5 scenario.

5. Application of the model for Global pluvial flood assessment at present and its validation

5.1 Introduction

In present globalized world, there is a large need of identifying the flood risk zone, and compare the risks of different regions across the world so that the region of higher flood risk be identified and mitigation and/or adaption measures could be applied. Winsemius *et al.* (2013) also stated the need of global flood risk assessment in present as well as in future socio-economic and climate change condition. Globally, annual flood damage was reported increasing from a few billion USD in 1980s to more than 20 billion USD by the end of 2000s (Kundzewicz *et al.*, 2013), although there was large spatial and temporal variation in damage amount. It is well known fact that all most every country in the world suffers from flooding and attributed to physical damage annually, partially because of the increase of exposure in flood plain zone, and un-engineered development activities in developing world. Hirabayashi *et al.* (2013) also revealed that increase in global flood exposure, particularly in Asia and Africa. Many researchers stressed that socio-economic factors mainly attributed to the increasing flood damage around the world for example Moel *et al.*, (2011); and Feyen *et al.*, (2012). Anthropogenic climate change which plays important role increasing extreme events frequency and amount can be another cause of increasing flood risk, although few studies established these relationship (Pall *et al.*, 2011).

To date, many researcher attempted to assess flood risk in global scale, however, there is no any common analytical framework established so far for such macro-level study. There is a large deficiency in global flood damage data which create a fundamental problem for calibration and validation of damage estimation, when scaling up micro scale model to macro level (Handmer *et al.*, 2012) for estimating damage amount. The loss model developed at a local scale cannot be applied globally, as there is large variation of vulnerability and resilience not only from one country to another, but also within a country (Handmer *et al.*, 2012). The nature of asset value and need of multi impact and resistance parameter for damage assessment further halt the use of present established model for global flood risk assessment.

Winsemius *et al.* (2013) presented a framework for global river flood risk assessment which combines hazard model and impact model to derive expected annual damage. Ward *et al.* (2013) also prescribed a model cascade for flood risk assessment in global scale and estimated global flood risk in terms of affected population, affected GDP, affected agriculture value, exposed urban property values, and urban damage amount using very high resolution (30-sec) global database. They performed the damage assessment with multiple return periods so that annual damage could be calculated by integration of all return period of hazard. However, use of a simple depth-damage function as vulnerability creates large uncertainties of their estimation in global scale. The method seems highly data extensive and requires large resources to perform damage estimation for all kind of hazard events. Moreover, to date, there is no any study reported which exclusively estimate the global pluvial flood damage, and vulnerability distribution of pluvial flood damage in the world.

In this regard, the newly developed statistical model was used to estimate global pluvial flood damage. The risk curves developed using the Japanese database, which establish the relation of hazard events with exposure and vulnerability is a simple empirical tool to estimate pluvial flood damage irrespective of individual flooding characteristics, asset values, and vulnerability of a location. However, to apply the relationships that were produced using Japanese database, for other nations, two basic assumptions were made.

i) Vulnerability distribution within a country is as same as the distribution in Japan. It means bigger cities within a nation have higher level of preparedness than smaller villages and towns, as similar to Japan.

ii) Vulnerability of each country is an inverse function of Human Development Index (HDI). It means the vulnerability of lower HDI country is higher than higher HDI country and varies inversely.

5.2 Forcing data

The global daily precipitation data, global digital elevation data, global population density data and global gross domestic product data were used from different sources, in different spatial and temporal scale. All data were interpolated on to 0.5° spatial

resolution. The EM-DAT damage data and some other country specific flood damage records were also used to perform validation of damage estimation. All forcing data used in this study are summarized in **Table 5.1** and briefly described in following subsections.

Table 5.1 Summary of forcing data, its source and other characteristics

Data	Source	Temporal resolution	Spatial resolution	Time Span	Final Spatial resolution prepared
CPC unified Gauge-based analysis of global daily precipitation	NOAA Climate prediction Center (CPC)	daily	0.5°x 0.5°	1979-2005	0.5°x 0.5°
Population density	RITE, ALPS project	Annual	0.5°x 0.5°	1990-2005	0.5°x 0.5°
Gross Domestic product (GDP)	RITE, ALPS project	Annual	0.5°x 0.5°	1990-2005	0.5°x 0.5°
Elevation	GTOPO30	-	30" x 30"	-	0.5°x 0.5°
Human Development Index (HDI)	United nation HDI reports (1990-2005)	Annual	National	1990-2005	0.5°x 0.5°

5.2.1 Precipitation data

The global daily precipitation data named CPC Unified Gauge-based Analysis of Global Daily Precipitation (Xie *et al.*, 2007, Chen *et al.*, 2008), which are the product of CPC unified precipitation project at NOAA climate Prediction Center, were used in this study. These data were produced at a spatial resolution of 0.5° based on gauged based observation over land and having consistent long term dataset from 1979 to present. The precipitation dataset were divided into two versions: one retrospective version (1979-2005) and other real-time version (2006 - present). The first version uses more than 30,000 gauges. The latter version uses about 17,000 gauges and need further processing to make consistent as retrospective version. To perform consistent analysis, the daily precipitation data for the period 1979-2005 were only utilized in this study.

5.2.1.1 Annual Maximum Daily Precipitation

Annual maximum daily precipitation data were computed from the daily precipitation data for each 0.5° grid, and thereby calculated the exceedance probability of annual

maximum daily precipitation. The average annual maximum daily precipitation for the period 1979-2005 is shown in **Fig. 5.1**.

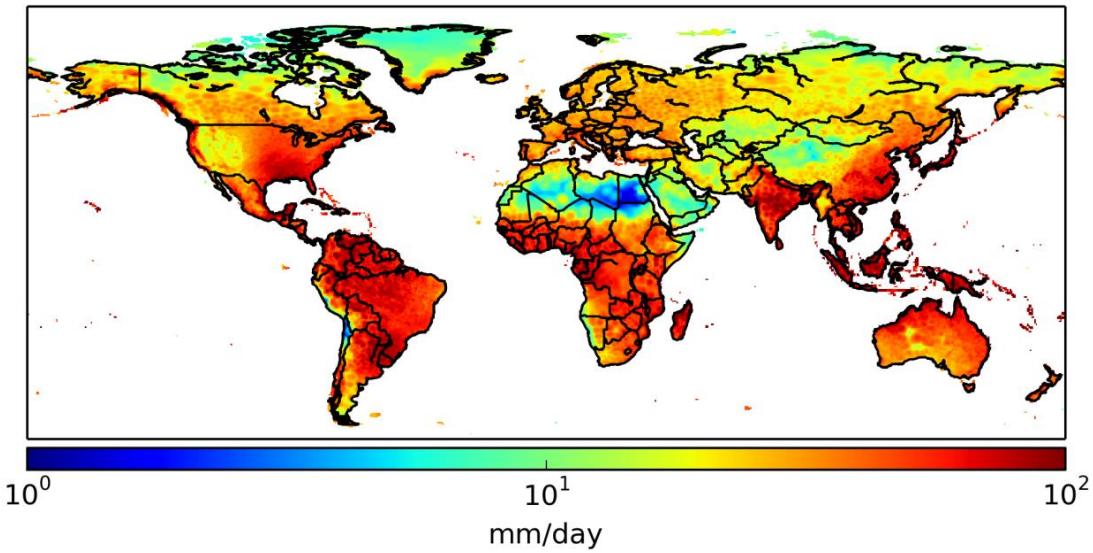

Fig. 5.1 Average annual maximum daily precipitation for the period 1979-2005

In this study, the annual maximum daily rainfall were assumed to follow a Gumbel distribution, and the period 1979-2005 (27 years) were used to calculate Gumbel parameters and thereby exceedance probability (return period) of daily rainfall as described in chapter 3 (section 3.5). The equations 3.4 and 3.5 were used to calculate the Gumbel scale parameter ('*a*') and location parameter ('*b*') respectively. **Figure 5.2** and **5.3** shows the parameter *'a'* and *'b'* respectively for all 0.5° grid in the world.

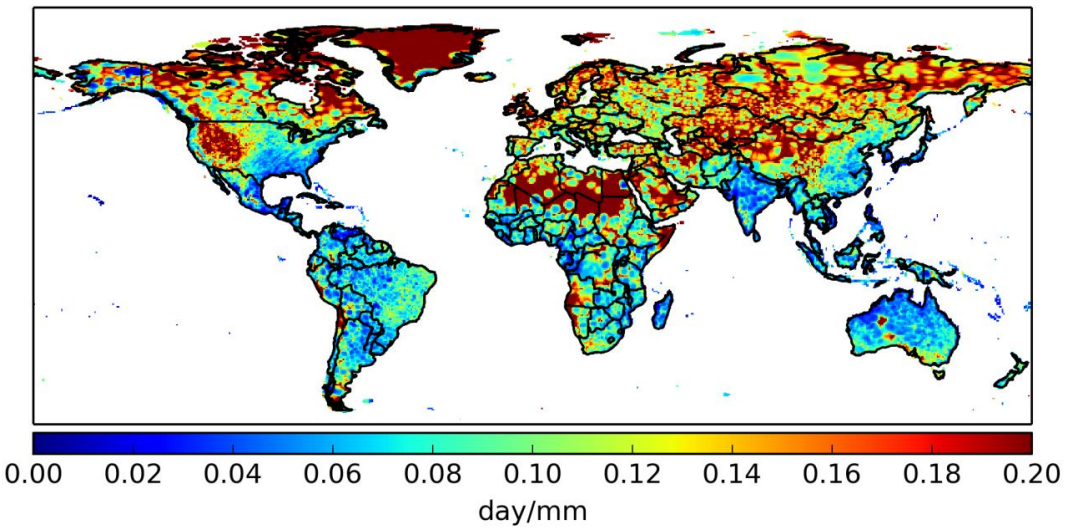

Fig. 5.2 Gumbel parameter "a" in each 0.5° grid in the world

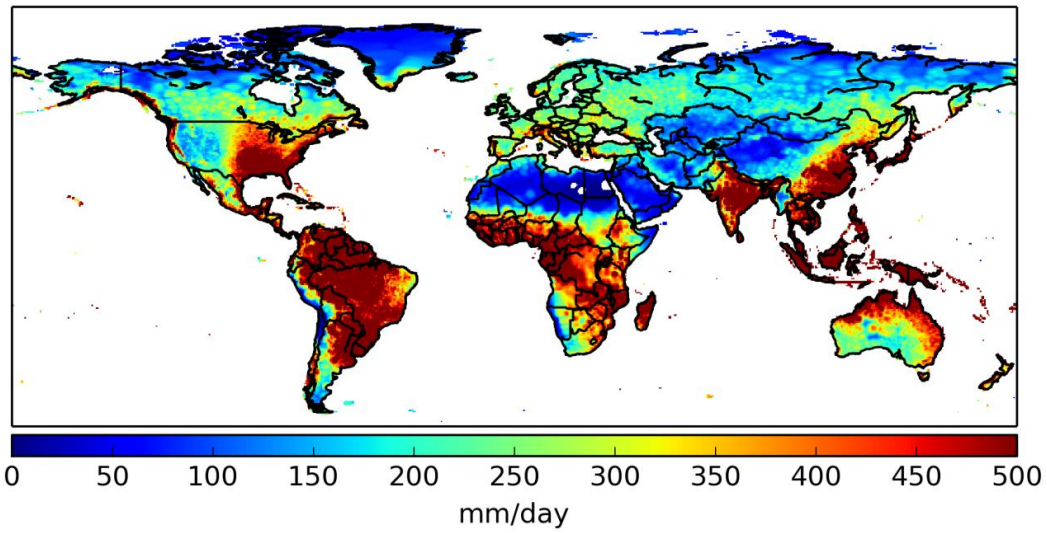

Fig. 5.3 Gumbel parameter "b" in each 0.5˚ grid in the world

5.2.1.2 Goodness of fit test for Gumbel distribution

The goodness of fit of Gumbel distribution to annual maximum daily rainfall in each grid was evaluated using the Probability Plot Correlation Coefficient (PPCC) as described by Vogel, (1986). Calculated PPCC value for each grid was compared with the critical PPCC at 5% significance level. The critical PPCC value tabulated in Vogel, (1986) at 5% significance level for 27 samples is 0.9488. The result shows that more than 79% grids have higher PPCC value than its critical value. **Figure 5.4** shows the grids which have higher PPCC values than critical PPCC showing their goodness to fit in Gumbel distribution for its annual maximum daily precipitation value. Some regions where the test for Gumbel distribution fails were basically attributed to arid African regions and Tibetan plateau. The numbers of gauge stations are highly associated with the accuracy of the precipitation data and the tropical African region is characterize with poor quality of data itself (Chen *et al.*, 2008). However, most other parts of the world showing applicability of Gumbel distribution for precipitation data and hence used in this study. The relation (3.3) and (3.6) were used to calculate exceedance probability of daily rainfall in each grid.

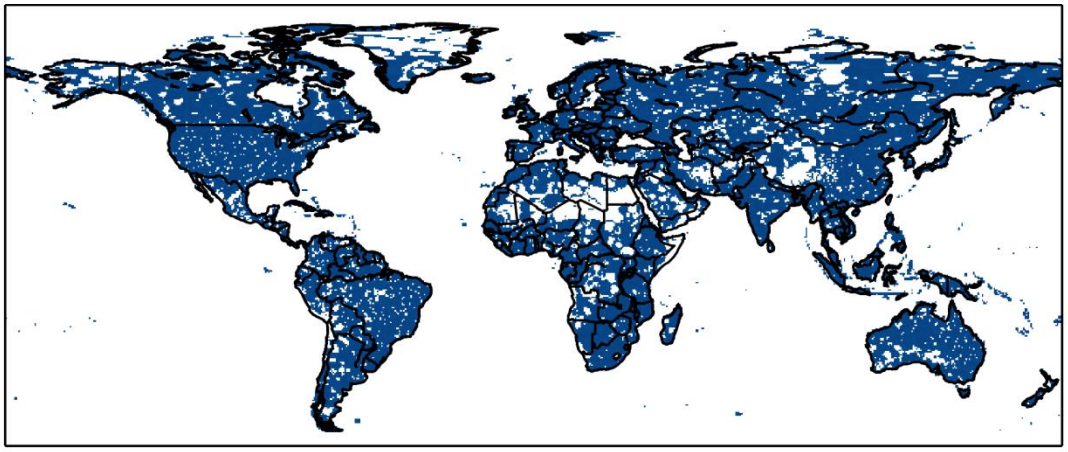

Fig. 5.4 Grids which shows PPCC value greater than critical PPCC in 5% significance level, reveals fitness of Gumbel distribution for annual maximum daily precipitation data

5.2.2 Population density data

Population data, developed under Alternative Pathways towards Sustainable Development and Climate Stabilization (ALPS) project (ALPS, 2011), were used in this study for the period 1990-2005. The population data were originally derived from UN population database, called World population prospect (The 2008 Revision) and gridded to 0.5 ° for entire globe. Population density in each grid was calculated dividing grid population by corresponding grid area. Latitude affect was considered during the process of calculating grid area. Average population density for the period 1990-2005 is shown in **Fig. 5.5**.

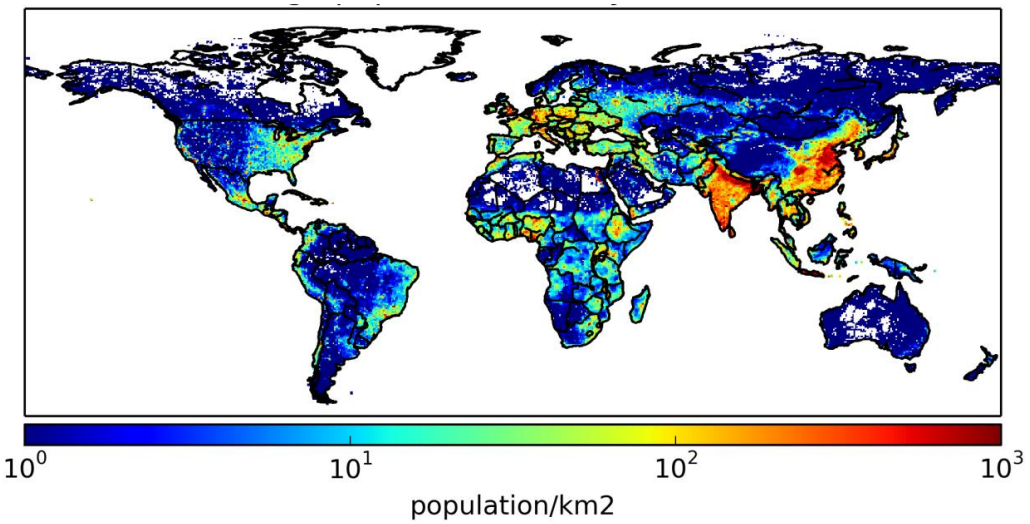

Fig. 5.5 Average population density distribution in the World [1990-2005]

5.2.3 Gross domestic product data

Gridded gross domestic product (GDP) data which were developed by ALPS project (ALPS, 2011) were used. The UN based GDP per capita for each nation was used to derive gridded GDP, hence gridded GDP is just a product of gridded population and GDP per capita of the corresponding nation. The spatial resolution of grid is 0.5° and the price of GDP in each grid is given in US dollar (price level at 2000). **Figure 5.6** shows the distribution of average GDP from 1990-2005 in each grid all over the world.

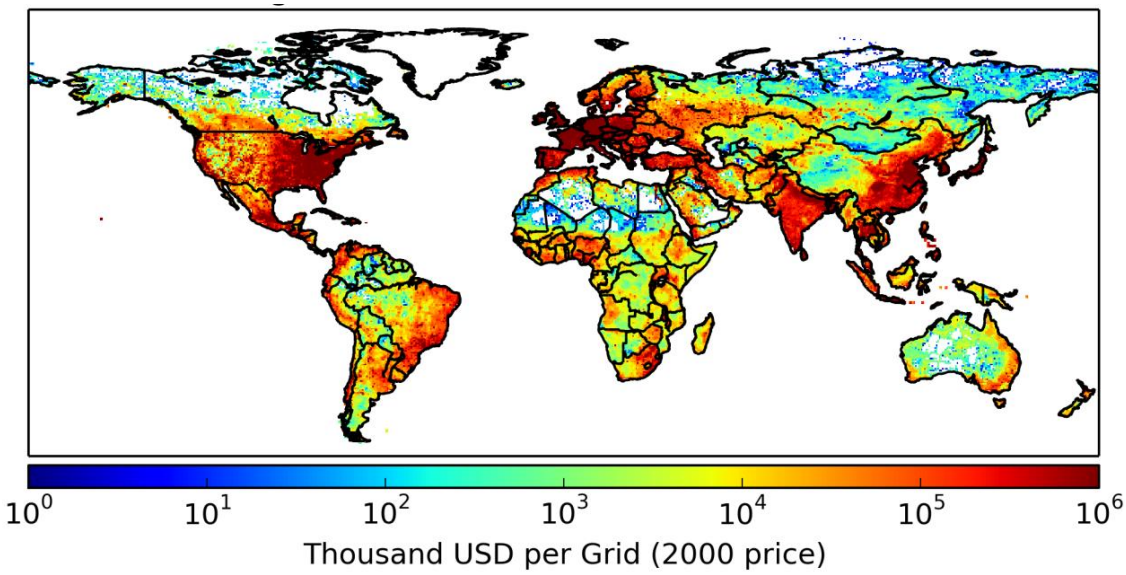

Fig. 5.6 Average gross domestic product distribution in each 0.5° grid in the World [1990-2005] in 2000 price.

5.2.4 Slope data

GTOPO30 digital elevation model (DEM) developed by United States Geological Survey's (USGS, 1996) were used to derive topographical slope in all over the world. These DEM data have spatial resolution of 30 arc-second (about 1 km), which covers latitude from 90° south to 90° north, and longitude of 180° west to 180° east. The original dimension for entire globe hence consists of 21,600 rows and 43,200 columns. Perhaps for easy handling of data and its distribution, these data were divided into 33 small tiles. An algorithm was developed to join all these tiles and prepare a global elevation data. Average maximum slope in each 0.5° grid were calculated as described in section 3.4.5. **Figure 5.7** shows the slope in percentage in each 0.5° grid computed

from method described in section 3.4.5, which was used as topographical slope (*S*) for each grid in the global pluvial flood damage assessment.

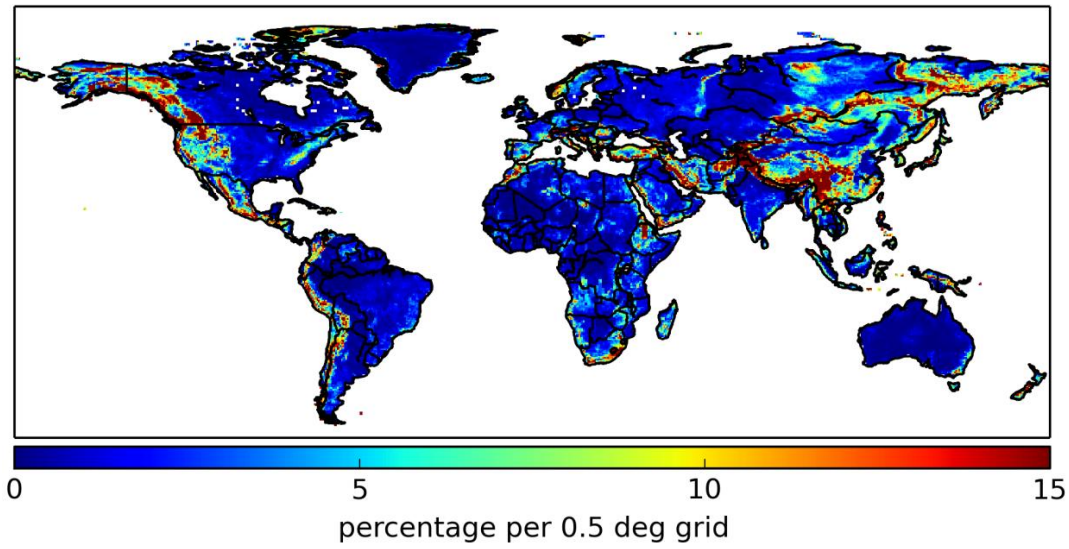

Fig. 5.7 Topographical slope (Average Maximum) for each 0.5˚grid derived from GTOPO30 DEM dataset.

5.2.5 Human development Index (HDI) data

UNDP (2013) described Human Development Index (HDI) as "a measure of average achievements of a country in three basic dimensions of human development: a long and healthy life, access to knowledge, and a decent standard of living". The indices for all three basic dimension are calculated based on life expectancy (years), mean and expected years of schooling, and gross national income per capita (PPP$) within a nation. HDI is the geometric mean of all these three dimension indices. The national scale HDI shows the overall capability of a nation in terms of both social and economic development with one single indicator and is comparable to one country to another. The scale of HDI varies from 0 to 1, and it is obvious that higher the HDI value (close to 1) shows higher social and technological development of a nation. Based on the Human Development Report 2013, **Table 5.2** shows top five and bottom five HDI countries in the world with their HDI values.

Although, the human development reports were published annually from 1990 to 2013, some definitions as well as number of countries included in each report vary,

and hence HDI values given in each report were unsystematic and incomparable to evaluate its temporal variation. The Human Development Report Office (HDRO) hence readjusted and calculated a consistent HDI from 1980 to 2012 [1980-2005 in five years interval and 2006-2012 annually] (HDRO, 2012). These data were used as HDI value from 1990-2005 in this study.

Table 5.2 Top five and Bottom five countries based on their HDI value as given in Human Development Report, 2013

Top five country			Bottom five country		
Rank	Country	HDI	Rank	Country	HDI
1	Norway	0.955	183	Burkina Faso	0.343
2	Australia	0.938	184	Chad	0.340
3	United States	0.937	185	Mozambique	0.327
4	Netherland	0.921	186	Dem. Rep. of Congo	0.304
5	Germany	0.920	186	Niger	0.304

Missing values for any country in any year was determined by linear interpolation/extrapolation method. Annual data from 1990-2005 were also generated using linear interpolation of each five years data. HDI values from 1990-2005 with its annual interpolation for all countries is shown in **Fig. 5.8**.

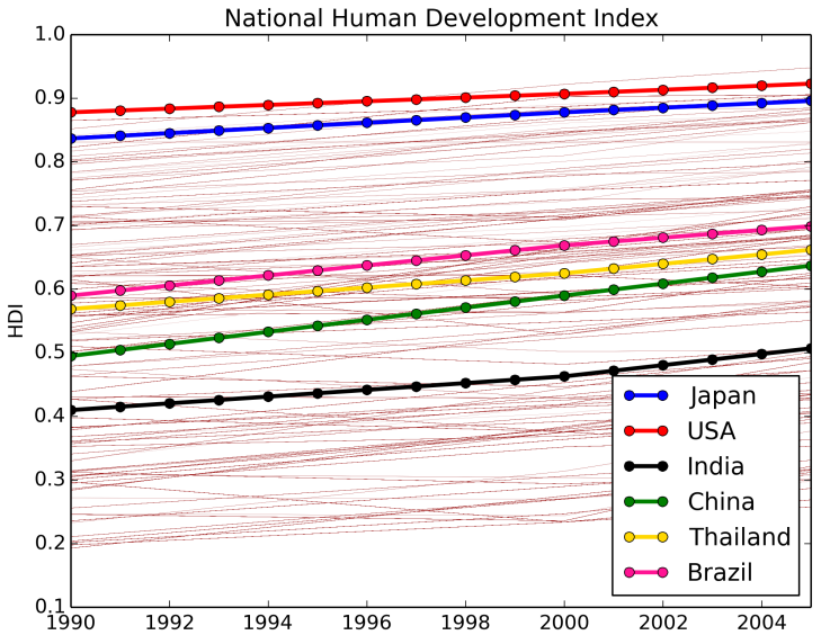

Fig. 5.8 Trend of HDI from 1990-2005 of various countries derived from linear interpolation of five years interval dataset

5.2.5.1 Gridded HDI data

As HDI values were reported for each nation with one value, gridded HDI value smaller than country scale grid were not available so far. For this study, an algorithm was developed to assign each national HDI value onto 0.5° grid. The 0.5° grid were first prepared in which grid value were given by UN national ID corresponding to the grid location. It means the grids falls in one nation were assigned by one ID, which was further used to assigning HDI value for each nation. All 0.5° grids in each nation have thus same HDI value. **Figure 5.9** shows the gridded HDI value in 0.5° grid for the year 1990, 1995, 2000, and 2005.

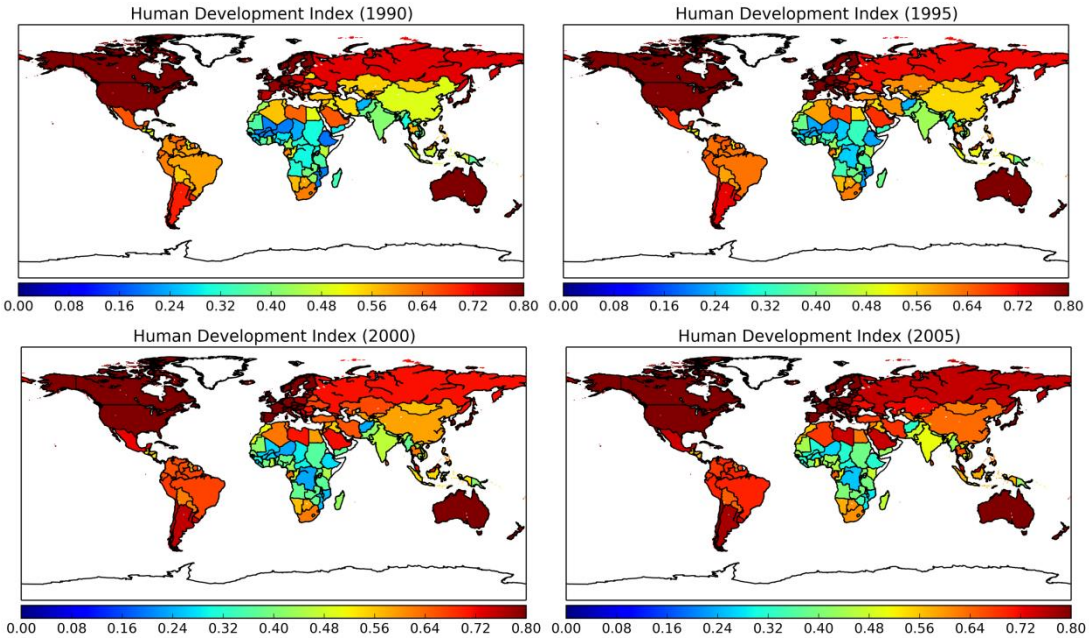

Fig. 5.9 Gridded HDI value in 0.5° grid for the year 1990, 1995, 2000, and 2005. All grids in one nation have same HDI value

5.2.5.2 HDI and national vulnerability

There is no any direct relation discovered so far between the human development index (HDI) of a country and country's vulnerability to natural disaster basically due to scarcity of data. However, some study adopted HDI as an indicator of vulnerability for example Peduzzi *et al.*, (2002), and proposed a relationship of disaster risk in terms of HDI, GDP, urban growth, percentage of arable land and population density depending on disaster type, including floods. The nations with lower HDI (developing

countries) often possess higher damage intensity in terms of disaster fatalities and economic losses expresses as a fraction of their real property values (Handmer *et al.*, 2012) showing higher vulnerability. As vulnerability at a location can be related with social and technological development and resources used for disaster preparedness, and HDI being an indicator of social and economic development of a location, these two are subjectively much similar to each other but inversely related. **Figure 5.10** shows a conceptual relationship between vulnerability (Damage per GDP (DpG)) and HDI.

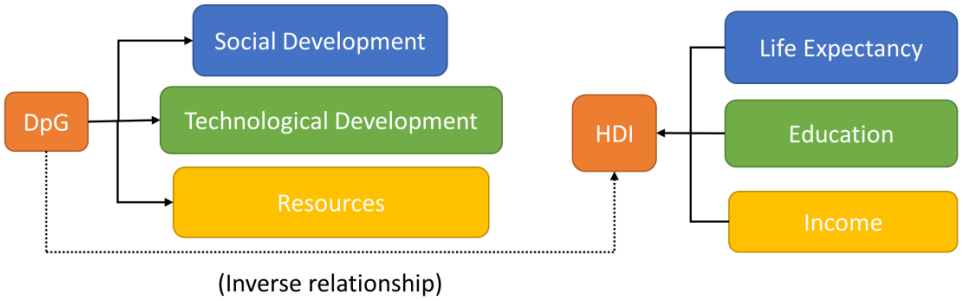

Fig. 5.10 Conceptual relationship between vulnerability and HDI

In this study, vulnerability is hence inversely related with national HDI of a country with one another. More specifically, vulnerability of a country is assumed as an inverse function of HDI to the vulnerability of Japan, so that the parameters value computed for vulnerability (damage cost function) in Japan could be transferred to any other nation. Based on this discussion, the relation 5.1 is adopted to transfer the scale parameter ("*p*") as given in relation (3.1) as:

$$p_o = p_j x \frac{HDI_J}{HDI_o} \text{ ---------- (5.1)}$$

Where, the subscript '*o*' is for other nations, and '*j*' is for Japan. As vulnerability parameter "*p*" is developed from the period 1993-2002 in Japan. An average HDI value for this period is given as 0.87. The relation (5.1) can further reduced to relation (5.2):

$$p_o = p_j x \frac{0.87}{HDI_o} \text{ ---------- (5.2)}$$

The relations (3.8), (3.9), (3.10) and (5.2) were applied to estimate the pluvial flood damage amount in the world, its distribution and estimate average annual national damage exclusively.

5.3 Results for global estimation of pluvial flood damage

The damage occurrence probability functions and damage cost function that derived from the statistical damage, and socio-economic data in Japan as described in chapter 3 were used for the whole globe with the forcing data described in this section. The vulnerability parameter for Japan was transferred to any other nation as relation (5.2) above. Annual damage value in each 0.5° grid was computed with the sum of probable damage amount by each daily rainfall. The results for distribution of global expected annual damage, expected annual national damage, and global annual damage were discussed in the following sub-sections.

5.3.1 Annual and expected annual global pluvial flood damage

Annual global pluvial flood damage were estimated using the mean DpG, 90 percentile DpG and 10 percentile DpG parameters as described in chapter 3 (section 3.6) for the period 1990-2005. The DpG parameter values were transferred to each nation by using relation (5.2) in each grid of 0.5°. Annual variation of total damage (derived from mean DpG parameter), and highest and lowest range (derived from 90^{th} percentile and 10^{th} percentile DpG parameter respectively) is shown in **Fig. 5.11**.

The expected annual pluvial flood damage in this period was 6.3 billion USD (2000 price). Due to the lack of actual pluvial flood damage record in the globe, it is hard to validate the result produced by our model. The exact figure for the total flood damage is also unavailable in global scale. Adikari and Yoshitani (2009) reported based on different global database that an average annual water-related damage during 1990s was about 50 billion USD, and about half of this (25 billion) seems to be caused by floods. Even these were very rough estimate of total flood damage amount; our estimation of global expected annual damage during 1990-2005 (6.3 billion USD) is around 25 % of the total flood damage.

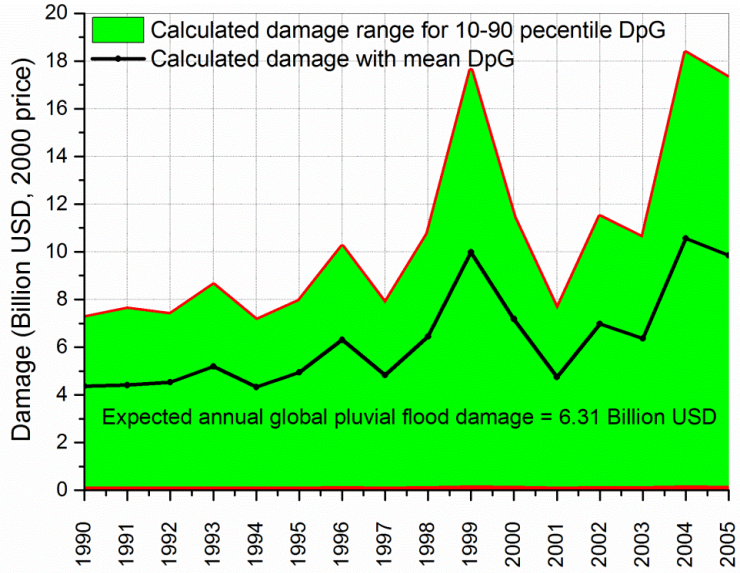

Fig. 5.11 Model estimate of total global pluvial flood damage shown by black line. The green shaded area shows the highest and lowest range of pluvial flood damage.

The model output shows some clear trend of pluvial flood damage as expected also in Adikari and Yoshitani, (2009) from 1990 to 2005. **Figure 5.12 s**hows two more estimates: (i) when the population density and GDP value were fixed at 1990 level; and (ii) population density, GDP, and HDI all three variables were fixed in 1990 level. The figure reveals that the trend is mainly attributed to the rise in GDP in different parts of the globe during 1990-2005.

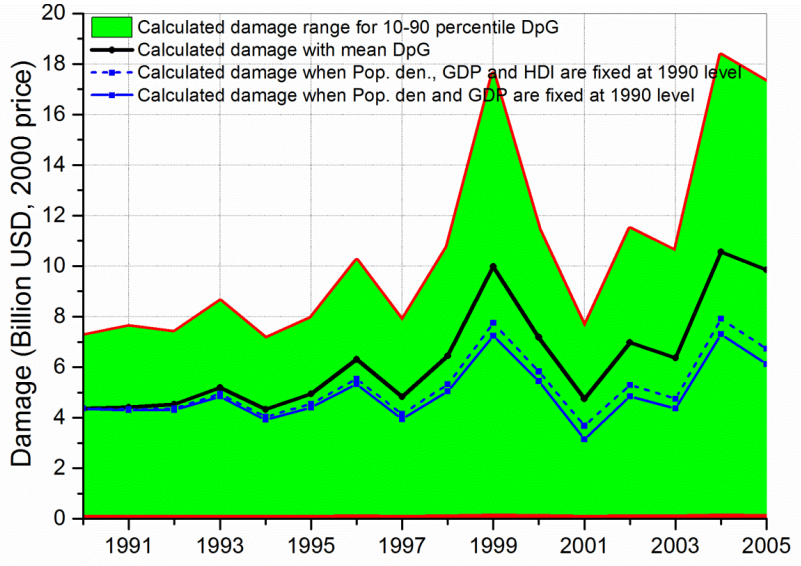

Fig. 5.12 Estimated annual total global pluvial flood damage shown by black line. The solid blue line shows the annual total damage value when population density and GDP are fixed at 1990 values, whereas dotted blue line shows the variation when Population density, GDP and HDI are fixed at 1990 level.

5.3.2 Distribution of expected annual pluvial flood damage in the world

Expected annual pluvial flood damage (1990-2005) in each 0.5˚grid were calculated with each daily rainfall event and the relation described above. The distribution of expected annual pluvial flood damage is shown in **Fig. 5.13.**

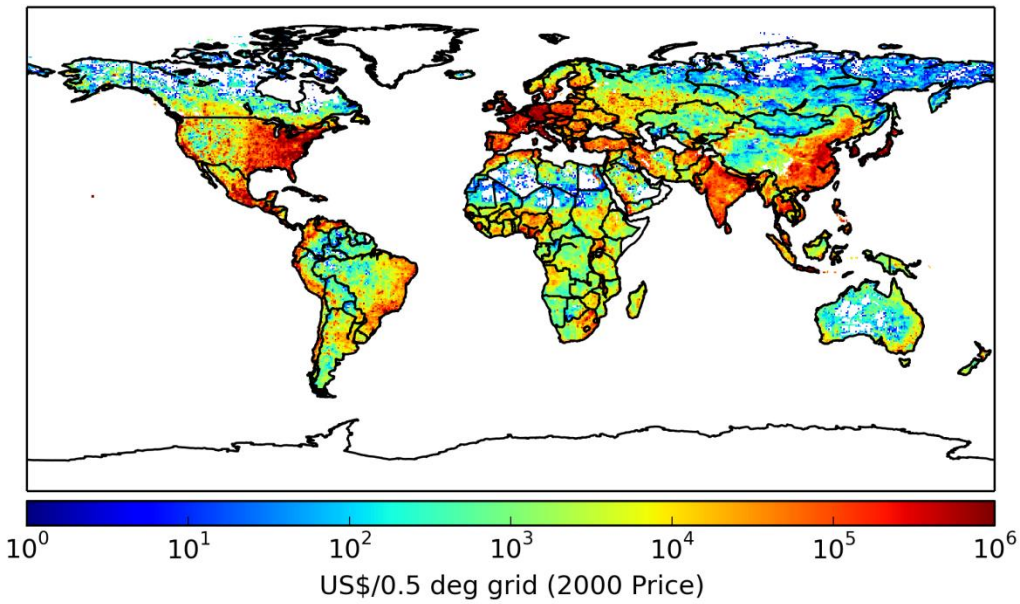

Fig. 5.13 Distribution of expected annual pluvial flood damage in the world in each 0.5˚grid for the period 1990-2005

The figure reveals that the pluvial flood damage is mainly attributed to the high population density and high GDP regions. Absolute amount of damage seems very large in eastern coast of North America, Western Europe, Northern India, Eastern China and Japan. The distribution of flood damage seems comparable with total economic loss distribution computed with different risk deciles in Dilley *et al.*, (2005). Also the distribution of flood damage by this model is similar with the geographic centers of large flood shown by Kundzewicz *et al.*, (2013). Moreover, the distribution of pluvial flood damage in absolute monetary term in global scale is unique and the first estimate to date.

5.3.3 National scale annual pluvial flood damage

As a capability of our model to estimate annual pluvial flood damage in each country, annual pluvial flood for different nations in the world through 1990 to 2005 were also

estimated. Examples for few countries are presented in **Figure 5.14** which shows the annual variation of pluvial flood damage in United States of America, Japan, Philippines, Bangladesh and India from 1990-2005 in million USD (2000 price). The direct validation of these results is very difficult due to the absence of damage record exclusively due to pluvial flooding in other countries (except Japan).

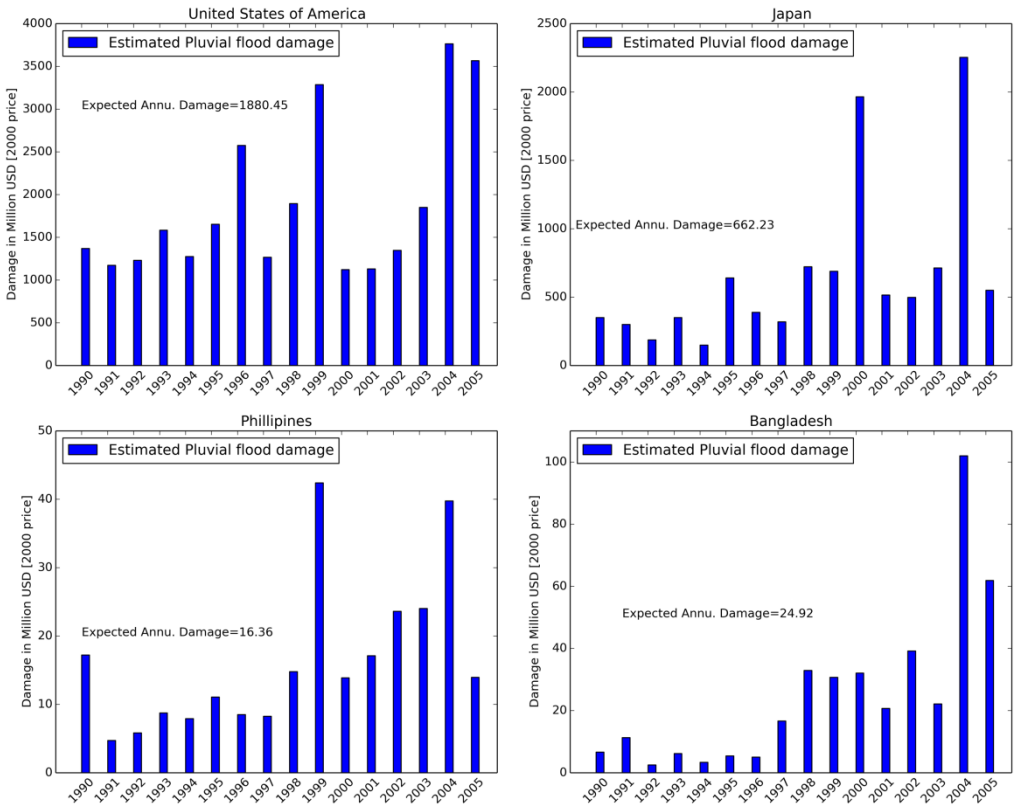

Fig. 5.14 Model estimate of annual variation of total pluvial flood damage in four different countries

5.4 Capability test of the model for other nations

As described in previous section, the damage records in other countries are not found separately due to pluvial flood only, even in developed countries. A long term flood damage data and its distribution from 1926-2000 in the United States of America were developed as National Weather Service (NWS) reanalysis data (Pielke *et al.*, (2002)), however these data also give total flood damage amount only. The definition of floods, damage types and damaged property across the years seems to be varying as well. Hence direct comparison of the result produced by our model could not be performed even in one single country due to the scarcity of recorded data. A comparison of total

flood records for United States of America (NWS reanalysis data) with our model estimate for pluvial flood damage for the period 1990-2000 is shown in **Fig. 5.15**. The figure reveals that most of the lower recorded flood damage years were associated with pluvial flood damage as estimated by the model.

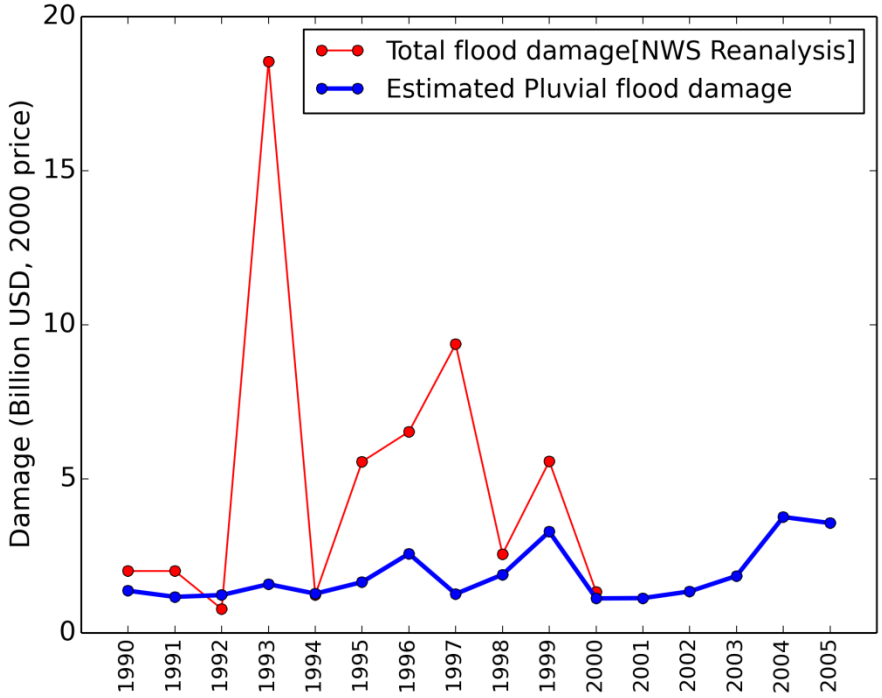

Fig. 5.15 A comparison between total recorded flood damage and estimated pluvial flood damage over the United States of America for the period 1990-2000

As described earlier, some global flood damage recoding databases are available in present day. One of the popular international databases for damage recording is Emergency Events Database (EM-DAT) (*www.emdat.be*) which is maintained by Center for Research on the Epidemiology of Disasters (CRED). The various types of disasters (event wise) are recorded in this database for 1900 through present. Flood damage data is one of them. Due to various criteria of disaster record, all damage produced was not recorded into the data. As described in EM-DAT official webpage (*www.emdat.be/criteria-and-defination*, 2014/05/31), at least one of the following criteria must be fulfilled to record in the database:

- Ten or more people reported killed.
- Hundred or more people reported affected.
- Declaration of a state of emergency.

- Call for international assistance.

Due to the various other social, political and technical reasons, and also due to the criteria, all flood damage in a countries produced by all hazard events were not recorded in these database as mentioned previously in section 3.4.3 and figure 3.5. Due to this reasons, the total annual damage in a country seems very large than recorded in these database especially for monetary flood damage.

The EM-DAT data base classified the flood disaster into three different types: (i) general floods, which include the flood from overflow from river etc., (ii) flash flood, which include the flood events mainly caused by heavy rainfall both in steep slopes river floods and flat slope urban (pluvial) flooding, and (iii) Coastal flood, along the sea-shores due to storm surge from sea water.

While going through the records for individual event and individual country, the author found that the economic damage records are very poor than the record of affected peoples and casualties. Physical losses due to an event are even less recorded for flash flood category. This is why the direct comparison between these data with our result was very difficult.

However, author calculated average annual damage recorded (general + flash) in EM-DAT database for selected 88 countries (countries are selected based on damage data available in the database) (time value of money is not considered for recorded damage data) and performed correlation test with model expected annual pluvial flood damage (2000 price) in same 88 countries. **Figure 5.15** shows the correlation of recorded average annual damage (general + flash) and expected annual pluvial flood damage. The correlation coefficient (=0.69) of these two seems quite good and prevails the national scale average annual damage estimation from proposed model and EM-DAT recorded total flood damage seems highly corresponds to each other in their national trend. However, as explained earlier, damage records in EM-DAT database do not have regular annual flood damage record for a country and only few damage records in monetary terms leads calculated pluvial damage are higher than total flood damage

recorded in many countries. Nevertheless, the nation wise flood producing capability shows its applicability to the whole world.

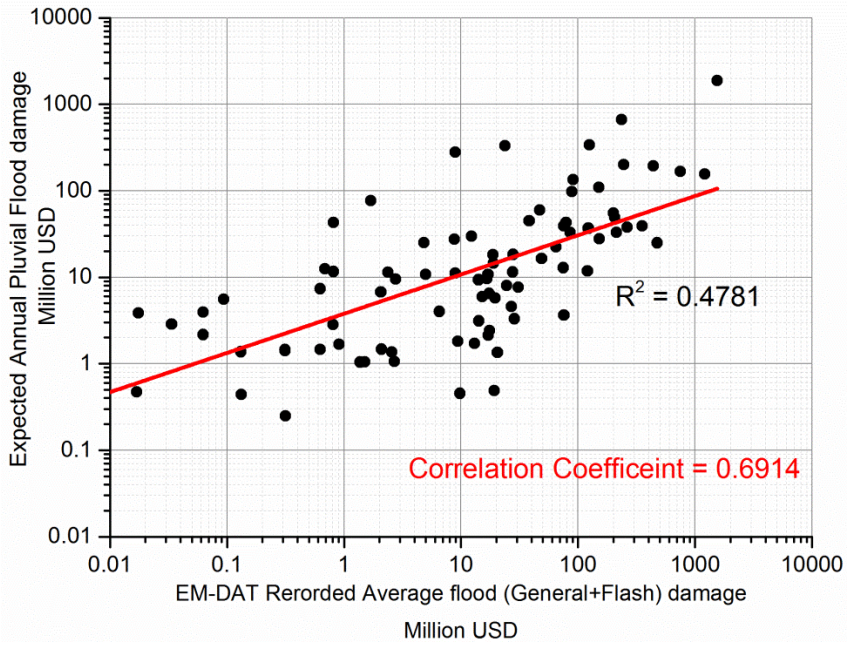

Fig. 5.16 Correlation between the recorded flood damage in EM-DAT (average annual) and expected annual pluvial flood damage in selected 88 nations in the world

5.5 Vulnerability in terms of expected annual DpG in the world

The vulnerability as defined in this study by damage per GDP (DpG) was also calculated to evaluate the vulnerability distribution in the world due to pluvial flood damage. The average annual damage in each grid for the period (1990-2005) in each grid was divided by its average annual GDP for the same period to calculate DpG. **Figure 5.16** shows the distribution of pluvial flood vulnerability in the world, as estimated by the present model.

The figure reveals that very low GDP and low HDI countries or regions have higher vulnerability. Many countries in the Central Africa and South Asia seem to have higher vulnerability than other regions. This vulnerability map also conveys that even very high absolute amount of damage in some developed regions, have very low damage with their property itself showing their resilience somehow to the pluvial flooding. More specifically **Table 5.3** shows the list of 20 countries which are expected to be higher vulnerability based on their annual damage per GDP for the

analysis period (1990-2005). The entire list for all 88 countries is given in appendix section.

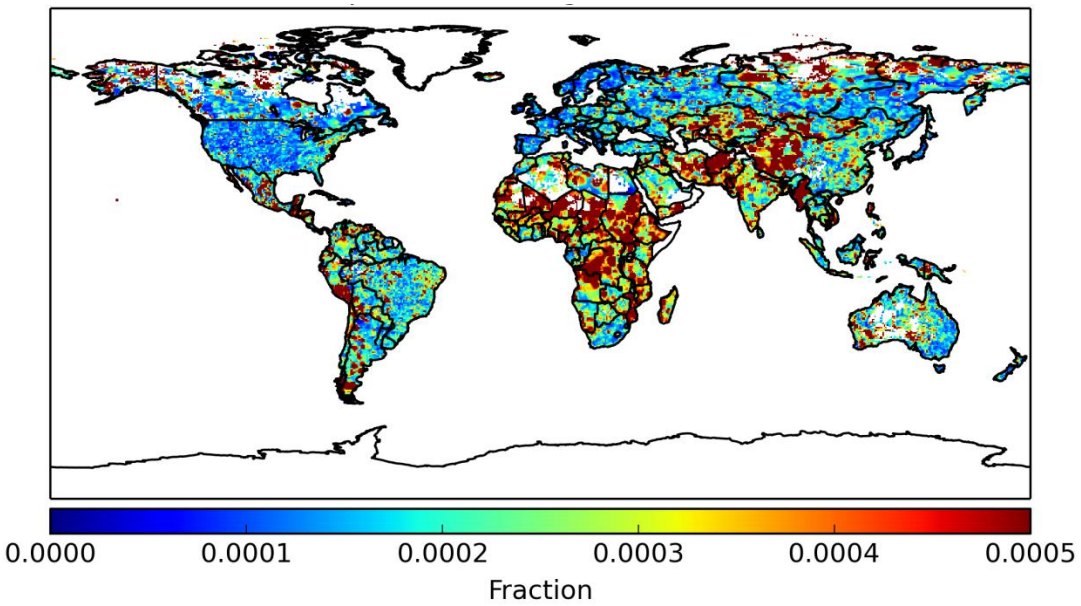

Fig. 5.17 Spatial distribution of expected annual damage per GDP per 0.5° for the period 1990-2005

Table 5.3 List of top 20 vulnerable countries in the world for pluvial flood damage

Vulnerability rank	Country	UN ID	Average HDI [1990-2005]	Expected Damage/GDP
1	Djibouti	262	0.365	0.002005680
2	Myanmar	104	0.374	0.001361891
3	Mozambique	508	0.245	0.001128205
4	Bolivia	68	0.608	0.000971042
5	Honduras	340	0.555	0.000895200
6	Sudan	736	0.351	0.000840865
7	Chad	148	0.281	0.000823175
8	Angola	24	0.364	0.000809908
9	Bangladesh	50	0.422	0.000610403
10	Nigeria	566	0.367	0.000562953
11	Venezuela	862	0.663	0.000539275
12	Brazil	76	0.652	0.000539097
13	Uganda	800	0.363	0.000524896
14	Mexico	484	0.707	0.000496456
15	Pakistan	586	0.429	0.000493045
16	El Salvador	222	0.601	0.000482291
17	Vietnam	704	0.515	0.000469433
18	Tanzania Uni Rep	834	0.372	0.000468695
19	Colombia	170	0.646	0.000463803
20	Yemen	887	0.363	0.000450244

5.6 Limitation of the model in global application

Due to the unavailability of exclusive pluvial flood damage records, the performance of the model in different countries could not be compared directly. The uncertainties of results may arise basically due to the assumptions made while applying the model derived from Japanese database to the globe. The vulnerability distribution within a nation might be different for different countries based on their political, social and economic development. The characteristics of population density distribution in many developing countries are very different than that in Japan. Densely populated regions of many mega cities in these countries often tend to have higher vulnerability due to very low preparedness to flood. A poor-engineered city in terms of flood defense structures (drainage systems) often tends to have larger vulnerability than the cities without such structures. Moreover, the geophysical characteristics other than topographical slope were not considered which might have significant impact on occurrence of pluvial flooding and vary among country to country.

The assumption regarding the inverse relation of vulnerability with human development index might have some uncertainties especially for the very low income counties. The assumption was based on the fact that the higher income nations have larger investment on flood defense infrastructures to mitigate flood risk than that of lower income countries. However, Kellenberg and Mobarak, (2008) argued the increment of disaster risks with income (upto GDP/capita $5044 for flood disaster) before they decreases and follows inverted-U relationship. This implies that the uncertainty in terms of vulnerability due to pluvial flooding seems quite large in very low HDI countries. Nevertheless, the present model seems highly applicable to the medium to high HDI countries which have actually very large physical damage in terms of absolute value.

5.7 Summary

This chapter dealt a way of applying of the statistical model derived in Japan to the entire world. The flexibility of the model in terms of readily available data for socio-economic and topographical characteristics led towards the global application of the

model. The chapter shows the application of the model in each nation, estimating its expected annual damage, and for entire world with gridded distribution of the damage data. Expected annual damage due to pluvial flood in the world is estimated to be around 6.3 billion USD (about 25 % of approximate total flood damage). The absolute damage seems quite large in some developed nations, whereas the distribution of damage per GDP seems to be very high in developing nations. The vulnerability rank produced by the presented model shows Djibouti is the highest vulnerable country in the world following by Myanmar, and then Mozambique. The limitations of the model while applying to other nations were also described in this chapter.

6. Conclusion and Recommendation

6.1 Conclusion

A statistical macro-scale model of risk assessment of pluvial flood damage at a location, incorporating socio-economic data, and topographical characteristics was developed. Based on the statistical database in Japan, two empirical relationships, the damage occurrence probability function and the damage cost function, were established. The former gives a way of calculating exposure, and the latter gives a way of calculating vulnerability of a location, and thereby the damage risk due to pluvial flooding. This newly developed model for estimating damage is depended on the hazard frequency of each daily rainfall event, and hence calculates probable damage from each hazard event and gives total annual damage estimate of a region with area averaged value. The model hence has capability to estimate probable damage from each daily rainfall event in a year, many of which are typically excluded when computing damage for low frequency rainfall events, although the contribution to total damage from medium to high frequency rainfall events are as equal as low frequency events. The author believes that the model will be a simple and robust tool for policy makers to estimate annual damage from pluvial flooding for short term planning and to estimate expected annual damage for long term planning of pluvial flood defense infrastructures.

The research concludes that the damage occurrence probability at a given location primarily depends on its population density and topographical slope. High population densities with gentle slopes result in high occurrence of damage owing to the high concentration of property and the poor natural drainage. The damage occurrence probability due to a hazard event hence is solely depends on the exposure of the location. On the other hand, the research concludes that the damage intensity is higher for smaller towns and cities showing their higher vulnerability. Typically in Japan, mega cities, for example Tokyo and Osaka, reflects their ability to withstand the disaster than some smaller cities and towns, even the occurrence of potentially hazardous rainfall events to these mega cities are very high.

Comparison of the model output with the recorded damage data especially in validation period reveals its capability of producing area averaged annual national damage. The expected annual damage during 1990-2009 (90 billion yen) is quite comparable with the recorded average annual damage (97 billion yen) for the period. The model also performed well to capture the inter-annual variation and also seasonal variation of pluvial flood damage, and concluded the sound performance of the newly developed model.

The model was applied to estimate pluvial flood damage in late 21st century and also to estimate the change of pluvial flood damage and its distribution over Japan. Monthly pluvial flood damage variation and its change in far-future were also presented. The overall trends of pluvial flood damage in 21st century in two future RCP scenarios were also presented. The results from model outputs show a large increment of pluvial flood damage in all over Japan in future for A1B and RCP8.5 scenarios. Total national damage due to pluvial flood over Japan will rise up to 177 ($\pm$44) billion yen in A1B scenario during late 21st century. The damage for RCP2.6 scenario will rise up to 116 ($\pm$17) billion yen and that for RCP8.5 is 274 ($\pm$92) billion yen at 2005 price in the late 21st century. Almost all parts of Japan show increment of pluvial flood damage. The increment seems more severe in central to western Japan. The results further conclude that the vulnerability of western Japan and Tohoku regions seems very high in future climate condition. The future analysis for Japan concludes the need of higher investments for flood control infrastructures (typically drainage facilities) in western Japanese's cities and towns. Further, the largest rise of flood damage is expected in both East Asian monsoon season (Jun-Jul) and typhoon season (Sep-Oct), hence there is a need of high attention and preparedness for both seasons.

In the dissertation, the author described a way of expanding the present model to the entire world, and concluded its applicability to each nations or regions. The vulnerability distribution within a nation was assumed to be distributed as same as Japan for all other nations. The vulnerability of each nation was linked with the popular human development index. Our results concludes that expected annual global

pluvial flood damage is around 6 billion USD (2000 price), which seems to be about 25% of annual total flood damage. The distribution of absolute damage amount shows that highly developed countries and regions are associated with higher damage value, basically due to the high damage occurrence probability as also revealed by Kundzewicz *et al.*, (2013). Expected annual pluvial flood damage on the national scale seems highly correlated with the total flood damage recorded so far and well capture the pluvial flood damage in each nation, although their direct validation cannot be performed due to unavailability of pluvial flood damage record in rest of the world. Moreover, it is concluded that the vulnerability to the pluvial flood is higher in some developing regions, typically in central Africa and South-Asia, owing to the fact of their low GDP and low HDI values. This conclusion with specific country level damage per GDP data is very alike to our understanding of vulnerability and damage. However, some uncertainties remain in the global scale estimation due to various limitations of current assumptions.

The author believes that the methodology described in this dissertation has a high capability of estimating pluvial flood damage to general property and very useful for all stockholders of risk assessment field. The model can be utilized by all level of technical and non-technical personnel for rapid estimation of damage associated with pluvial flooding.

6.2 Achievements and Scientific significance

The research elaborated in this dissertation brought out with a macro-scale model for pluvial flood damage estimation, which itself is a worthy scientific gain in the field of disaster risk assessment. The model can estimate total national annual damage which is a very useful data to engineers and policy makers for economic evaluation of proposed infrastructure plan, typically in feasibility study. The elimination of the use of advance hydrological models and irrespective of types of property at a location widens the scope of this model for all levels of technical expertise and in all regions in the world. The need of macro scale readily available data extends its application to the global scale analysis. The model further can be used to see the different scenarios for

future climate and can be used in future adaptation planning, which is a great concern of today's society.

The study further contributes to understand the relation between hazard, exposure and vulnerability. Each governing components of disaster risk are well quantified in numeric values, and finally provides the absolute damage amount. The author believes that this study will be a mile-stone to identify proper parameters for hydrological models, and vulnerability models and their improvements in regard to damage assessment due to all types of flooding.

6.3 Recommendation

The future scope of this research work is to expand the model further to both micro and meso scales. There is still a large need of micro scale damage assessment so that economic valuation of a particular small flood control infrastructure could be achieved. The author recommends the use of the prescribed methodology in some urban areas. Some parameters, for example land use pattern, and urban drainage density could be incorporated to define the damage occurrence probability and damage cost functions for micro scale use of the proposed model. The model has a capability to be used in hydrological basin scale, however proper calibration of the parameters in each catchment might be necessary with data in higher spatial resolutions.

The validation of results for other nations are still a big challenge for the proposed model, basically due to the lack of pluvial flood damage record in other nations. However, author claims that the proposed methodology can be applied to every nation, if their data permits for calibration of DOP and DpG parameters independently. Nevertheless, this study proposed a way to transfer the parameters value optimized for Japan to other nation and the results seem reasonable. The author further recommends studying of pluvial damage using this model and evaluates characteristics of pluvial flooding in some nations as a case study. The inverse relation between HDI and vulnerability can be redefined so that the uncertainty in the vulnerability calculation on very low income countries can be reduced; however validation of the results still

demands the recorded data. A future projection of pluvial flood damage in global scale is also recommended.

During the research progress, author feels that the international database should be well standardized for all nations and their temporal and spatial disintegration are further needed. The actual damage type and flood type should be well defined so that calibration and validation of model output could be performed for specific flood and damage type. Further, many small scale damages were not recorded in these international database, in this regard, the author recommends to expand the technical matters to tie up with national scale damage database.

The statistical model described in this study only accounts tangible general property damage. Author recommends incorporating other tangible damages, for example agriculture, and infrastructures. However, both have very large uncertainty in damage amount, which might also depend on timing and duration of an event. Moreover, author considers that the same methodology could be applied for fluvial flood damage assessment, so that the total flood damage could be estimated.

Practically pluvial flood damage is more sensitive to sub-daily scale precipitation. Intense rainfall in few hours often causes a huge flooding in some urban regions. This feature is not captured well in the present study, as daily rainfall data relate the daily damage amount. Present damage data recording technique is not sufficient for a statistical model to estimate sub-daily scale damage. At this stage, author recommends for concern authorities to advance the damage recording technique. Spatial and temporal both features are very important. Damage records could be given by latitude and longitude of spatial extent of flooding (at least center of flooding area). The damage records are often recorded for some duration (days). The temporal disintegration could be done as per the observation, and daily damage could be given with the percentage of total damage during an event period.

Further, the functions and results discussed with this research provide some insight for further improvement of present integrated physical hydrological modelling technique

for flood risk assessment which might have capability to assess flood damage in micro scale and also incorporate localized heavy rainfall of sub-daily scale.

Appendix

A. Annual GDP adopted from IMF database for Japan from 1980-2012

YEAR	JAPAN
1980 年	246464.5
1981 年	264966.3
1982 年	278179.0
1983 年	289314.6
1984 年	307498.7
1985 年	330260.6
1986 年	345644.5
1987 年	359458.4
1988 年	386427.8
1989 年	416245.9
1990 年	449392.3
1991 年	476431.0
1992 年	487961.5
1993 年	490934.2
1994 年	495743.5
1995 年	501706.9
1996 年	511934.8
1997 年	523198.3
1998 年	512438.6
1999 年	504903.1
2000 年	509860.0
2001 年	505543.3
2002 年	499147
2003 年	498854.7
2004 年	503725.4
2005 年	503903.0
2006 年	506687.0
2007 年	512975.2
2008 年	501209.3
2009 年	471138.6
2010 年	481784.5
2011 年	468191.1
2012 年	474558.6

billion yen

(c)世界経済のネタ帳

出典: IMF - World Economic Outlook Databases(2012 年 10 月版)

B. Probability Plot Correlation coefficient basic theory based on Vogel, (1986)

The probability Plot Correlation Coefficient (PPCC) is given as:

$$PPCC = \frac{\sum_{i=1}^{n}(X_i - \bar{X})(M_i - \overline{M})}{\sqrt{\sum_{i=1}^{n}(X_i - \bar{X})^2 \sum_{i=1}^{n}(M_i - \bar{M})^2}}$$

Where, X_i = Ordered observation of annual maximum values.

M_i = Ordered statistical median derived from Gumbel distribution

For Gumbel distribution, the cumulative distribution function can be written as:

$F(x) = e^{-exp\{-a(x-b)\}}$

Where, Gumbel parameter *a* and *b* is calculated by the method of moment (Euler's Formula):

$$a = \frac{\sqrt{6\pi}}{6\sigma}$$

where, σ is the standard deviation of observed data series.

$$b = \mu - \frac{0.5772}{a}$$

where, μ is the mean of observed data series.

The inverse of Gumbel cumulative distribution function can be written as:

$$F^{-1}(F'(x_i)) = [a*b - ln(-ln(F'(x_i)))]/a = M_i$$

This relation is used the calculation of i^{th} statistical median. Gringorten plotting position for Gumbel distribution is used to calculate $F'(X_i)$ for i^{th} order median value and given as:

$$F'(X_i) = \frac{i - 0.44}{n + 0.12}$$

The calculated *PPCC* value is compared with *Critical PPCC* as given in *Critical Point table.*

C. Critical value table for Gumbel distribution (Based on Vogel (1986))

Table: Critical point of 1000(1-r'), where r' is the Gumbel probability plot correlation coefficient						
	Significance Level					
n	**0.005**	**0.01**	**0.05**	**0.10**	**0.25**	**0.50**
10	156.000	137.000	91.600	74.000	49.600	32.000
20	114.000	294.000	61.000	48.300	33.330	21.700
30	99.200	80.900	47.400	37.800	25.400	16.900
40	85.900	71.400	40.600	31.100	21.400	13.800
50	73.700	61.100	35.400	27.100	18.200	12.100
60	66.600	53.300	31.500	24.000	16.100	10.600
70	57.200	49.400	28.000	21.300	14.400	9.430
80	59.700	47.500	25.300	19.600	13.100	8.610
90	53.000	44.600	23.600	18.100	11.900	7.970
100	48.300	40.400	22.100	16.900	11.200	7.390
200	30.100	23.700	13.400	10.200	6.730	4.450
300	22.500	18.100	9.790	7.490	4.910	3.230
500	15.300	12.200	6.670	5.010	3.330	2.200
1000	8.230	6.660	3.780	2.920	1.930	1.280
2000	4.770	3.820	2.090	1.610	1.090	0.736
3000	3.230	2.610	1.500	1.160	0.779	0.528
5000	1.950	1.590	0.975	0.756	0.507	0.344
10000	1.120	0.858	0.525	0.414	0.277	0.190
This table is based upon 10,000 replicate experiments						

D. DOP calculation table for population density class 0-250 km^2

Exceedance probability bins		Mean Value	Dam Day	Total days	Probability of Damage
0	0.01	0.005	12	118	0.10169492
0.01	0.1	0.055	279	3592	0.07767261
0.1	0.2	0.15	211	3885	0.05431145
0.2	0.3	0.25	141	4064	0.03469488
0.3	0.4	0.35	120	4777	0.02512037
0.4	0.5	0.45	139	6175	0.02251012
0.5	0.6	0.55	106	7962	0.01331324
0.6	0.7	0.65	97	10711	0.00905611
0.7	0.8	0.75	104	16965	0.00613027
0.8	0.9	0.85	139	39947	0.00347961
0.9	0.95	0.925	97	43478	0.00223101
0.95	0.99	0.97	127	153740	0.00082607
0.99	1	0.995	535	2994588	0.00017866

E. DOP calculation table for population density class 250-2000 km^2

Exceedance probability bins		Mean Value	Dam Day	Total days	Probability of Damage
0	0.01	0.005	23	54	0.425925926
0.01	0.1	0.055	213	1008	0.211309524
0.1	0.2	0.15	173	1154	0.149913345
0.2	0.3	0.25	162	1341	0.120805369
0.3	0.4	0.35	121	1423	0.085031623
0.4	0.5	0.45	117	1620	0.072222222
0.5	0.6	0.55	128	2201	0.058155384
0.6	0.7	0.65	101	2937	0.034388832
0.7	0.8	0.75	115	4594	0.025032651
0.8	0.9	0.85	128	8891	0.014396581
0.9	0.95	0.925	109	10582	0.010300510
0.95	0.99	0.97	215	33997	0.006324087
0.99	1	0.995	651	835248	0.000779409

F. GTOPO30 DEM tiles for its Global scale data and its nomenclature

GTOPO30 tiles

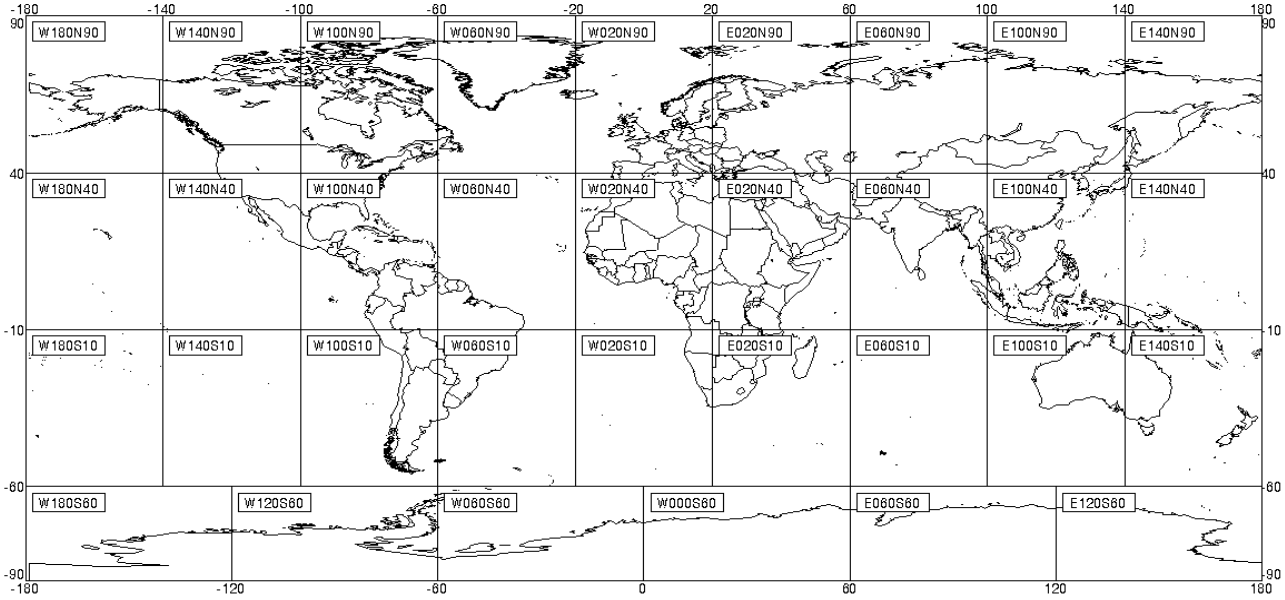

ftp://edcftp.cr.usgs.gov/data/gtopo30/global/

Tile	Latitude Min.	Latitude Max.	Longitude Min.	Longitude Max.	Elevation Min.	Elevation Max.	Elevation Mean	Elevation Std. Dev.
W180N90	40	90	-180	-140	1	6098	448	482
W140N90	40	90	-140	-100	1	4635	730	596
W100N90	40	90	-100	-60	1	2416	333	280
W060N90	40	90	-60	-20	1	3940	1624	933
W020N90	40	90	-20	20	-30	4536	399	424
E020N90	40	90	20	60	-137	5483	213	312
E060N90	40	90	60	100	-152	7169	509	698
E100N90	40	90	100	140	1	3877	597	455
E140N90	40	90	140	180	1	4588	414	401
W180N40	-10	40	-180	-140	1	4148	827	862
W140N40	-10	40	-140	-100	-79	4328	1321	744
W100N40	-10	40	-100	-60	1	6710	375	610
W060N40	-10	40	-60	-20	1	2843	212	168
W020N40	-10	40	-20	20	-103	4059	445	298
E020N40	-10	40	20	60	-407	5825	727	561
E060N40	-10	40	60	100	1	8752	1804	1892
E100N40	-10	40	100	140	-40	7213	692	910
E140N40	-10	40	140	180	1	4628	549	715
W180S10	-60	-10	-180	-140	1	2732	188	297
W140S10	-60	-10	-140	-100	1	910	65	124
W100S10	-60	-10	-100	-60	1	6795	1076	1356
W060S10	-60	-10	-60	-20	1	2863	412	292
W020S10	-60	-10	-20	20	1	2590	1085	403
E020S10	-60	-10	20	60	1	3484	893	450
E060S10	-60	-10	60	100	1	2687	246	303
E100S10	-60	-10	100	140	1	1499	313	182
E140S10	-60	-10	140	180	1	3405	282	252
W180S60	-90	-60	-180	-120	1	4009	1616	1043
W120S60	-90	-60	-120	-60	1	4743	1616	774
W060S60	-90	-60	-60	0	1	2916	1866	732
W000S60	-90	-60	0	60	1	3839	2867	689
E060S60	-90	-60	60	120	1	4039	2951	781
E120S60	-90	-60	120	180	1	4363	2450	665
ANTARCP	-90	-60	-180	180	1	4748	2198	1016

G. Rank of 88 selected countries as per the vulnerability level for pluvial flood damage with their DpG value

Vulnerability rank	Country	UN ID	Average HDI [1990-2005]	Calculated Damage/GDP
1	Djibouti	262	0.365	0.00200568
2	Myanmar	104	0.374	0.001361891
3	Mozambique	508	0.245	0.001128205
4	Bolivia	68	0.608	0.000971042
5	Honduras	340	0.555	0.0008952
6	Sudan	736	0.351	0.000840865
7	Chad	148	0.281	0.000823175
8	Angola	24	0.364	0.000809908
9	Bangladesh	50	0.422	0.000610403
10	Nigeria	566	0.367	0.000562953
11	Venezuela	862	0.663	0.000539275
12	Brazil	76	0.652	0.000539097
13	Uganda	800	0.363	0.000524896
14	Mexico	484	0.707	0.000496456
15	Pakistan	586	0.429	0.000493045
16	El Salvador	222	0.601	0.000482291
17	Vietnam	704	0.515	0.000469433
18	Tanzania Uni Rep	834	0.372	0.000468695
19	Colombia	170	0.646	0.000463803
20	Yemen	887	0.363	0.000450244
21	Iran	364	0.626	0.000427546
22	Ecuador	218	0.658	0.000419846
23	Mongolia	496	0.581	0.000417302
24	Cambodia	116	0.425	0.000407226
25	Sri-Lanka	144	0.648	0.000402163
26	Cuba	192	0.702	0.000398455
27	Ethiopia	231	0.261	0.000393816
28	India	356	0.460	0.000390558
29	Nepal	524	0.390	0.000376206
30	Nicaragua	558	0.526	0.000375914

31	Congo	178	0.499	0.000375247
32	Madagascar	450	0.413	0.000369271
33	Kazakhstan	1007	0.643	0.000356929
34	Belgium	56	0.861	0.000356409
35	Tunisia	788	0.618	0.000354019
36	Morocco	504	0.503	0.000335904
37	Ghana	288	0.459	0.000318007
38	Papua New Guinea	598	0.404	0.000312343
39	Thailand	764	0.618	0.000312281
40	Egypt	818	0.573	0.000312204
41	Malawi	454	0.336	0.00031065
42	Australia	36	0.907	0.000309812
43	Belarus	112	0.643	0.000305134
44	Zimbabwe	716	0.385	0.000299436
45	Senegal	686	0.404	0.000297196
46	Chile	152	0.750	0.000290724
47	Romania	642	0.723	0.000289611
48	Tajikistan	762	0.575	0.000289038
49	Algeria	12	0.622	0.000280465
50	Laos	418	0.442	0.000279670
51	Botswana	72	0.592	0.00027766
52	Kyrgyzstan	417	0.597	0.00026338
53	Philippines	608	0.670	0.000262175
54	Ukraine	804	0.701	0.000262071
55	Moldova	498	0.626	0.000260887
56	Indonesia	360	0.531	0.000255382
57	Hungary	348	0.774	0.000245396
58	Poland	616	0.771	0.000245084
59	South Korea	410	0.821	0.000244077
60	Kenya	404	0.460	0.000242902
61	Bulgaria	100	0.727	0.000237301
62	South Africa	710	0.615	0.000236612
63	Malaysia	458	0.696	0.000223948
64	USA	840	0.902	0.000219141
65	Canada	124	0.886	0.000210225

66	Austria	40	0.837	0.000204363
67	Greece	300	0.814	0.00019644
68	Argentina	32	0.742	0.000192436
69	Germany	276	0.858	0.000191157
70	Costa Rica	188	0.700	0.000184002
71	Turkey	792	0.632	0.000181378
72	New-Zealand	554	0.876	0.000163218
73	France	250	0.838	0.000161296
74	Italy	380	0.824	0.000160578
75	Japan	392	0.870	0.000159282
76	Switzerland	756	0.873	0.000153075
77	Panama	591	0.712	0.000151136
78	Slovakia	703	0.784	0.000147943
79	UK	826	0.830	0.000142819
80	Ireland	372	0.859	0.000141612
81	Netherland	528	0.877	0.000139467
82	Portugal	620	0.764	0.000139144
83	Spain	724	0.822	0.000133922
84	Norway	578	0.907	0.000132978
85	Dominican Republic	214	0.631	0.000124309
86	Swaziland	748	0.513	0.000116798
87	Slovenia	705	0.830	0.000110662
88	Luxemburg	442	0.844	8.17102E-05

References

Adikari, Y. and Yoshitani, J., 2009. Global Trends in Water-Related Disasters : an insight for policymakers The United Nations World Water Development Report 3 Water in a Changing World. Paris, France.

Allen, K. M., 2006. Community-based disaster preparedness and climate adaptation: local capacity-building in the Philippines. *Disasters* 30(1), 81–101. doi:10.1111/j.1467-9523.2006.00308.x

ALPS, 2011. No Title. *Development of Long-term Socioeconomic Scenarios*. Retrieved from http://www.rite.or.jp/Japanese/labo/sysken/research/alps/baselinescenario/E-ScenarioOutline_POPGDP_20110815.pdf

Apel, H., Aronica, G. T., Kreibich, H. and Thieken, A. H., 2009. Flood risk analyses—how detailed do we need to be? *Natural Hazards* 49, 79–98. doi:10.1007/s11069-008-9277-8

Arakawa, A. and Schubert, W. H., 1974. Interaction of a Cumulus Cloud Ensemble with the Large-Scale Environment, Part I. *Journal of the Atmospheric Sciences* 31, 674.

Asian Development Bank, 2013. Investing in Resilience: Ensuring a Disaster-Resistant Future. Mandaluyong City, Philippines. Retrieved from www.adb.org

Baddiley, P., 2003. The flood risk in Cairns. *Natural hazards* 155–164. Retrieved from http://link.springer.com/article/10.1023/A:1026114316844

Baldassarre, G. Di, Montanari, A., Lins, H., Koutsoyiannis, D., Brandimarte, L. and Blöschl, G., 2010. Flood fatalities in Africa: From diagnosis to mitigation. *Geophysical Research Letters* 37(22). doi:10.1029/2010GL045467

Bentsen, M., Bethke, I., Debernard, J. B., Iversen, T., Kirkevåg, a., Seland, Ø., Drange, H., Roelandt, C., Seierstad, I. a., Hoose, C. and Kristjánsson, J. E., 2013. The Norwegian Earth System Model, NorESM1-M – Part 1: Description and basic evaluation of the physical climate. *Geoscientific Model Development* 6(3), 687–720. doi:10.5194/gmd-6-687-2013

Birkmann, J., 2007. Risk and vulnerability indicators at different scales:Applicability, usefulness and policy implications. *Environmental Hazards* 7(1), 20–31. doi:10.1016/j.envhaz.2007.04.002

Blaikie, P., Cannon, T., Davis, I. and Wisner, B., 1994. *At Risk: Natural Hazards, People's vulnerability and Disaster*, 1st ed. Routledge, London.

Bouwer, L. M., Bubeck, P. and Aerts, J. C. J. H., 2010. Changes in future flood risk due to climate and development in a Dutch polder area. *Global Environmental Change* 20(3), 463–471. doi:10.1016/j.gloenvcha.2010.04.002

Bouwer, L. M., 2013. Projections of future extreme weather losses under changes in climate and exposure. *Risk analysis* 33(5), 915–30. doi:10.1111/j.1539-6924.2012.01880.x

Brown, C. A. and Graham, W. J., 1988. ASSESSING THE THREAT TO LIFE FROM DAM FAILURE1 Loss of Life]. *Water Resources Bulletin* 24(6).

Büchele, B., Kreibich, H., Kron, a., Thieken, a., Ihringer, J., Oberle, P., Merz, B. and Nestmann, F., 2006. Flood-risk mapping: contributions towards an enhanced assessment of extreme events and

associated risks. *Natural Hazards and Earth System Science* 6(4), 485–503. doi:10.5194/nhess-6-485-2006

Chan, L. S., Chen, Y., Chen, Q., Liu, J., Dong, W. and Shah, H., 1998. Assessment of global seismic loss based on macroeconomic indicators. *Natural hazards* 269–283. doi:10.1023/A:100806051037

Chen, M., Shi, W., Xie, P., Silva, V. B. S., Kousky, V. E., Wayne Higgins, R. and Janowiak, J. E., 2008. Assessing objective techniques for gauge-based analyses of global daily precipitation. *Journal of Geophysical Research* 113(D4), D04110. doi:10.1029/2007JD009132

Choi, O. and Fisher, A. N. N., 2003. THE IMPACTS OF SOCIOECONOMIC DEVELOPMENT AND CLIMATE CHANGE ON SEVERE WEATHER CATASTROPHE LOSSES: MID-ATLANTIC REGION (MAR) AND THE U.S. *Climatic Change* 58, 149–170. Kluwer Academic Publishers.

Cross, J. A., 2001. Megacities and small towns : different perspectives on hazard vulnerability. *Environmental Hazards* 3(2001), 63–80.

CSIS UT, 2013. Tools and utilities using the position reference technology - Geocoding Tools & Utilities. Retrieved October 17, 2013, from http://newspat.csis.u-tokyo.ac.jp/geocode/

Davidson, R., 1997. *An Urban Earthquake Diaster Risk Index*, report no. Standford, California: The John A. Blume Earthquake Engineering Center.

Dekay, M. L. and Mcclellandl, G. H., 1993. Predicting Loss of Life in Cases of Dam Failure and Flash Flood. *Risk analysis* 13(2).

Dilley, M., Chen, R. S., Deichmann, U., Lerner-Lam, A. . and Arnold, M., 2005. Natural Disaster Hotspots: A Global Risk Analysis: Synthesis Report.

Dilley, M., Chen, R. S., Deichmann, U., Lerner-Lam, A. L., Arnold, M., Agwe, J., Buys, P., Kjkstad, O., Lyon, B. and Yetman, G., 2005. Natural Disaster Hotspots: A Global Risk Analysis-Synthesis Report. World bank.

Dirks, K. N., Hay, J. E., Stow, C. D. and Harris, D., 1998. High-resolution studies of rainfall on Norfolk Island Part II : Interpolation of rainfall data. *Journal of Hydrology* 208, 187–193.

Douglas, I., 2009. Climate change, flooding and food security in south Asia. *Food Security* 1(2), 127–136. doi:10.1007/s12571-009-0015-1

Dunne, J. P., John, J. G., Adcroft, A. J., Griffies, S. M., Hallberg, R. W., Shevliakova, E., Stouffer, R. J., Cooke, W., Dunne, K. a., Harrison, M. J., Krasting, J. P., Malyshev, S. L., Milly, P. C. D., Phillipps, P. J., Sentman, L. T., Samuels, B. L., Spelman, M. J., Winton, M., Wittenberg, A. T. and Zadeh, N., 2012. GFDL's ESM2 Global Coupled Climate–Carbon Earth System Models. Part I: Physical Formulation and Baseline Simulation Characteristics. *Journal of Climate* 25(19), 6646–6665. doi:10.1175/JCLI-D-11-00560.1

Dunne, J. P., John, J. G., Shevliakova, E., Stouffer, R. J., Krasting, J. P., Malyshev, S. L., Milly, P. C. D., Sentman, L. T., Adcroft, A. J., Cooke, W., Dunne, K. a., Griffies, S. M., Hallberg, R. W., Harrison, M. J., Levy, H., Wittenberg, A. T., Phillips, P. J. and Zadeh, N., 2013. GFDL's ESM2 Global Coupled Climate–Carbon Earth System Models. Part II: Carbon System Formulation and Baseline Simulation Characteristics*. *Journal of Climate* 26(7), 2247–2267. doi:10.1175/JCLI-D-12-00150.1

Dutta, D., Herath, S. and Musiake, K., 2003. A mathematical model for flood loss estimation. *Journal of Hydrology* 277(1-2), 24–49. doi:10.1016/S0022-1694(03)00084-2

Dutta, D., Herath, S. and Musiake, K., 2006. An application of a flood risk analysis system for impact analysis of a flood control plan in a river basin. *Hydrological Processes* 20(6), 1365–1384. doi:10.1002/hyp.6092

Escuder-Bueno, I., Castillo-Rodríguez, J. T., Zechner, S., Jöbstl, C., Perales-Momparler, S. and Petaccia, G., 2012. A quantitative flood risk analysis methodology for urban areas with integration of social research data. *Natural Hazards and Earth System Science* 12(9), 2843–2863. doi:10.5194/nhess-12-2843-2012

FEMA, 1998. Costs and benefits of natural hazard mitigation. Washington DC.

FEMA, 2003. HAZUS:Multi-hazard loss estimation model methodology. Washington DC.

Feyen, L., Dankers, R., Katalin, B., Peter, S. and Barredo, J. I., 2012. Fluvial flood risk in Europe in present and future climates. *Climatic Change* 112, 47–62. doi:10.1007/s10584-011-0339-7

Förster, S., Kuhlmann, B., Lindenschmidt, K.-E. and Bronstert, A., 2008. Assessing flood risk for a rural detention area. *Natural Hazards …* 311–322. Retrieved from http://www.nat-hazards-earth-syst-sci.net/8/311/2008/nhess-8-311-2008.html

Fukubayashi, N., 2012. *Probability of Water-Related Disaster Occurrence and Risk Evaluation in Japan, Master thesis*. The University of Tokyo.

Glade, T., 2003. Vulnerability assessment in landslide risk analysis. *DieErde* 134, 123–146.

Green, C. H. and Penning-Rowsell, E. C., 1988. Flooding and the Quantification of " Intangibles ." *IWEM: 1998 Annual Symposium* (8), 27–30.

Grünthal, G., Thieken, a. H., Schwarz, J., Radtke, K. S., Smolka, a. and Merz, B., 2006. Comparative Risk Assessments for the City of Cologne – Storms, Floods, Earthquakes. *Natural Hazards* 38(1-2), 21–44. doi:10.1007/s11069-005-8598-0

Hall, J. W., Sayers, P. B. and Dawson, R. J., 2005. National-scale Assessment of Current and Future Flood Risk in England and Wales. *Natural Hazards* 36(1-2), 147–164. doi:10.1007/s11069-004-4546-7

Handmer, J., Honda, Y., Kundzewicz, Z. W., Arnell, N., Benito, G., Hatfield, J., Mohamed, I. ., Peduzzi, P., Wu, S., Sherstyukov, B., Takahashi, K. and Yan, Z., 2012. Changes in impacts of climate extremes:human systems and ecosystem, 231–290. Cambrige University Press, Cambridge.

Handmer, J., 2003. The chimera of precision : Inherent uncertainties in disaster loss assessment. *The Australian Journal of Emergency Management* 18(2), 88–97.

Hara, Y., Umemura, K., Kato, K., Connor, R. and Sato, Y., 2009. The development of flood vulnerability index applied to 114 major river basin around the world. *Journal of Japan Society of Hydrology and Water Resources* 22, 10–23.

Haraguchi, M. and Lall, U., 2013. Background paper: Global assessment report on disaster risk reduction. *Journal of the American Podiatric Medical Association*, Vol. 103. Geneva, Switzerland.

HDRO, 2012. International Human Development Indicators. *Human Development Index (HDI) value*. New York, USA. Retrieved February 25, 2013, from http://hdr.undp.org

Hempel, S., Frieler, K., Warszawski, L., Schewe, J. and Piontek, F., 2013. A trend-preserving bias correction – the ISI-MIP approach. *Earth System Dynamics Discussions* 4(1), 49–92. doi:10.5194/esdd-4-49-2013

Hinkel, J., 2011. "Indicators of vulnerability and adaptive capacity": Towards a clarification of the science–policy interface. *Global Environmental Change* 21(1), 198–208. doi:10.1016/j.gloenvcha.2010.08.002

Hirabayashi, Y., Kanae, S., Emori, S., Oki, T. and Kimoto, M., 2008. Global projections of changing risks of floods and droughts in a changing climate Global projections of changing risks of floods and droughts in a changing climate. *Hydrological Sciences Journal* 53, 754–772.

Hirabayashi, Y., Mahendran, R., Koirala, S., Konoshima, L., Yamazaki, D., Watanabe, S., Kim, H. and Kanae, S., 2013. Global flood risk under climate change. *Nature Climate Change* 3(9), 816–821. Nature Publishing Group. doi:10.1038/nclimate1911

Hourdin, F., Foujols, M.-A., Codron, F., Guemas, V., Dufresne, J.-L., Bony, S., Denvil, S., Guez, L., Lott, F., Ghattas, J., Braconnot, P., Marti, O., Meurdesoif, Y. and Bopp, L., 2012. Impact of the LMDZ atmospheric grid configuration on the climate and sensitivity of the IPSL-CM5A coupled model. *Climate Dynamics* 40(9-10), 2167–2192. doi:10.1007/s00382-012-1411-3

Hydrotec, 2001. Teil I: Berichte und Anlagen. Studie im Auftrag des StUA Dusseldorf, Aachen.

ICPR, 2001. Atlas on the risk of flooding and potential damage due to extreme floods of the Rhine. Koblenz, Germany.

Ikeda, S., Sato, T. and Fukuzono, T., 2007. Towards an integrated management framework for emerging disaster risks in Japan. *Natural Hazards* 44, 267–280. doi:10.1007/s11069-007-9124-3

Inter-American Development Bank, 2007. Indicators of Disaster Risk and Risk Management. Washington DC. Retrieved from http://www.iadb.org/exr/disaster/pvi.cfm?language=EN&parid=4

IPCC, 2000. IPCC special report on emission scenarios.

IPCC, 2001. Third Assessment Report: Climate Change (TAR).

IPCC, 2012. Managing the Risks of Extreme Events and Disasters to Advance Climate Change Adaptation. A Special Report of Working Groups I and II of the IPCC. (C. B. Field, V. Barros, T. F. Stocker & Q. Dahe, Eds.), 582. Cambrige University Press, Cambridge, UK, and New York, NY, USA: Cambridge University Press. doi:10.1017/CBO9781139177245

Iwasada, M., Sasaki, K. and Murakami, M., 1999. The damage of river structure and natural bank protection in Kochi flood disaster in 1998. *Shikoku-based affiliate of Japan Society of Civil engineers*, 128–129.

Jha, A. K., Bloch, R. and Lamond, J., 2011. Cities and Flooding: A guide to integrated urban flood risk management for the 21st century-A summary for policy makers. Washington DC. Retrieved from www.worldbank.org

Jongman, B., Hochrainer-Stigler, S. and Feyen, L., 2014. Increasing stress on disaster risk finance due to large floods. *Nature Climate Change* (5). doi:10.1038/NCLIMATE2124

Jongman, B., Kreibich, H., Apel, H., Barredo, J. I., Bates, P. D., Feyen, L., Gericke, A., Neal, J., Aerts, J. C. J. H. and Ward, P. J., 2012a. Comparative flood damage model assessment: towards a European approach. *Natural Hazards and Earth System Science* 12(12), 3733–3752. doi:10.5194/nhess-12-3733-2012

Jongman, B., Ward, P. J. and Aerts, J. C. J. H., 2012b. Global exposure to river and coastal flooding: Long term trends and changes. *Global Environmental Change* 22(4), 823–835. Elsevier Ltd. doi:10.1016/j.gloenvcha.2012.07.004

Kain, J. S. and Fritsch, M., 1990. A One-Dimensional Entraining/Detraining Plume Model and Its Application in Convective Parameterization. *Journal of the Atmospheric Sciences* 47(23), 2784.

Kazama, S., Sato, A. and Kawagoe, S., 2009. Evaluating the cost of flood damage based on changes in extreme rainfall in Japan. *Sustainability Science* 4(1), 61–69. doi:10.1007/s11625-008-0064-y

Kellenberg, D. K. and Mobarak, A. M., 2008. Does rising income increase or decrease damage risk from natural disasters? *Journal of Urban Economics* 63(3), 788–802. doi:10.1016/j.jue.2007.05.003

Kelman, I. and Spence, R., 2004. An overview of flood actions on buildings. *Engineering Geology* 73(3-4), 297–309. doi:10.1016/j.enggeo.2004.01.010

Kreibich, H., Piroth, K., Seifert, I., Maiwald, H., Kunert, U., Schwarz, J., Merz, B. and Thieken, A. H., 2009. Is flow velocity a significant parameter in flood damage modelling? *Natural Hazards and Earth System Science* 9(5), 1679–1692. doi:10.5194/nhess-9-1679-2009

Kreibich, H., Seifert, I., Merz, B. and Thieken, A. H., 2010. Development of FLEMOcs – a new model for the estimation of flood losses in the commercial sector. *Hydrological Sciences Journal* 55(8), 1302–1314. doi:10.1080/02626667.2010.529815

Kreibich, H., Thieken, a. H., Petrow, T., Müller, M. and Merz, B., 2005. Flood loss reduction of private households due to building precautionary measures – lessons learned from the Elbe flood in August 2002. *Natural Hazards and Earth System Science* 5(1), 117–126. doi:10.5194/nhess-5-117-2005

Kreibich, H. and Thieken, A. H., 2008. Assessment of damage caused by high groundwater inundation. *Water Resources Research* 44(9), n/a–n/a. doi:10.1029/2007WR006621

Kundzewicz, Z. W., Kanae, S., Seneviratne, S. I., Handmer, J., Nicholls, N., Peduzzi, P., Mechler, R., Bouwer, L. M., Arnell, N., Mach, K., Muir-Wood, R., Brakenridge, G. R., Kron, W., Benito, G., Honda, Y., Takahashi, K. and Sherstyukov, B., 2013. Flood risk and climate change: global and regional perspectives. *Hydrological Sciences Journal* 59(1), 1–28. Taylor & Francis. doi:10.1080/02626667.2013.857411

Lavell, A., Oppenheimer, M., Diop, C., Hess, J., Lempert, R., Liu, J., Muir-Wood, R. and Myeong, S., 2012. Climate change:new dimensions in disaster risk, exposure, vulnerability, and resilence., 25–64. Cambrige University Press, Cambridge.

Lehner, B., Döll, P., Alcamo, J., Henrichs, T. and Kaspar, F., 2006. Estimating the Impact of global change on flood and drought risks in Europe: A continental, Integrated Analysis. *Climatic Change* 75(3), 273–299. doi:10.1007/s10584-006-6338-4

Linde, a. H. te, Bubeck, P., Dekkers, J. E. C., Moel, H. de and Aerts, J. C. J. H., 2011. Future flood risk estimates along the river Rhine. *Natural Hazards and Earth System Science* 11(2), 459–473. doi:10.5194/nhess-11-459-2011

Maaskant, B., Jonkman, S. N. and Bouwer, L. M., 2009. Future risk of flooding: an analysis of changes in potential loss of life in South Holland (The Netherlands). *Environmental Science & Policy* 12(2), 157–169. doi:10.1016/j.envsci.2008.11.004

Merz, B., Kreibich, H., Schwarze, R. and Thieken, A., 2010. Review article "Assessment of economic flood damage." *Natural Hazards and Earth System Science* 10(8), 1697–1724. doi:10.5194/nhess-10-1697-2010

Merz, B., Kreibich, H., Thieken, A., Schmidtke, R. and Hydrology, S. E., 2004. Estimation uncertainty of direct monetary flood damage to buildings. *Natural Hazards and Earth System Science* 153–163.

Messner, F. and Meyer, V., 2005. UFZ-Discussion Papers. Retrieved from http://www.researchgate.net/publication/235642120_Criteria_for_ILTSER_(International_Long_Term_Socio-Ecological_Research)_Sites_selection_Criteria_for_ILTSER_(International_Long_Term_Socio-_Ecological_Research)-Sites_selection/file/32bfe51238a309b2e0.pdf

Meyer, V., Becker, N., Markantonis, V., Schwarze, R., Bergh, J. C. J. M. van den, Bouwer, L. M., Bubeck, P., Ciavola, P., Genovese, E., Green, C., Hallegatte, S., Kreibich, H., Lequeux, Q., Logar, I., Papyrakis, E., Pfurtscheller, C., Poussin, J., Przyluski, V., Thieken, a. H. and Viavattene, C., 2013. Review article: Assessing the costs of natural hazards – state of the art and knowledge gaps. *Natural Hazards and Earth System Science* 13(5), 1351–1373. doi:10.5194/nhess-13-1351-2013

MLIT, 2006. Flood disaster statistics 2006. Tokyo.

MLIT, 2008a. Climate Change Adaptation Strategies to cope with Water-related Disasters due to Global Warming (Policy Report).

MLIT, 2008b. Sewerage-mitigation of inundation damage. Retrieved October 16, 2013, from http://www.mlit.go.jp/crd/sewerage/policy/01.html

MLIT, 2009. Flood disaster statistics 1993-2009. Tokyo.

Moel, H. de, Aerts, J. C. J. H. and Koomen, E., 2011. Development of flood exposure in the Netherlands during the 20th and 21st century. *Global Environmental Change* 21(2), 620–627. Elsevier Ltd. doi:10.1016/j.gloenvcha.2010.12.005

Moel, H. de and Aerts, J. C. J. H., 2010. Effect of uncertainty in land use, damage models and inundation depth on flood damage estimates. *Natural Hazards* 58(1), 407–425. doi:10.1007/s11069-010-9675-6

Montz, B. E., 1992. The effects of flooding on residential property values in three new zealand communities. *Disasters* 16(4), 283–98. doi:10.1111/j.1467-7717.1992.tb00411.x

Morgan, M. and Henrion, M., 1990. *"Uncertainty: a Guide to dealing with uncertainty in quantitatie risk and policy analysis."* New York, USA: Cambridge University Press.

Morita, M., 2011. Quantification of increased flood risk due to global climate change for urban river management planning. *Water Science & Technology* 63(12), 2967. doi:10.2166/wst.2011.172

Moss, R. H., Babiker, M., Brinkman, S., Calvo, E., Carter, T., Edmonds, J., Elgizouli, I., Emori, S., Erda, L., Hibbard, K., Jones, R., Kainuma, M., Kelleher, J., Lamrque, J. F., Manning, M., Matthews, B., Meehl, J., Meyer, L., Mitchell, J., Nakicenovic, N., O'Neill, B., Pichs, R., Riashi, K., Rose, S. K., Runchi, P., Stouffer, R. J., Vuuren, D. P. van, Weyant, J. P., Wilbanks, T. J., Ypersele, J. P. van and Zurek, M., 2008. Towards New Scenarios for Analysis of Emissions, Climate Change, Impacts, and Response Strategies., 132. Geneva.

Moss, R. H., Edmonds, J. a, Hibbard, K. a, Manning, M. R., Rose, S. K., Vuuren, D. P. van, Carter, T. R., Emori, S., Kainuma, M., Kram, T., Meehl, G. a, Mitchell, J. F. B., Nakicenovic, N., Riahi, K., Smith, S. J., Stouffer, R. J., Thomson, A. M., Weyant, J. P. and Wilbanks, T. J., 2010. The next generation of scenarios for climate change research and assessment. *Nature* 463(7282), 747–56. Nature Publishing Group. doi:10.1038/nature08823

Mouri, G., Minoshima, D., Golosov, V., Chalov, S., Seto, S., Yoshimura, K., Nakamura, S. and Oki, T., 2013. Probability assessment of flood and sediment disasters in Japan using the Total Runoff-Integrating Pathways model. *International Journal of Disaster Risk Reduction* 3, 31–43. Elsevier. doi:10.1016/j.ijdrr.2012.11.003

Munich Re, 2004. Megacities-Megarisks Trends and chalenges for insurance and risk management. Germany.

MURL, 2000. Potentielle Hochwasserschaden am Rhein in NRW, Dusseldorf: MURL Report.

Nicholas, J., Holt, G. D. and Proverbs, D. G., 2001. Towards standardising the assessment of flood damaged properties in the UK. *Structural Survey* 19(3), 163–172.

Nicholls, R. J., 2004. Coastal flooding and wetland loss in the 21st century: changes under the SRES climate and socio-economic scenarios. *Global Environmental Change* 14(1), 69–86. doi:10.1016/j.gloenvcha.2003.10.007

NRE, 2000. Rapid Appraisal Method (RAM) for floodplain Management, Report prepared by Read Sturgess and Associates. Melbourne, Australia.

Okazawa, Y., Yeh, P. J.-F., Kanae, S. and Oki, T., 2011. Development of a global flood risk index based on natural and socio-economic factors. *Hydrological Sciences Journal* 56(5), 789–804. doi:10.1080/02626667.2011.583249

Olsen, B. J. R., Beling, P. A., Lambert, J. H. and Haimes, Y. Y., 1998. INPUT-OUTPUT ECONOMIC EVALUATION OF SYSTEM OF LEVEES By J. Rolf Olsen; Peter A. Beling/ James H. Lambert/ Member, ASCE, and Yacov Y. Haimes,4 Fellow, ASCE. *Journal of water resources planning and management* (October), 237–245.

Pall, P., Aina, T., Stone, D. A., Stott, P. A., Nozawa, T., Hilberts, A. G. J., Lohmann, D. and Allen, M. R., 2011. Anthropogenic greenhouse gas contribution to flood risk in England and Wales in autumn 2000. *Nature* 470(7334), 382–5. doi:10.1038/nature09762

Peduzzi, P., Dao, H. and Herold, C., 2002. Global Risk And Vulnerability Index Trends per Year (GRAVITY), Phase II: Development, analysis and results. Geneva.

Pelling, M. and Uitto, J. I., 2001. Small island developing states: natural disaster vulnerability and global change. *Environmental Hazards* 3(2), 49–62. Taylor & Francis. doi:10.3763/ehaz.2001.0306

Penning-Rowsell, E., Johnson, C., Tunstall, S., Tapsell, S., Morris, J. and J, C., 2005. The benefits of flood and coastal risk management: a manual of assessment techniques. London.

Pielke, R. a., Downton, M. W. and Miller, J. Z. B., 2002. Flood Damage in the United States , 1926 – 2000 A Reanalysis of National Weather Service Estimates by. P.O. Box 3000, Boulder, Colorado 80307-3000.

Pistrika, A. K. and Jonkman, S. N., 2009. Damage to residential buildings due to flooding of New Orleans after hurricane Katrina. *Natural Hazards* 54(2), 413–434. doi:10.1007/s11069-009-9476-y

Ranger, N., Hallegatte, S., Bhattacharya, S., Bachu, M., Priya, S., Dhore, K., Rafique, F., Mathur, P., Naville, N., Henriet, F., Herweijer, C., Pohit, S. and Corfee-Morlot, J., 2011. An assessment of the potential impact of climate change on flood risk in Mumbai. *Climatic Change* 104(1), 139–167. doi:10.1007/s10584-010-9979-2

Rodda, H. J. E., 2005. The Development and Application of a Flood Risk Model for the Czech Republic. *Natural Hazards* 36(1-2), 207–220. doi:10.1007/s11069-004-4549-4

Scawthorn, C., Flores, P., Blais, N., Seligson, H., Tate, E., Chang, S., Mifflin, E., Thomas, W., Murphy, J., Jones, C. and Lawrence, M., 2006. HAZUS-MH Flood Loss Estimation Methodology. II. Damage and Loss Assessment. *Natural Hazards Review* 7(2), 72–81. doi:10.1061/(ASCE)1527-6988(2006)7:2(72)

Schmidt-Thomé, P., Greiving, S., Kallio, H., Fleischhauer, M. and Jarva, J., 2006. Economic risk maps of floods and earthquakes for European regions. *Quaternary International* 150(1), 103–112. doi:10.1016/j.quaint.2006.01.024

Schreider, S. Y., Smith, D. I. and Jakeman, A. J., 2000. Climate change impacts on urban flooding. *Climatic Change* 47, 91–115. Kluwer Academic Publishers.

Seneviratne, S. I., Nicholls, N., Easterling, D., C.M, G., Kanae, S., Kossin, J., Luo, Y., Marengo, J., Mclnnes, K., Rahimi, M., Reichstein, M., Sorteberg, A., Vera, C. and Zhang, X., 2012. Changes in climate extremes and their impacts on the natural physical environment, 109–230. Cambrige University Press, Cambridge.

Smith, D., 1994. 1994 flood damage estimation-A review of urban stage-damage curves and loss function (Smith, 1994).pdf. *Water SA* 20, 231–238.

Smith, K., 1996. *Environmental Hazards: Assessing Risk and Reducing Disaster*, Second. Routledge, London.

UNDP, 2004. Reducing disaster risk: A challenge for development. New York, USA. Retrieved from http://www.undp.org/content/dam/undp/library/

UNDP, 2013. Human Development Report 2013 (Technical notes). New York, USA. Retrieved from http://hdr.undp.org/sites/default/files/hdr_2013_en_technotes.pdf

UNISDR, 2009. UNISDR Terminology on Disaster Risk Reduction. Geneva.

USGS, 1996. GTOPO30 global digital elevation model. *United States Geological Survey,Sioux Falls, South Dakota, EROS data centers*. Retrieved January 11, 2013, from ftp://edcftp.cr.usgs.gov/data/gtopo30/global/

Utsumi, N., Seto, S., Kanae, S., Maeda, E. E. and Oki, T., 2011. Does higher surface temperature intensify extreme precipitation? *Geophysical Research Letters* 38(16). doi:10.1029/2011GL048426

Vogel, R. M., 1986. The Probability Plot Correlation Coefficient Test for the Normal, Lognormal, and Gumbel Distributional Hypotheses. *Water Resources Research* 22(4), 587–590. doi:10.1029/WR022i004p00587

Wake, B., 2013. Flooding costs. *Nature Climate Change* 3(9), 778–778. Nature Publishing Group. doi:10.1038/nclimate1997

Ward, P. J., Jongman, B., Weiland, F. S., Bouwman, A., Beek, R. van, Bierkens, M. F. P., Ligtvoet, W. and Winsemius, H. C., 2013. Assessing flood risk at the global scale: model setup, results, and sensitivity. *Environmental Research Letters* 8(4), 044019. doi:10.1088/1748-9326/8/4/044019

Warszawski, L., Frieler, K., Huber, V., Piontek, F., Serdeczny, O. and Schewe, J., 2014. The Inter-Sectoral Impact Model Intercomparison Project (ISI-MIP): project framework. *Proceedings of the National Academy of Sciences of the United States of America* 111(9), 3228–32. doi:10.1073/pnas.1312330110

Watanabe, S., Hajima, T., Sudo, K., Nagashima, T., Takemura, T., Okajima, H., Nozawa, T., Kawase, H., Abe, M., Yokohata, T., Ise, T., Sato, H., Kato, E., Takata, K., Emori, S. and Kawamiya, M., 2011. MIROC-ESM: model description and basic results of CMIP5-20c3m experiments. *Geoscientific Model Development Discussions* 4(2), 1063–1128. doi:10.5194/gmdd-4-1063-2011

Wind, H. G., Nierop, T. M., Blois, C. J. de and Kok, J. L. de, 1999. Analysis of flood damages from the 1993 and 1995 Meuse Floods. *Water Resources Research* 35(11), 3459–3465. doi:10.1029/1999WR900192

Winsemius, H. C., Beek, L. P. H. Van, Jongman, B., Ward, P. J. and Bouwman, a., 2013. A framework for global river flood risk assessments. *Hydrology and Earth System Sciences* 17(5), 1871–1892. doi:10.5194/hess-17-1871-2013

Xie, P., Chen, M., Yang, S., Yatagai, A., Hayasaka, T., Fukushima, Y. and Liu, C., 2007. A Gauge-Based Analysis of Daily Precipitation over East Asia. *Journal of Hydrometeorology* 8(3), 607–626. doi:10.1175/JHM583.1

Yamamoto, H., Iwaya, K., K, S. and Hayakawa, S., 1999. Heavy rainfall disaster in September of 1998 by Akisame Front in Kochi Prefecture. *Journal of Japan Society for Natural Disaster Science* 18(2), 213–226. Retrieved from http://sciencelinks.jp/j-east/article/199922/000019992299A0923670.php

Yamazaki, D., Kanae, S., Kim, H. and Oki, T., 2011. A physically based description of floodplain inundation dynamics in a global river routing model. *Water Resources Research* 47(4), n/a–n/a. doi:10.1029/2010WR009726

Yoshimura, K., Sakimura, T., Oki, T., Kanae, S. and Seto, S., 2008. Toward flood risk prediction: a statistical approach using a 29-year river discharge simulation over Japan. *Hydrol Res Lett* 2(April), 22–26. doi:10.3178/HRL.2.22

Yukimoto, S., Yoshimura, H., Hosaka, M., Sakami, T. and Tsujino, H., 2011. Meteorological Research Institute-Earth System Model Version 1 (MRI-ESM1), Model Description. Tsukuba, Japan. Retrieved from http://www.mri-jma.go.jp/Publish/Technical/DATA/VOL_64/tec_rep_mri_64.pdf

Zhou, Q., Mikkelsen, P. S., Halsnæs, K. and Arnbjerg-Nielsen, K., 2012. Framework for economic pluvial flood risk assessment considering climate change effects and adaptation benefits. *Journal of Hydrology* 414-415, 539–549. Elsevier B.V. doi:10.1016/j.jhydrol.2011.11.031